JET PROPULSION

Journal of the

AMERICAN ROCKET SOCIETY

Rocketry . . . . . Jet Propulsion Sciences . . . . . Astronautics

VOLUME 25 **MAY 1955** **NUMBER 5**

ARS SUMMER MEETING BOSTON, MASS., JUNE 22–23 SEE PAGE 241


LAUNCHING DEVICES by RMI
DROP OF THE FLAG . . .
Aircraft powerplants
Special propulsion
Auxiliary power units
Boundary layer control
RMI
ROCKAWAY, NEW JERSEY Special Products
Test Areas DOVER, NEW JERSEY
REACTION MOTORS, Inc.
DENVILLE, NEW JERSEY
Engineering Research Administration
AFFILIATED WITH OLIN MATHIESON CHEMICAL CORPORATION

Scope of JET PROPULSION

JET PROPULSION, the Journal of the American Rocket Society, is devoted to the advancement of the field of jet propulsion through the publication of original papers disclosing new knowledge and new developments. The term "jet propulsion" as used herein is understood to embrace all engines that develop thrust by rearward discharge of a jet through a nozzle or duct; and thus it includes systems utilizing atmospheric air and underwater systems, as well as rocket engines. JET PROPULSION is open to contributions, either fundamental or applied, dealing with specialized aspects of jet and rocket propulsion, such as fuels and propellants, combustion, heat transfer, high temperature materials, mechanical design analyses, flight mechanics of jet-propelled vehicles, astronautics, and so forth. JET PROPULSION endeavors, also, to keep its subscribers informed of the affairs of the Society and of outstanding events in the rocket and jet propulsion field.

Limitation of Responsibility

Statements and opinions expressed in JET PROPULSION are to be understood as the individual expressions of the authors and do not necessarily reflect the views of the Editors or the Society.

Subscription Rates

One year (twelve monthly issues)	$10.00
Foreign countries, additional postage add	.50
Single copies	1.75
Special issues, single copies	2.50
Back numbers	2.00

Change of Address

Notices of change of address should be sent to the Secretary of the Society at least 30 days prior to the date of publication.

Information for Authors

Preparation of Manuscripts

Manuscripts must be double spaced on one side of paper only with wide margins to allow for instructions to printer. Submit two copies: original and first carbon. Include a 100–200 word abstract of paper. The title of the paper should be brief to simplify indexing. The author's name should be given without title, degree, or honor. A footnote on the first page should indicate the author's position and affiliation. Include only essential illustrations, tables, and mathematics. References should be grouped at the end of the manuscript; footnotes are reserved for comments on the text. Use American Standard symbols and abbreviations published by the American Standards Association. Greek letters should be identified clearly for the printer. References should be given as follows: For Journal Articles: Title, Authors, Journal, Volume, Year, Page Numbers. For Books: Title, Author, Publisher, City, Edition, Year, Page Numbers. Line drawings must be made with India ink on white paper or tracing cloth. Lettering on drawings should be large enough to permit reduction to standard one-column width, except for unusually complex drawings where such reduction would be prohibitive. Photographs should be clear, glossy prints. Legends must accompany each illustration submitted and should be listed in order on a separate sheet of paper.

Security Clearance

Manuscripts must be accompanied by written assurance as to security clearance in the event the subject matter of the manuscript is considered to lie in a classified area. Alternatively, written assurance that clearance is unnecessary should be submitted. Full responsibility for obtaining authoritative clearance rests with the author.

Submission of Manuscripts

Manuscripts should be submitted in duplicate to the Editor-in-Chief, Martin Summerfield, Professor of Aeronautical Engineering, Princeton University, Princeton, N. J.

Manuscripts Presented at ARS Meetings

A manuscript submitted to the ARS Program Chairman and accepted for presentation at a national meeting will automatically be referred to the Editors for consideration for publication in JET PROPULSION, unless a contrary request is made by the author.

To Order Reprints

Prices for reprints will be sent to the author with the galley proof, and orders should accompany the corrected galley when it is returned to the Assistant Editor.

JET PROPULSION

Journal of the

AMERICAN ROCKET SOCIETY

JET PROPULSION, the Journal of the American Rocket Society, published monthly by the American Rocket Society at 20th and Northampton Streets, Easton, Pa., U.S.A. The Editorial Office is located at 500 5th Ave., New York 36, N. Y. Price $1.75 per copy, $10.00 per year: Entered as second-class matter at the Post Office at Easton, Pa., under the Act of March 3, 1879.

Ten Years That Changed the World

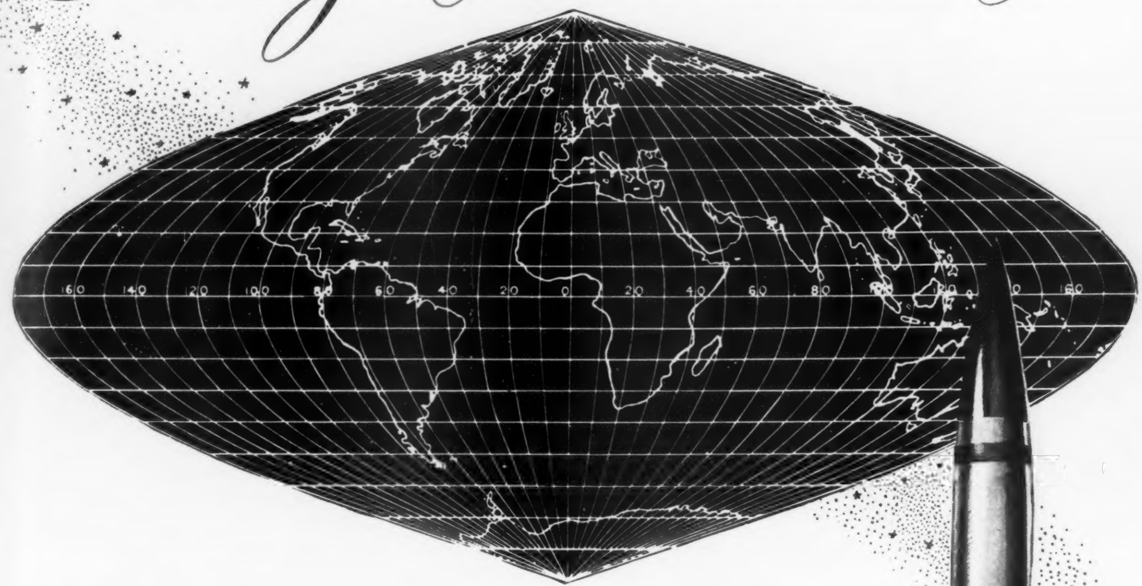

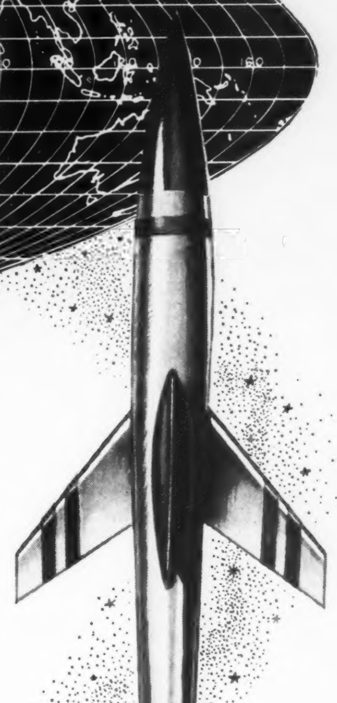

History records no more radical changes in the military sciences than those of the past decade. The period 1945-1955 saw not only the advent of nuclear weapons but, equally important, new systems of defense and new means of offense – guided missiles.

Just ten short years ago guided missiles were only a visionary concept. Today they are on the verge of becoming the base on which the security of Western Civilization and the peace of the world will rest. Although largely masked by the necessities of military security, tremendous strides are being made by all the branches of the U. S. Armed Forces in this crucial period.

The Fairchild Guided Missiles Division is proud to have a part in the missile programs of our Armed Services. Starting in 1945 with the first of this country's true guided missiles – the Navy's surface-to-air "Lark" – the Fairchild Guided Missiles Division has been continuously engaged in designing, developing and producing missiles, radar and associated equipment. It has supplied missiles and missile weapons systems to the Navy, the Air Force and the Army.

In the years ahead, Fairchild can be counted upon to continue its role as one of the leaders in our missiles program.

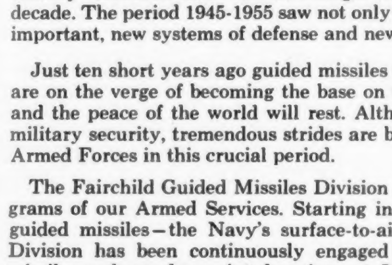

"where the future is measured in light-years"

ENGINE AND AIRPLANE CORPORATION

FAIRCHILD

Guided Missiles Division

WYANDANCH, L. I.

Other Divisions: Aircraft Division, Hagerstown, Md. American Helicopter Division, Manhattan Beach, Calif.; Engine Division, Farmingdale, N. Y.; Kinetics Division, New York, N. Y.; Speed Control Division, St. Augustine, Fla.; Stratos Division, Bay Shore, N. Y.

Now Solve

ATTITUDE CONTROL

Best with this New Clary A-mount Gyroscope!

CLARY CG-100 GYROSCOPE. Here in this one small unit (no bigger than your hand) is your newest and best answer to the problem of controlling attitude of aircraft and guided missiles... where vibration and steady-state accelerations are moderate to heavy.

Our intensive Gyroscope Test Program assures dependable precision of every unit.

Our unique design assures handmade dependability in volume production.* We are proud to be the supplier of all the gyroscope equipment for the famous "Corporal" guided missiles.

For full details, please call or write: Automatic Controls Division, Dept. J55, Clary Corporation, San Gabriel, Calif.

**90-day delivery*

HIGHLIGHTS

Weight: 7½ pounds

Dimensions: 5¾" diameter x 6¼" long.

Mounting Flange: Gyro axes referenced to mounting holes and mounting plane within 0.25°.

Vibration: Along any principal axis—sinusoidal motion:
- 12g 100-200 c.p.s.
- 6g 20-100 c.p.s.
- 6g 200-500 c.p.s.

Pickoffs: 3 Wire synchro, each axis:
- Null voltage: 50 mv or less
- Input voltage: 26 V., 400 c.p.s., single phase.

Motor: Supply Voltage: 115 V., 400 c.p.s., three phase.

J-55

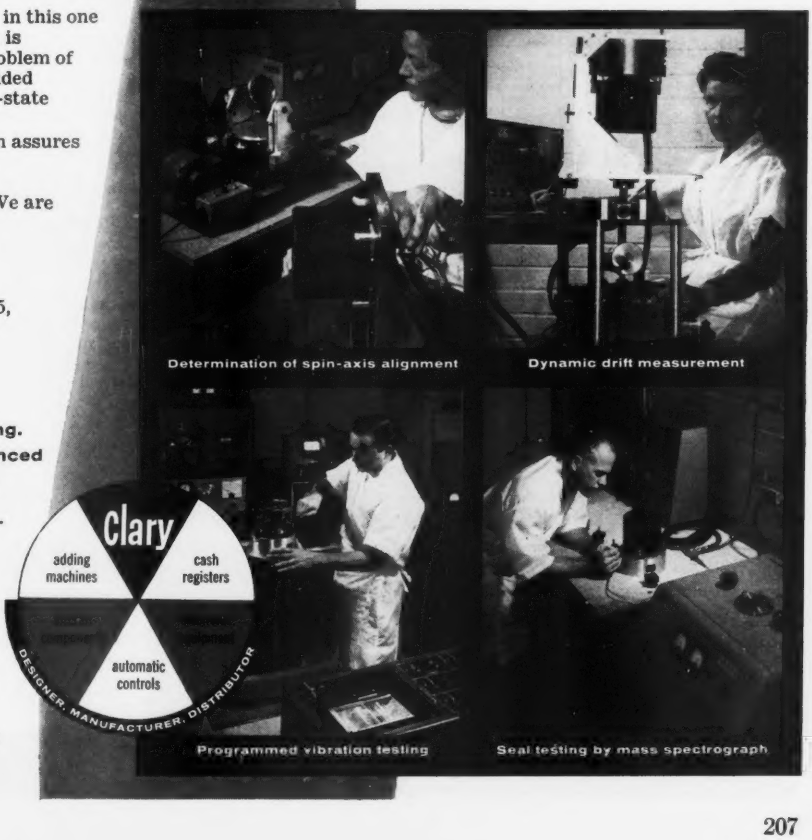

Determination of spin-axis alignment

Dynamic drift measurement

Programmed vibration testing

Seal testing by mass spectrograph

MAY 1955

VOLUME 25 NUMBER 5

JET PROPULSION

Journal of the

AMERICAN ROCKET SOCIETY

Editor-in-Chief

MARTIN SUMMERFIELD

Review of Biological Effects of Subgravity and Weightlessness

DAVID G. SIMONS[1]

Aero Medical Field Laboratory, Holloman Air Development Center, N. Mex.

Disorientation and discoordination resulting from exposure to subgravity and weightlessness depend upon the response of the sensory modalities of equilibrium, vision, and kinesthesis. These modalities are influenced by altered stimulus-sensation responses, illusions, and sensory inconsistencies. Experimental evidence of disorientation and discoordination due to exposure to subgravity and weightlessness is cited from both animal and human experiments. It is concluded that the vestibular apparatus plays a critical role in the physiological and psychological responses to subgravity exposure. The experimental evidence available to date suggests that incapacitating disorientation may occur under specific conditions.

Introduction

CONTINUED progress in rocket research brings us closer to the day when earthly missiles will penetrate the realm of interplanetary space. The prospect of manning such vehicles brings with it many problems (1, 2)[2] in the fields of physiology and psychology. One of the most interesting of these problems involves human responses to subgravity and weightless conditions (3, 4).

After a brief review of the organs man employs to orient himself in space (5), the experiments that have been conducted under subgravity conditions will be reviewed, correlating the effects observed with the organs involved. Finally, the nature and importance of the problem to a space traveler will be estimated.

Space Orientation Organs

Man establishes his orientation in space by means of three sensory systems: the vestibular apparatus, the visual apparatus, and the mechano-receptor apparatus.

Part of the vestibular apparatus (6) can be thought of as a pair of three-dimensional accelerometers, one situated in each middle ear on either side of the head. One unit consists of three semicircular canals lying in the three planes of space like three sides of a box coming together to form a corner. Near their common junction, each canal has a slight enlargement which contains a christa that behaves like critically damped torsion pendulum. Angular acceleration in any plane is detected with these structures. Another part of the vestibular apparatus, an enlargement at the junction point of the semicircular canals (at the corner of the box) contains a macular plate of the otolith organ which is largely responsible for translational accelerative sensations. Each plate is equipped with tiny grains of sand called otoliths, which are supported upon sensitive hairs by a jellylike material. Under normal one-"g" conditions, these hairs support the weight of the otoliths against the accelerative force of the pull of gravity. Any translatory acceleration superimposed on this one-g background is sensed in terms of deformation of the sensitive hair in the same manner that angular acceleration moves the fluid in one or more canals, displacing its christa. The brain is continually receiving vestibular impulses caused by the force of gravity except for brief moments when one is diving, jumping, or falling.

This vestibular sense of balance is a very deep-seated sensory system closely connected to the autonomic nervous system that controls such automatic functions as digestion, heart rate, sweating, and vasomotor control. Because of these close connections, disturbance of the vestibular sense can produce an incapacitating, shocklike state. Anyone who has been severely motion-sick will vouch for the havoc disoriented vestibular sensation can play with one's ability to function effectively.

Of the three orienting senses, vision is the one of which we are most conscious. The fact that one learns to correlate visual sensations with tactile and vestibular sensations is not self-evident because the process occurs so early in life. This is brought out vividly when an individual acquires sight for the first time later in life. For such a person, relative directions and distances conveyed through visual stimuli become meaningful only after they have been defined through experience with the already familiar world of vestibular and tactile sensations.

The kinesthetic or body position sensory apparatus includes both the familiar skin sensations of touch and pressure as well as proprioceptive sense. This latter sense of body position permits one to realize the position of an arm or leg with relation to the rest of the body. It is based on sensory messages sent from pressure detectors placed within the muscles and on joint surfaces. The fact that such a sensation exists is difficult to realize until it has been removed by a disease process. Its absence can be dramatically illustrated by having an afflicted subject close his eyes. When his hand is grasped firmly and his arm is stretched to one side, to the front, and lowered to his side, he is completely unable to state in what position it was being placed. These sensations, too, are closely associated with the autonomic nervous system.

Sensory Responses to Subgravity

To date, exposure of human subjects to subgravity conditions have been limited to about 20 seconds. During these

Presented at the ARS Fall Meeting, White Sands Proving Ground, N. Mex., September 22, 1954.

[1] Major, U.S.A.F. (MC); Chief, Space Biology Branch. Mem. ARS

[2] Numbers in parentheses indicate References at end of paper.

brief exposures, Von Beckh (7) has noted significant neuromuscular discoordination, and Yeager has described severe disorientation. It is possible that continued exposure might result in a form of motion sickness comparable to seasickness. The possibility of an incapacitating autonomic "storm" must be considered because of altered stimulus-sensation relationships, illusions, and sensory inconsistencies.

When the possible consequences of prolonged exposure to weightlessness (sometimes called zero g) were first contemplated, Gauer and Haber (8) postulated that the intensity of sensation from the vestibular and kinesthetic system might follow the Weber-Fechner law to very low levels of stimulation. (The Weber-Fechner law states that the intensity of sensation is proportional to the logarithm of the intensity of the stimulus.) As applied to the vestibular and proprioceptive senses, the logarithmic sensory response to small accelerative forces in a weightlessness field would be greatly disproportionate to that normally perceived. These strange, unidentified, and unaccountable sensations might in themselves produce neuromuscular discoordination when physical movement is attempted. It is expected that any difficulties from this source would be resolved by learning after repeated or prolonged exposure to weightlessness.

To date, no experiment has been designed which clearly isolates altered stimulus-sensation relationships as a factor during subgravity exposure. Determination of the extent to which this factor contributes to performance difficulties is of interest because adaptation to altered sensation is generally prompt and effective.

Illusions can be very disturbing (9). The dizziness one experiences after spinning like a top is accompanied by the strong sensation that the room is still spinning. This is partly because the fluid in the semicircular canals is still flowing and partly because the eyes are performing a sweeping motion called nystagmus. The visual and vestibular sensations add up to a spinning room, but all mechano-receptor sensations indicate a fixed position.

In the absence of a normal gravitational reference, it is not unlikely that translational acceleration may be perceived as rotational acceleration (10). Graybiel (11) and others have demonstrated that linear acceleration will generate the visual illusion of apparent motion and displacement of an object vertically in space. Gerathewohl (10) has discussed extensively the importance of ocular illusory phenomena with respect to subgravity exposure.

Inconsistent sensations may produce autonomic disturbance, particularly when the conflict is between sensations closely related to the autonomic nervous system. The experiment mentioned previously, of making one's self dizzy by spinning like a top, if prolonged, can result in a distressing autonomic "storm" very similar to motion sickness. This abnormal stimulation of the vestibular apparatus and discordant reports from the senses of balance and position are not taken lightly by the body.

Consideration of the pattern characterized by motion sickness may give some hint as to how individuals may react to the stress of weightlessness. When the ocean suddenly becomes rough, it takes an appreciable time of exposure, something on the order of 15 or 20 minutes, before most neophyte passengers become thoroughly sick. Many hours later the seasoned sailors are still unaffected. There are many similarities between the factors producing motion sickness and its possible counterpart, space sickness. The differences are sufficient that there may or may not be the same 20-minute latent period upon initial exposure with acclimatization after repeated or prolonged exposure.

The occurence of serious functional disturbance during exposure to weightlessness may well depend upon mental set. The experience of being unsupported in space can be thought of equally well as floating or falling. The difference in body responses, however, may be definitive.

Experiments

1 In the summer of 1951, Crossfield used a YF-84 aircraft to produce weightlessness (12) for periods of 15 to 20 seconds on 30 occasions. Only on the first five flights was a sensation of "befuddlement" experienced while entering the subgravity state. No sensation of falling was observed, although the sensation of being weightless was described as feeling "unnatural." The only evidence of muscular discoordination was a tendency to overshoot on reaching out rapidly with his arm.

2 At the same time Ballinger (13) was performing a series of similar experiments on passive subjects in a modified F-80E. His subjects were given 15 to 20-second exposures to less than $^1/_{50}$ g by flying the aircraft in a Keplerian trajectory. The subjects, held firmly in place, were able to maintain their sense of orientation by fixing a point of visual reference. Head-shaking had no adverse effects; however, the opinion was stated that had the subjects been unrestrained and blindfolded, disorientation might have been extreme.

3 One instance of serious disorientation is recorded under similar conditions by Haber (14). C. Yeager, Major, U.S.A.F., in his thirteenth second of weightlessness "got the impression that he was spinning around slowly in no particularly defined direction. After fifteen seconds he became lost in space, and pulled out of the parabola. With his returning weight, his badly needed orientation was restored, too." At a panel discussion (15) Yeager added the following comment: "It feels as though the blood pressure is increasing. You get quite a swelling of the head, literally, that is."

4 The latest series of such experiments has been reported by Von Beckh (7). Each subject was required to draw squares in two different formats under four conditions of acceleration with eyes open, and again with eyes closed, always constrained with safety harness. The four conditions of acceleration were: (a) Straight and level flight; (b) radial positive acceleration; (c) direct exposure to weightlessness; and (d) exposure to weightlessness following exposure to plus 6.5 g. The subjects had difficulty placing the crosses accurately during exposure to weightlessness with their eyes open. With eyes closed, the line of crosses was typically deviated 90 degrees upward. It is very interesting to note that all subjects improved noticeably on subsequent flights, that a pilot trained in instrument flying showed the greatest rate of improvement, and that performance clearly deteriorated when supporting harness was reduced to a minimum and fitted loosely.

These human experiments clearly indicate that the first exposure to subgravity is associated with a moderate degree of neuromuscular discoordination. They suggest that it is not of a serious degree unless performed without vision, and that subjects can learn to properly interpret the altered sensations that occur during exposure to weightlessness. Apparently, the fact that the brain is being presented with contradictory stimuli from the vestibular apparatus, versus the visual and kinesthetic senses, does not in itself cause any serious disturbance. The experience of Yeager, however, indicates that serious disorientation can occur.

The work of both Ballinger and Von Beckh suggests that in the absence of both sensory and visual orienting sensations there is considerable likelihood of complete spatial disorientation. It is of considerable interest that Yeager experienced an episode of disorientation and none of the other subjects did. One possible answer is that he skillfully eliminated the residual longitudinal acceleration and verticle bumps which are very difficult to eliminate in aircraft flying within the lower atmosphere. The difference between a subgravity exposure with residual acceleration and a true weightless condition may be critical. It is also possible that Yeager achieved a mental set for falling, whereas other experimenters experienced floating. Present published data do not permit the degree of weightlessness attained to be assessed as a parameter. Only

very accurate instrumentation can resolve this question.

5 Von Beckh (7) also reported the behavior of normal specimens of the South American water turtle *Hydromedusa tactifera* when exposed to subgravity conditions compared to that of a specimen which had lost its vestibular or labyrinthine functions due to accidental overexposure to heat. The injured turtle took several weeks to learn to strike normally for its food using only visual and kinesthetic clues. However, after it had become adapted to the complete absence of labyrinthine sensations, this animal was able to feed normally during a subgravity run, whereas its normal brethren showed the same symptoms of disturbed orientation and coordination evidenced by the first turtle immediately after its accident.

The above experiment emphasizes the critical role played by the sense of equilibrium located in the vestibular apparatus or labyrinth of the middle ear. It is interesting to note that the normal turtles were able to adapt only partially to subgravity conditions after 30 runs.

6 A similar experiment using mice in an Aerobee rocket vehicle was performed by Henry, et al. (16). In this case a normal mouse and a purposely labyrinthectomized mouse were each given a compartment in a rotating smooth-walled drum with an irregularity that afforded a possible foothold for each. During this experiment, the animal without vestibular function quietly rode around the drum clinging to the irregularity during the subgravity phase of the rocket flight, whereas the normal animal clawed at the air, suggesting disorientation.

In a later rocket experiment, the same authors flew two normal mice in a similar drum. On this flight, one mouse was provided a paddle with a convenient foothold. The other compartment was completely smooth. Throughout the subgravity portion of the flight, the mouse with the paddle rode around the drum clinging securely to its perch. During most of the subgravity phase of the flight the rocket rotated slowly, producing approximately $^1/_{20}$ g. However, for about 15 seconds, between the time the nose section was separated from the body of the rocket and when it re-entered the atmosphere, there was a true weightless situation. Until this time, the mouse without a perch rode quietly against the "down" side of its cage, orienting himself with the slight accelerative force supplied by the rotation of the nose. However, during the 15 seconds that there was no "down," this moused hopped disconcertedly back and forth, unable to "stick" to any surface of its compartment. It is not known why the normal mouse with a foothold should react so quietly to weightlessness whereas the normal mouse in the previous experiment was so disturbed, unless the animal in the earlier experiment was simply unable to find its foothold.

This experiment suggests that a little g can go a long way in supplying helpful orientation. Since the mouse without a perch had such a relatively short time to adjust to a completely weightless status, it is impossible to say whether it was truly disoriented or just slow to adjust its landing reflexes to the fine precision required to just cancel its forward momentum.

Other studies associated with the above experiments, using monkeys, clearly established the fact that the weightless state itself produces no disturbance of circulation in terms of heart rate or arterial and venous blood pressures. This does not mean that the circulation might not be involved secondarily due to emotional and autonomic reactions to weightlessness. Such secondary reactions are essentially the same whether caused by weightlessness, a rough sea, or an obnoxious mother-in-law.

Conclusions

The turtle and mouse experiments demonstrate the critical role played by the vestibular apparatus in causing disorientation and discoordination under subgravity conditions. As the result of many human exposures to subgravity conditions lasting 15 to 20 seconds, it is generally agreed that minimal discoordination and no disorientation are experienced as long as the subject retains tactile and visual references. There are insufficient data available to establish clearly what will happen if the latter conditions are not met, but indications are that severe disorientation can occur. Until more accurate instrumentation is used in conjunction with these experiments, the question of the difference between factional subgravity exposure and true weightlessness exposure cannot be resolved. The relation of mental set to the problem needs clarification. On purely theoretical grounds, there is good reason to suspect that once severe disorientation has occurred due to prolonged weightlessness, the process of re-establishing autonomic equanimity may be a difficult one.

Although the physiological and psychological responses to subgravity will likely present problems to a wayfarer in space, by employing at least one of the three orienting sensory modalities at all times, accumulating evidence indicates that it should be possible to avoid an attack of incapacitating "space sickness."

References

1 "Aeromedical Problems of Space Travel," by H. G. Armstrong, H. Haber, and H. Strughold, *J. Aviation Medicine*, vol. 20, 1949, pp. 383–417.

2 "Medizinische Probleme der Raumfahrt," by H. V. Diringshofer, Oldenbourg, Germany, 1952.

3 "Zür Frage der Orientierung im schwerefreien Zustand. IV," Intern. Astronaut Congr., S. J. Gerathewohl, Zürich, Switzerland, August 2–8, 1953.

4 "Physics and Psychophysics of Weightlessness," by H. Haber and S. J. Gerathewohl, *J. Aviation Medicine*, vol. 22, 1951, p. 180.

5 "Orientation in Space," by P. A. Campbell, chapter 5, pp. 62–69 in "Space Medicine," edited by J. P. Marbarger, Univ. of Illinois Press, 1951.

6 "The Effect of Vision Produced by Stimulation of the Semi-Circular Canals by Angular Acceleration and Stimulation of the Otolith Organs by Linear Acceleration," by Ashton Graybiel, chapter XXI, in "Physics and Medicine of the Upper Atmosphere," edited by White and Benson, p. 152.

7 "Experiments with Animals and Human Subjects under Sub and Zero Gravity Conditions During the Dive and Parabolic Flight," by H. J. A. Von Beckh, *J. Aviation Medicine*, vol. 25, 1954, pp. 235–241.

8 "German Aviation Medicine in Word War II," vol. I, chapter VI-G, by Otto Gauer and Heinz Haber, Dept. of the Air Force, U. S. Government Printing Office, Washington 25, D. C., pp. 641–644.

9 "Some Problems of Orientation in the Gravity-Free State," by S. J. Gerathewohl, First Annual Meeting of the Southwestern Psychological Association, San Antonio, Tex., December 3–5, 1953.

10 "Physics and Psychophysics of Weightlessness—Visual Perception," by S. J. Gerathewohl, *J. Aviation Medicine*, vol. 23, 1952, pp. 373–395.

11 "The Illusory Perception of Movement Caused by Angular Acceleration and by Centrifugal Force During Flight. I, II, III, and IV," by A. Graybiel, B. Clark, and K. MacCorquodale, Naval School Aviation Medicine, U. S. Naval Air Training Base, Pensacola, Fla., 1946.

12 "Possible Methods of Producing the Gravity-Free State for Medical Research," by F. Haber and H. Haber, *J. Aviation Medicine*, vol. 21, 1950, p. 395.

13 "Human Experiments in Subgravity and Prolonged Acceleration," by E. R. Ballinger, *J. Aviation Medicine*, vol. 23, 1952, p. 319.

14 "Man in Space," by H. Haber, The Bobbs-Merrill Co., Inc., New York, 1st ed., 1953, pp. 171–172.

15 Panel discussion, Symposium on Frontiers of Man-Controlled Flight, by H. Haber, The Institute of Transportation and Traffic Engineering, University of California, 1953.

16 "Animal Studies of Subgravity States during Rocket Flight," by J. P. Henry, E. R. Ballinger, P. M. Maher, and D. G. Simons, *J. Aviation Medicine*, vol. 23, 1952, pp. 421–432.

Fabrication of Titanium Components

ARNOLD S. ROSE[1]

I-T-E Circuit Breaker Company, Philadelphia, Pa.

The fabrication of titanium rocket and jet engine components has necessitated the use of techniques peculiar to this material. Such operations as forming, forging, spinning, resistance, and fusion welding are described in detail. Inasmuch as considerable usage of titanium has been for the fabrication of prototype material models, tooling has generally been adapted from those used for stainless steel fabrications. Hot working is required for most forming and spinning. Fusion welding is performed in a helium-filled chamber which totally encloses the work and provides protection against contamination for the weld and adjacent heat-affected zones.

Introduction

THE fabrication of titanium components for aircraft gas turbine, guided missile, or rocket assembly has developed over the past few years in an unprecedented manner. Fabrication techniques have been modified from existing practice when available, and in some instances techniques peculiar to the requirements imposed by the properties of titanium have been developed. Many of these have been amply reported in the literature by industrial and government organizations, contributing greatly to the rapid advance in titanium technology. This report presents a further review of some of the principal operations utilized in the assembly of titanium components.

Titanium Alloys

A discussion of titanium, as related to fabrication, may be divided into two phases. One concerns the commercially pure and alloy grades which are weldable; the other, those high-strength alloys which because of their composition are considered not capable of being welded. The latter type will be omitted from this paper inasmuch as fusion welding is a fundamental requirement for the components under consideration here.

The weldable grades are primarily commercially pure titanium alloys which are classified under such grades as AMS 4900, AMS 4901, AMS 4921, and under commercial designations such as Ti-75A, RC-A55, RC-A70, RS-70, MST Grade III, etc. Commerically pure titanium at room temperature and at temperatures up to approximately 1600 F exists in a hexagonal close-packed crystal structure, the alpha phase. This structure allows the material to be bent and formed with some effort at room temperature although heating to approximately 1000 F–1200 F increases its ductility measureably, as indicated in Fig. 1. This, in combination with the drop in yield strength at elevated temperatures, greatly improves the formability.

Inasmuch as these grades transform to the ductile alpha state at room temperature, no difficulty is experienced with postwelding embrittlement. This is contrasted to the results obtained where beta is retained at room temperature, in which case considerable hardening of the weld bead and adjacent heat-affected zone is noted. In Fig. 2 this is shown graphically by means of a hardness traverse across fusion-welded, commercially pure titanium and alloy titanium such as RC-

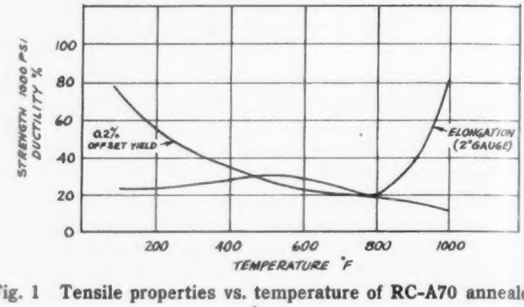

Fig. 1 Tensile properties vs. temperature of RC-A70 annealed sheet

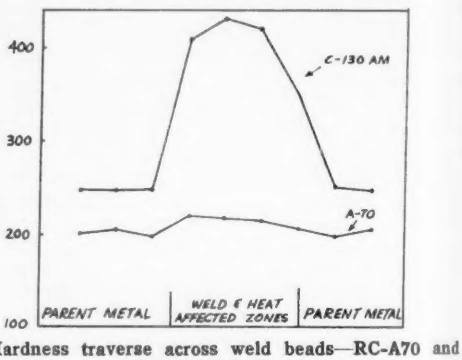

Fig. 2 Hardness traverse across weld beads—RC-A70 and RC-C130AM

C130AM. The latter alloy is titanium alloyed with 4 per cent manganese and 4 per cent aluminum and retains some beta phase at room temperature. The weld zone hardnesses resulting from mixed alpha-beta structure are sufficiently high that cracking ensues on cooling from the welding temperature.

A recently developed variation from the commercially pure titanium is an all alpha phase weldable alloy containing 4 per cent aluminum and 2 per cent tin; Rem-Cru's A-110AT grade. This alloy, whose properties at elevated temperature are superior to the commercially pure grades, is readily weldable

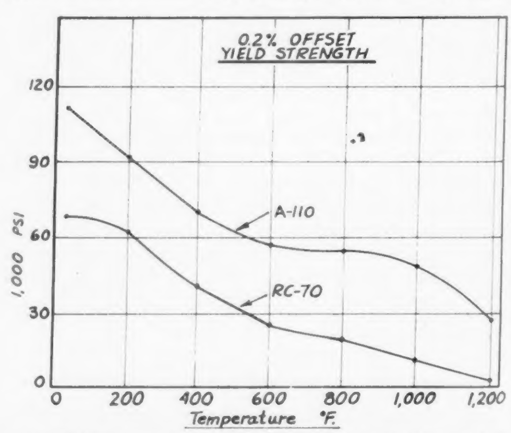

Fig. 3 Yield strength. vs. temperature of RC-A70 and RC-A110AT

Presented at the ARS Summer Meeting, Pittsburgh, Pa., June 24, 1954.

[1] Supervisor, Research and Development Laboratory, Special Products Division.

and amenable to fabrication. A comparison is shown in Fig. 3 of the yield strengths of this alloy and the commercially pure titanium.

Thus we have available for construction, in addition to the commercially pure grade, an aluminum-tin alloy grade. The superior properties of the latter obviously make it more difficult to bend and form, requiring somewhat higher fabricating temperatures to achieve comparable metal movement. When proper consideration is given to this factor in design no difficulty should be experienced.

Forming Operatons

The type of tooling utilized for various forming operations is dependent upon the quantity of parts to be produced. Since, in our experience, the greatest usage of titanium has been in the production of prototype models requiring only one or two units of a kind, our tooling has generally been adapted from existing tools or has been of a temporary nature. For example, bending and rolling of sheet and bar stock has been performed on rollers and mills commonly found in a stainless steel sheet metal shop, and forming of parts has been almost exclusively with Kirksite dies on a drop hammer. Sheet metal RC-A70 varying in thickness from 0.025 in. to 0.140 in. has been rolled into cylinders and conical sections with diameters ranging from 10 in. to 48 in. These have been rolled at room temperature with no difficulty. Sheet titanium 0.180 in. thick and bar stock ranging in section between $\frac{1}{2} \times \frac{1}{2}$ in. to 3 in. $\times$ 4 in. have required hot rolling. This was done by placing the flat stock into a 1300 F recirculating air furnace and holding for a length of time sufficient only to uniformly heat the material which was then transferred to the rolling machine. Surface pyrometer observation disclosed that even the heaviest bar sections were rolled into rings at temperatures varying from 900 F to 700 F.

Similarly, in view of their low volume requirements and correspondingly high value, almost all parts have been hot formed using the techniques outlined above. The titanium blanks were heated in an air oven to 1300 F and then placed immediately on the drop hammer. As mentioned previously, Kirksite dies were generally used. Several blows were struck to form the part with surface pyrometer observation between blows. When required, the partially finished parts were reheated and hit with finishing strokes. Although we have successfully formed parts as thin as 0.025 in., it has not been found necessary to resort to internally heated dies for this grade of titanium. At most, slight preheating of the dies to approximately 200 F has been required occasionally. Several parts formed in this manner as shown in Figs. 4 and 5. It is of interest to note here that although the zinc alloy Kirksite dies were used on heated parts, no die pickup was observed and there was no difficulty during forming or subsequent welding and assembly.

Fig. 4 Parts hot formed on drop hammer

Fig. 5 Duct hot formed on drop hammer

Forging

The forging of titanium parts also requires heating. Since the forged parts generally are machined subsequent to forging, they may be heated to higher temperatures than those used for sheet metal forming. Normally, the forging temperature is approximately 1800 F and a hard skin forms on the part as a result of contamination by the atmosphere. If this skin were not removed prior to welding, embrittlement of the weld bead would obviously result. In order to minimize the formation of this skin, heating in an inert atmosphere has been used, but is not required where sufficient skin removal follows forging.

The forging of the plate illustrated in Fig. 6 began with a section of RC-A70 bar stock 2 in. $\times$ 4 in. $\times$ 14 in. which was upset into a billet 4 in. $\times$ 4 in. $\times$ 7 in. The starting blank was placed on the cleaned hearth of an oil-fired air atmosphere furnace and heated to 1800 F. The upsetting blows were discontinued when the temperature fell to 1450 F, at which point the blank was reheated to 1800 F. In order to complete the initial upsetting, four reheats were required. Following upsetting, the billet was sprued and then forged to shape in dies on the drop hammer. Approximately 30 hammer blows and four additional reheats were required to produce the finished forging.

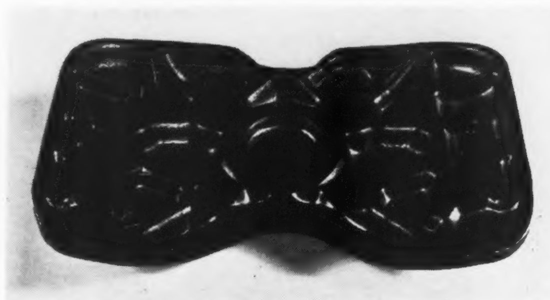

Fig. 6 Forged RC-A70 plate

The flow of the titanium under the drop hammer compared to that experienced with stainless steel of the AISI 300 series. Filling of the dies was exceptionally good. It is considered good practice to finish the forging in the lower temperature range at the end of a series of hammer blows in order to achieve a finer grain size with its accompanying improvement in physical properties.

Spinning

Spinning is one of the most readily adaptable methods for the production of prototype units for jet engines where cylindrical and conical sheet metal parts are widely used. When applied to the forming of titanium, a departure from normal practice is necessary since titanium must be spun at an elevated temperature. In order to accomplish this heating, a group of manifolded oxygen-gas burners was set up above the spinning lathe as illustrated in Fig. 7. These burners were adjustable relative to the work being spun by means of a handwheel geared arrangement which permitted lateral and vertical adjustment along the chuck. The burners were lit as the work rotated and heated a narrow 2-in. band of the titanium cone to which the spinning tool was applied. It was found that, inasmuch as the localized heating caused rapid charring of the chuck, a method of protection was necessary to prevent its eventual destruction.

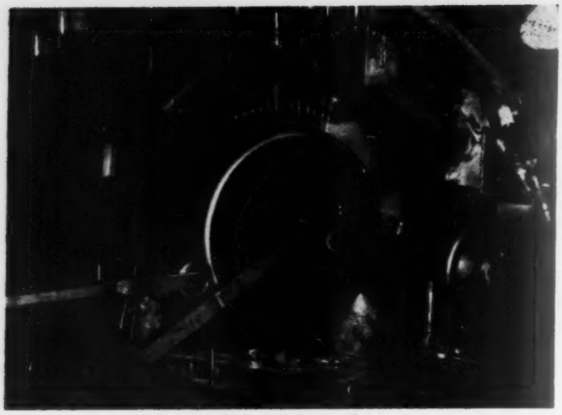

Fig. 7 Hot spinning of cone

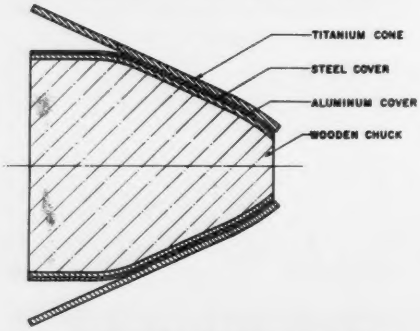

Fig. 8 Schematic view of chuck protection

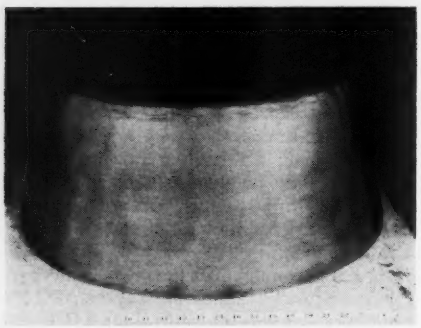

Fig. 9 Spun cone of 0.140-in. thick titanium

This involved spinning an aluminum cone over the chuck and in turn covering this with a mild steel shell, all conforming to the chuck contour as shown in Fig. 8. The high thermal conductivity of the aluminum cone served the purpose of rapidly diffusing the heat away from the heated band and greatly minimizing the chuck charring.

A typical spinning is shown in Fig. 9. It was spun from a rolled conical section of 0.140-in. thick titanium on which the mating edges had been welded by means of an inert gas-shielded tungsten arc. The resulting cone was placed over the chuck and clamped with an end plate. The burners were then lit and positioned over the rotating cone. Spinning was performed manually, as shown in Fig. 7, by means of a hardened steel roller mounted on a scissor tool. When the temperature of the heated area reached the desired 1300 F, the spinning roller was applied by the operator to force the titanium into conformation with the chuck. The heating fires were kept aligned with the roller so that only the heated, and therefore ductile, titanium was spun.

A mechanized version which differs markedly from conventional hand spinning is involved in the shear forming of sheet metals to produce conics. This process, which has been used extensively for the manufacture of metal cones for television tubes, actually produces a reduced section in the portion being spun. The essential differences between the two processes are illustrated graphically in Fig. 10. With manual

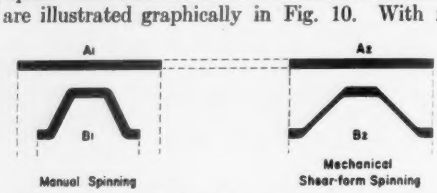

Fig. 10 Differentiation between manual and mechanical shear-form spinning

spinning, reduction in the finished part diameter results, as shown by the cone B_1, spun from an original blank size A_1. With mechanical shear forming, and starting with the same blank A_1, the cone wall is reduced (as a function of the sine of the spinning angle) and the finished cone diameter is precisely that of the initial blank. As an example, a 16-in.-diam blank, 0.100 in. in thickness may be mechanically spun into a 16-in.-diam cone B_2 whose wall thickness is 0.045 in.

The equipment used in this process is shown in Fig. 11. On this machine, the spinning force is applied hydraulically by steel rollers against the blank which is mounted on a rotating steel chuck.

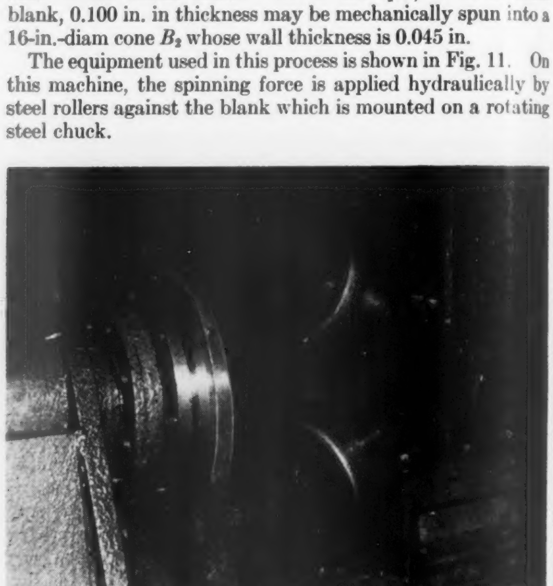

Fig. 11 Mechanical spinning machine

Fig. 12 Titanium cone spinning

It was felt that an attempt to mechanically spin titanium could serve the purposes of subjecting the metal to an exceedingly severe forming operation and of establishing data for future application. Accordingly, 16-in.-diam blanks of RC-A70 titanium were prepared for spinning and an initial trial was run with the metal at room temperature. Immediately upon application of the spinning rollers, the blank was severed into two pieces, coming apart with a brittle fracture. Subsequent trials showed that hot spinning was necessary and since the spinning time was of such a short duration—40 sec—the required heating could be accomplished prior to spinning rather than by playing fires on the work. A blank was then preheated in an oven to 1300 F, transferred to the spinner chuck, and spun immediately. Surface pyrometer indications at various stages showed that blank temperature fell to about 800 F during the 15–20-sec transfer time, and at the conclusion of spinning had dropped to approximately 600 F. A photograph of the finished 16-in.-diam titanium cone is shown in Fig. 12.

Welding

A basic consideration in the welding of titanium is the requirement that the molten metal be shielded from contact with air. Above 1500 F the titanium reacts with the oxygen and nitrogen of the atmosphere, becoming brittle and unworkable. In fusion welding, the argon or helium associated with the inert-arc welding process in conjunction with an auxiliary supply of gas provide the necessary protection. In resistance welding, the molten nugget at the joint interface is sufficiently protected by the parent metals that gas coverage is not required and the welds are made in air.

The spot, overlap spot, and seam welding of the RC-A70 titanium was performed with no difficulty and with excellent results. Initial sample setups were made with those values of time, pressure, and current normally used for stainless steel, and when the parts were actually welded, only slight variations from these were required. A typical welder setting for spot welding 0.062 in. to 0.062-in. thicknesses required a pressure of 1350 lb, a welding current of approximately 10,000 amperes of 6 cycles duration using $^1/_2$-in. Elkonite 10W3 electrodes and giving a tensile strength of 3750 lb. A typical seam weld for 0.045 in. to 0.045-in. thicknesses required a pressure of 1400 lb; a welding current of approximately 15,000 amperes of 8 cycles duration; 8 welds per in. at a speed of 15 in. per min. The seam welding electrodes were 10-in.-diam wheels, $^1/_2$ in. thick with a 3-in. radius at their faces.

One outstanding feature of resistance welding on titanium is the tendency to excessive penetration of the weld nugget into the parent materials. This effect may be limited by proper welder setups to acceptable values. It is important when inspecting etched cross sections of weld nuggets that differentiation be made between the actual dendritic cast metal of the nugget and the surrounding heat-affected zone. Casual examination will give an exaggerated impression of the penetration, since the structure of the heat-affected zone is somewhat similar in appearance to that of the nugget. Careful examination, however, will reveal the differences in structure and allow calculation of the actual penetration.

When seam or spot welding dissimilar thicknesses, it was found that penetration into the thinner sheet titanium increased as the disparity in thicknesses increased. When welding a combination where the heavier metal was four times the thickness of the thinner sheet, penetration over the permissible 80 per cent was obtained. A practical working limit, therefore, for dissimilar metal thicknesses may be taken as $(t_1/t_2) = 3$. The photomacrographs (Figs. 13 and 14) illustrate this limit.

The assembly of engine components calls for a wide variety of fusion welding which may be conveniently outlined as follows: (a) Butt: 1—longitudinal, 2—circumferential; (b) fillet; (c) plug or slot; (d) edge; (e) lap.

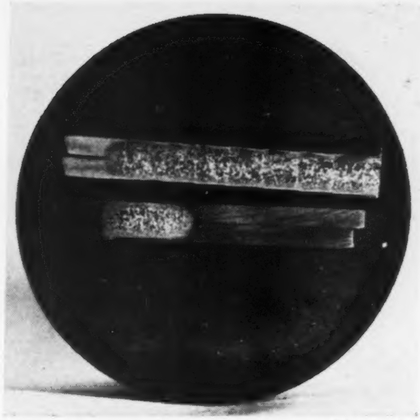

Fig. 13 Photomacrograph 4 ×. Seam weld; 0.062 in. to 0.062-in. thicknesses, RC-A70 titanium

Fig. 14 Photomacrograph 4 ×. Spot weld; 0.062 in. to 0.180-in. thicknesses, RC-A70 titanium

In view of the widely varying nature of the welding, it was essential that some universal means of shielding the molten weld metal be utilized. It was recognized that for straight longitudinal butt joints a close fitting copper backup would protect the weld underbead, and that the shielding gas flowing from the inert-arc torch would provide similar protection to the top of the weld. However, such a method proved suitable only for relatively thin sheets. Titanium over 0.100 in. thick required high welding currents (approximately 200 amperes) and a heat input so great that the weld bead remained at red heat for a considerable length of time after the shielding gas issuing from the torch had moved on. The titanium was thus left unprotected, oxidized badly, and consequently became embrittled. Solution to this difficulty was provided by an elongated cup into which gas flowed covering approximately a 4-in. length of seam. It was obvious, however, that such a method would be effective only for straight seams and would be useless for lap, contoured, or various types of fillet welds, etc., where the gas protection could not be maintained because of the physical irregularity of the parts.

In order to provide gas protection to the titanium weld bead for all types of joints, a gas chamber, such as is shown in Fig. 15, was constructed into which the work was placed. Welds were made using either water or gas-cooled inert-arc tungsten electrode torches which were manipulated by an operator working with his arms encased in gas-tight rubber gloves. The various water, gas, and electrical leads for the torches were fitted through gas-tight ports into the gas cham-

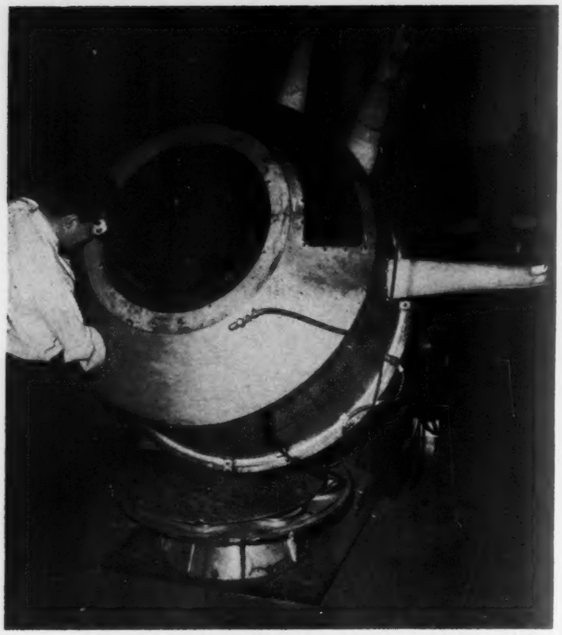

Fig. 15 View of helium-filled chamber for fusion welding titanium

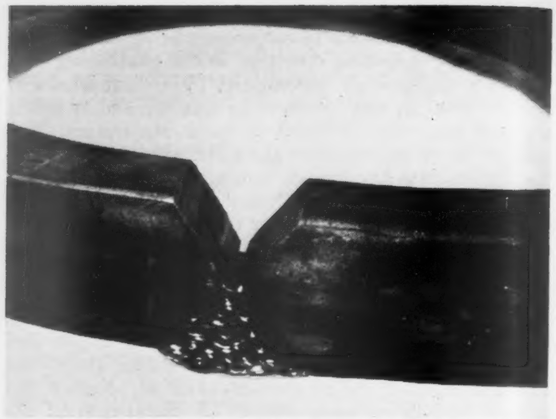

Fig. 16 Partially welded RC-A70 bar; 30-in. diameter, 2 in. by $3^1/_2$-in. section. Joint preparation is shown

ber, 52 in. in diam and 30 in. high, which was constructed of mild steel with strategically located gloves and windows. The windows were made of ultraviolet-absorbing Plexiglas so that the operator needed only goggles and did not require full face protection against the welding arc rays.

The bottom of the chamber was rubber gasketed to minimize gas leakage, and clamped firmly to a welding positioner capable of being rotated and/or tilted. The sequence of operations for a typical weld involved clamping the work to the positioner table following which the torch, filler wire supply, extra tungsten electrodes, and various hand tools were placed on the table. The chamber was lowered into place and fastened by means of the bolt clamps.

Rotation of the work inside the chamber was made possible by the inclusion of a separate turntable to which the work was clamped.

In order to expel the air from the chamber, a vent cock was opened and a flow of helium gas initiated into the chamber. This purging, which consisted simply of displacement of the air by helium was accomplished in approximately one hour. The extent of purging was tested periodically after $^1/_2$ hour by maintaining an arc with the inert-arc torch on a scrap piece of titanium for a few seconds. Discoloration of the melted section after cooling served as an indication of the presence of residual oxygen. An interesting sidelight with respect to this test is that it served not only as an oxygen indicator but also as an oxygen remover with the molten titanium acting as a getter.

When the test bead appeared bright and shiny, showing that the chamber was completely purged, the actual welding was started with additional helium added only through the torch. The welding proceeded normally in a manner similar to ordinary inert-arc practice.

Examples of titanium welded in the helium-filled chamber include heavy 2 in. × 2 in. titanium bar stock which had been rolled into ring shape. It was welded in the chamber by making deep 90-degree "V" bevel cuts on the mating ends and filling the grooves by depositing stringer beads of titanium weld metal, as illustrated in Fig. 16. Inasmuch as only a small quantity of 0.090 in. wire (RC-55) was available, sheet stock RC-A70 was sheared into narrow strips and utilized as filler rod. On this heavy work it was found that, after a few minutes of welding, the weld metal began to discolor even though the chamber had been purged sufficiently to give satisfactory test beads. Attempts to minimize this condition led to the inclusion of a dry-ice alcohol tube on which considerable quantities of water condensed and froze but which had little effect on the discoloration. The only feasible solution was to weld for short periods on the heavy work and to resume welding when the part had cooled. In order to hasten this cooling, an internally water-cooled copper block was introduced into the chamber. This was mildly helpful but proved so cumbersome that its use was discontinued.

The quality of welding performed in the chamber is shown by a series of tests run on RC-A70 titanium comparing the ductility of material as-received against welded samples. No significant change in the as-welded ductility from that of parent material was noted. This was checked by selecting only the welded portion of a 0.140-in.-thick butt joint for tensile testing. The value of 22 per cent elongation (in 2 in.) for the all-weld-cast-metal sample is approximately equivalent to that of the parent wrought material. Such values are are also obtainable on welds made outside the chamber, but it should be emphasized that complete shielding of the weld is essential for such ductility to be maintained consistently.

When molten, the RC-A70 titanium forms an exceptionally fluid, free-flowing liquid pool. As a result, it was desirable to position the work so that the welding took place in as nearly a horizontal plane as possible. It was found that welding vertically was difficult because the molten titanium tended to flow away from the joint. Another factor of this fluidity was the tendency of the titanium to freeze in a bridging fashion over unwelded areas, thereby leaving large voids. Constant care was exercised at all times to prevent this bridging and to make sure that 100 per cent penetration was achieved. The only other defects observed were minor in nature, such as small amounts of porosity, tungsten electrode inclusions, and undercutting—all of which may be minimized by careful welding.

Another example of the type of work which can be done only in a completely protective atmosphere, such as provided by the chamber, was in the fabrication of airfoil contour struts. The outer skin of the struts was made by butt welding 0.063 in. to 0.140-in. sheet thicknesses. This was done by clamping the pieces against a grooved copper backup and welding in the chamber. Following this, the strut halves were formed, as described previously, to airfoil contour. The halves were then slotted and assembled into a fixture with the stiffeners in place. The joint between stiffeners and skin was "through"-welded through the slotted skin and with copious

(*Continued on page 234*)

Mixture Ratio and Temperature Surveys of Ammonia-Oxygen, Rocket Motor Combustion Chambers[1]

DWIGHT I. BAKER[2]

Jet Propulsion Laboratory, California Institute of Technology, Pasadena, Calif.

Probing methods were applied to the study of combustion in NH_3-liquid oxygen, rocket motor combustion chambers. Temperature was measured by a pneumatic double-sonic-nozzle probe, and mixture ratio was determined by analyzing gas samples. Chemical methods were employed to analyze some of the samples, and a mass spectrometer was used for the others. Reasonable correlation was found to exist between sample composition and temperature for each value of local mixture ratio in both the high-performance and the low-performance injectors. Correlation also existed between external performance parameters and internal temperature measurements. At over-all mixture ratios near stoichiometric, high performance was associated with small variation in local mixture ratio and almost complete combustion, whereas low performance was associated with large variation in local mixture ratio and locally incomplete combustion. At over-all mixture ratios far above and far below stoichiometric, high performance was obtained with an injector which gave low performance at mixture ratios near stoichiometric. Gas analyses, together with measurements of temperature and performance in addition to considerations of extrapolated reaction-kinetic data, indicate that at low over-all mixture ratios and for the injectors tested the combustion process consists of (*a*) reaction of oxygen with ammonia in stoichiometric proportions, and (*b*) mixing of the products with undecomposed excess ammonia. Included is a summary of theoretical calculations for the NH_3-LO_2 system which extend over a range of values of mixture ratio from 0.12 to 16.0 and are based on chemical equilibrium at chamber temperature and at room temperature.

Nomenclature

A = throat area of nozzle
c = effective exhaust velocity $= F/(w/g) = c^*C_F$
c^* = characteristic velocity $= p_cf_t/(w/g)$
C = nozzle discharge coefficient ($\sim$0.98 for nozzles)
C_F = exhaust-nozzle thrust coefficient $= F/p_cf_t$
C_p = specific heat of gas at constant pressure
C_v = specific heat of gas at constant volume
f_c = chamber cross-sectional area
f_t = exhaust-nozzle throat area
F = thrust $= (w/g)c$
g = acceleration due to gravity
I_{sp} = specific impulse $= F/w$
K = probe constant determined from adiabatic calibration with nitrogen from $(p_2/p_c)^2$
L^* = characteristic length of combustion chamber $= V_c/f_t$
M = molecular weight
p = pressure
p_c = chamber pressure
p_2 = pressure measured upstream from downstream nozzle N_2
q_m = average heat flow per unit area including combustion chamber and nozzle
r = propellant mixture ratio $= w_o/w_f$
r_l = local mixture ratio
r_o = over-all mixture ratio
R = universal gas constant
t = time
T = absolute temperature
T_c = temperature of gases in combustion chamber
T_l = local temperature of gases in combustion chamber
T_2 = temperature measured upstream from downstream nozzle N_2
V_c = volume of combustion chamber up to the throat of exhaust nozzle
w = rate of propellant consumption (total), or flow of gas through probe nozzle
w_f = rate of fuel consumption
w_o = rate of oxidizer consumption
γ = ratio of specific heats C_p/C_v

Subscripts

1 = parameter associated with upstream probe nozzle, N_1
2 = parameter associated with downstream probe nozzle, N_2

I Introduction

PROBING studies of rocket motor combustion chambers have been made since July 1950, under a contract with the Navy Bureau of Aeronautics. The purpose of the program was to conduct an investigation of the combustion process in liquid-propellant rocket motors to determine experimentally the gas-temperature and gas-composition distributions throughout the thrust chamber and to correlate the internal distributions with the observed motor performance.

Initial work on the temperature-measuring probe and the radio-frequency mass spectrometer (which was to have been used in determining local mixture ratio) has been reported in (1, 2, 3).[3] The pneumatic method for measuring temperature has been employed by others, reported in (4, 5, 6). A series of temperature surveys was reported in (7) in which the surveys were found to correlate approximately with specific impulse. An additional series of tests has been made in order to determine the relationship between measurements of local temperature T_1 and local mixture ratio r_1. These measurements were combined with photographic techniques for some tests with the ammonia-acid system (cf. Ref. 8). Probing and photographic studies were expected to lead to a better understanding of the combustion process and thus aid in the development of rocket motors.

2 Apparatus and Procedure

The experimental apparatus and procedure used in this investigation were the same in general as those described in (1) and (7). A description of the way in which the probe is manufactured and used is included in an appendix.

Temperature was measured as before by bleeding combus-

Received August 24, 1954.

[1] This paper presents the results of one phase of research carried out at the Jet Propulsion Laboratory, California Institute of Technology, under Contract Number NOa(s)-53729 sponsored by Department of the Navy, Bureau of Aeronautics.

[2] Senior Research Engineer; now with Propulsion Field Laboratory, North American Aviation, Chatsworth, Calif. Mem. ARS.

[3] Numbers in parentheses indicate References at end of paper.

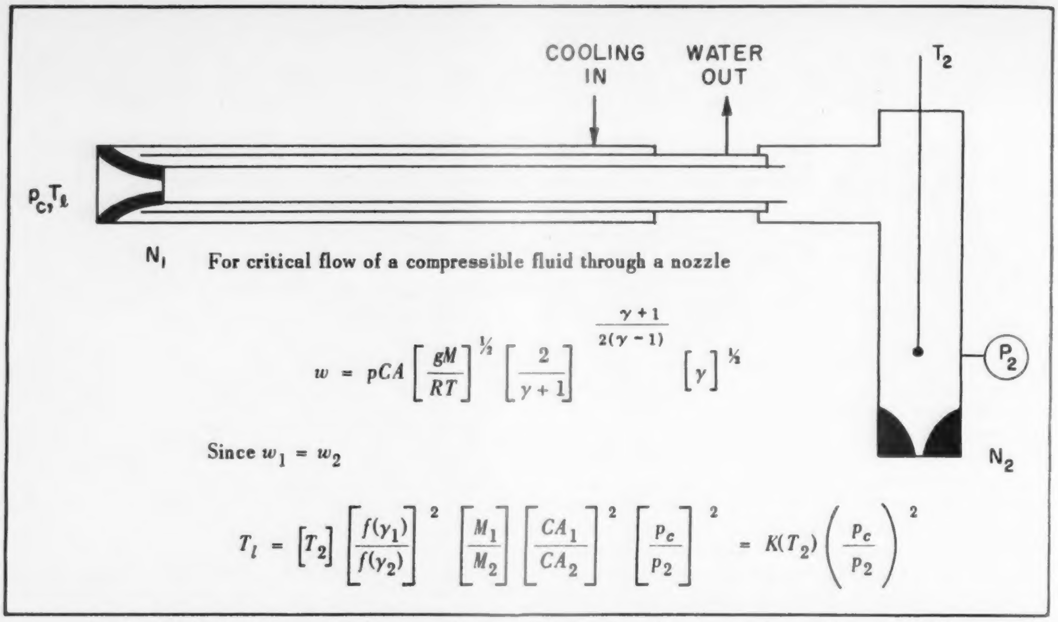

Fig. 1 Derivation of equation for determining combustion-chamber temperature with a pneumatic, double-sonic-nozzle probe

tion products through two sonic-flow nozzles in series (cf. Fig. 1), heat being extracted from the gas between the two nozzles. Temperature in the combustion chamber was determined from a simplified thermodynamic equation and was equal to the product of temperature measured upsteam from the second nozzle, a calibration constant, and the ratio squared of chamber pressure to pressure upstream from the second nozzle. Because of zero shifts in the Wiancko gages, temperature data obtained with high-response equipment (using a Miller recorder) were less reproducible than data reported in (1) and (7). Unexplained large shifts in probe calibration constants for tests 253 and 266 through 272 nullified temperature data for these tests.

Fig. 2 is a cross-sectional view of the motor which was tested, showing the probe in pad position 3. The like-on-like injector which is shown could be rotated between tests in increments of 30 degrees. This injector could be replaced with an Enzian-type injector (impinging multiorifice on splash plate). Provision was made so that the probe could be moved radially into the combustion chamber during a test.

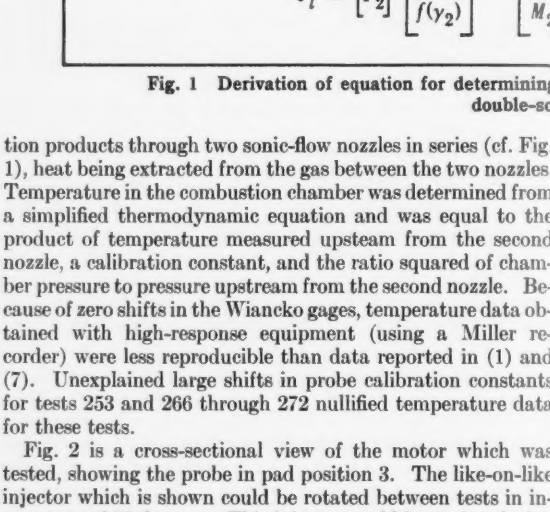

Fig. 2 Test motor of 1300-lb thrust for combustion study with probes

A heated, insulated line (not shown in Fig. 2) was used to carry the bled gases over to a manifold in the control room. Velocity of the bled gases in this line was approximately 100 fps. Static pressure in the line downstream from the probe was less than 5 psig. In order to prevent condensation of water, the line and manifold were heated by means of a nichrome wire to a temperature of 250 F. Six evacuated, stainless-steel, gas-sampling bottles of 75-cc capacity were attached to the manifold which was open to the atmosphere through a $^3/_8$-in. line.

Each gas sample was collected during an interval of 2 sec, the final pressure in the bottle being between $^1/_2$ and 1 atm. A period of 3 sec was allowed for moving the probe and for purging the gas-sample line. Collection of the sample was coordinated with radial position of the probe in the combustion chamber. The gas samples were analyzed either by local contractors or by the chemistry section of this Laboratory. A conventional mass spectrometer (cf. Ref. 9) was used for some of the analysis since the radio-frequency mass spectrometer (cf. Ref. 10) was not yet available; chemical methods were employed for other analyses.

Each sample analyzed in the mass spectrometer was volatilized into an evacuated volume of 7 liters. For the samples which indicated air leakage, as shown by the presence of argon gas, a correction based on the argon content was applied by the contractor. Precision of the determination was normally expected to be within 1 mole per cent. Analyses which did not have the correct N_2/H_2 weight ratio (4.63 for NH_3, the only source of nitrogen and hydrogen in the system) were corrected by adjusting the percentage of water. This correction for water was justified primarily on the basis of the final results obtained. There seems to be inherent difficulty in mass-spectrometer analysis for water caused by fractionation of the sample and by adsorption of water on wall surfaces. A difference of 8 mole per cent in water was found between the synthetic composition of a standard sample and the mass-spectrometer analysis of the sample. The correction for percentage of water was much larger for some samples analyzed by the mass spectrometer than for some analyzed by chemical methods.

Standard analysis techniques were adapted for the samples analyzed by chemical methods. The water and ammonia were frozen out of the sample in a trap cooled by liquid nitrogen.

Water and ammonia were weighed, and the percentage of ammonia was obtained by titration. O_2, N_2, and H_2 were determined manometrically. With the exception of percentage of water, the chemical analyses of standard samples agreed with known values, the different being less than 1 per cent of total.

3 Results

The results of this investigation are presented in Figs. 3 through 8. Reasonable correlation was found to exist between temperature and local mixture ratio, the best correlation being found in reaction zones near the nozzle of the rocket motor. Experimental results agreed with calculated values based on certain assumptions. However, selection of the proper assumptions to be used posed a difficult problem. Although the assumption of chemical equilibrium may be reasonable for over-all mixture ratios near stoichiometric, nonequilibrium conditions would seem to be the more realistic assumption at low mixture ratios. At the low mixture ratios the final temperatures are lower, and the combustion processes are slower. As a result, a final equilibrium may not be attained for such mixtures.

Theoretical values which were calculated for various assumed conditions are given in Fig. 4. The solid curves give temperature and gas composition as a function of mixture ratio for chemical equilibrium at 300 psia and at adiabatic reaction temperature. Gas composition for O, H, and N atoms are not shown since they exist in concentrations of less than 1 per cent. Such theoretical values of gas composition, with the exception of those of OH and NO, might be expected from probing experiments in a region of the motor where the reaction had gone to completion and where the rate of cooling the gases in the probe was fast enough to keep components from reassociating. The dashed curves give gas composition for chemical-equilibrium conditions at room temperature. These values might be expected in a region of the motor where the reaction had gone to completion and where the rate of cooling of the gases in the probe was slow enough to permit maintaining chemical-equilibrium conditions. These composition curves correspond closely (from $r = 0.12$ to 1.0) to those calculated for the assumption that gas in stoichiometric proportions and in chemical equilibrium for the final calculated temperature is mixed with undecomposed excess ammonia. The dash-dot curve shows combustion temperature corresponding to this assumption. Although other assumptions (i.e., incomplete reaction) can be made which would change the theoretical curves somewhat, the curves shown are believed to be the most useful for interpreting the experimental results which were obtained.

The interpretation of results should be based in part on an analysis of the factors which govern the rate of attainment of chemical equilibrium in liquid-propellant rocket motors. However, as summarized in (11), such an analysis is difficult because of (*a*) the unknown effects of the interaction of hydrodynamic components, and (*b*) the lack of information on the kinetics of reaction of heterogeneous and homogeneous chemical systems at elevated temperatures and pressures. Decomposition-rate data for NH_3 were extrapolated[4] to 3000 K and 20.4 atm from data obtained at 1000 K and 1 atm (cf. Ref. 12). At 1000 K and 1 atm it required 6×10^5 sec to decompose 50 per cent of the ammonia, whereas at 3000 K and 20.4 atm the extrapolation indicates that it requires only 3×10^{-10} sec. Unpublished data[5] obtained at this Laboratory show that, for the NH_3-O_2 system at stoichiometric mixture ratio, the half-life reaction at 1000 K and 1 atm requires 9.6×10^2 sec. Extrapolation[4] of the data to 3000 K and 20.4 atm indicates that only 2.5×10^{-3} sec is required for the half-like reaction. In this connection, it should be mentioned that residence time of the propellant gases in the rocket motor (80-in. L^*) is approximately 3×10^{-3} sec. These data based on extrapolation should be used with caution since the values give only a qualitative indication of the magnitude of the effect of temperature (primary) and pressure (secondary) on the reaction-rate data.

Interpretation of the data should also be based on a study of some of the other factors that influence local temperature in the combustion chamber (e.g., heat transfer, diffusion, and liquid drops).

Heat transfer to or from other propellants in the chamber and/or the motor wall may either increase or decrease the temperature of the gas sampled. Temperatures even higher than stoichiometric might exist locally on a macroscopic scale for conditions such that the propellants in the chamber are preheated before reaction. A point of interest in this connection is concerned with extremely high temperatures calculated[6] at the California Institute of Technology by Goldsmith using methods discussed in (13) relative to the burning of single drops of fuel in an oxidizing atmosphere. Although high temperatures calculated for the microscopic combustion zones may at first be considered unlikely, a physical mechanism can be postulated whereby the results calculated could be quite realistic when based on reasoning similar to that discussed for possible high local macroscopic zone temperatures in a rocket-motor combustion chamber. This postulate assumes that the products of combustion diffusing away from the high-temperature reaction zone (plus the effect of any inert chemical molecular matrix acting as a regenerative heat-transfer device) serve to preheat the fuel and oxidizer diffusing into the high-temperature zone. This burning-rate mechanism may have practical significance when the combustion of extremely small drops is considered. However, these possible microscopic combustion zones of extremely high temperature are not expected to affect temperatures indicated by the standard double-sonic-nozzle probe.

A question as to the possible effect of relative diffusion rates of different chemical species (into and out of the local macroscopic zone being sampled by the probe) on local mixture ratio and temperature has been raised but has not been evaluated. The correction of gas analyses (for percentage of water) to the proper N_2/H_2 ratio for ammonia tacitly assumes this effect to be negligible. This effect is nil for uniform distributions of temperature and mixture ratio in the chamber and is believed to be small for nonuniform distributions.

The effect of the evaporation and reaction of small drops of liquid on local temperature in the combustion chamber may be either to increase or to decrease the temperature of the gas, the magnitude of the effect being a function of local mixture ratio, as determined by gas-sample analysis, and of whether the drop is fuel or oxidizer. The temperature measured by the probe in a mixture of gas and liquid will be the temperature of the gas for conditions such that small liquid drops pass through both nozzles of the probe without evaporating. The evaporation and reaction of small drops of liquid which pass through the first nozzle and evaporate before passing through the second would decrease measured temperature. The evaporation of liquid between nozzles corresponding to 10 per cent of the mass flowing through the first nozzle would cause approximately 19 per cent reduction in measured temperature for no change in molecular weight, since for each critical flow nozzle, p is proportional to mass rate of flow of gas and T is proportional to p^2.

Fig. 3 shows the results of tests with the Enzian-type injector (no. 2), a cross-sectional view of which is shown at the bottom of the graph. All points are identified by test and bottle number (e.g., 269-21), circle points being temperatures shown at the left and square points being local mixture ratio shown at the right. Points are plotted as a function of radial position from the motor wall for pad positions 3, 2, 1, and 0; the points for over-all mixture ratios of approximately 1.4

[4] This extrapolation was made by H. Wise at this Laboratory.
[5] This work was carried out by H. Wise and M. Frech.

[6] The calculations were made by M. Goldsmith.

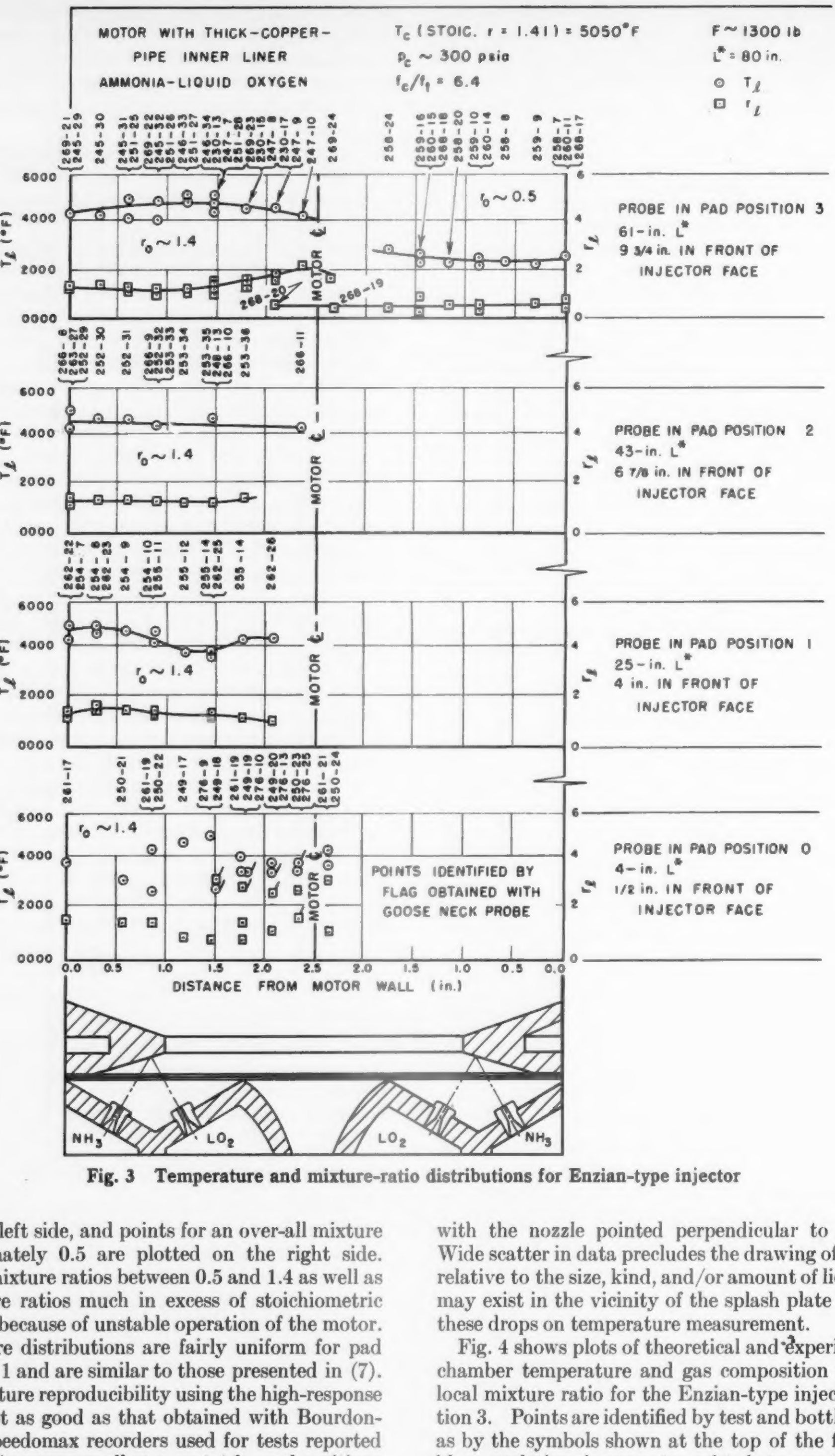

Fig. 3 Temperature and mixture-ratio distributions for Enzian-type injector

are plotted at the left side, and points for an over-all mixture ratio of approximately 0.5 are plotted on the right side. Tests at over-all mixture ratios between 0.5 and 1.4 as well as at over-all mixture ratios much in excess of stoichiometric were unsuccessful because of unstable operation of the motor. Radial temperature distributions are fairly uniform for pad positions 3, 2, and 1 and are similar to those presented in (7). However, temperature reproducibility using the high-response equipment was not as good as that obtained with Bourdon-tube gages and Speedomax recorders used for tests reported in (7). Variation in r_l was small at $r_o \sim 1.4$ for pad positions 3, 2, and 1, and at $r_o \sim 0.5$ for pad position 3. Variation in local mixture ratio and temperature was relatively large for pad position 0. The large variation in r_l may be explained by considering orientation of the probe nozzle (N_1) relative to the motion of assumed drops of liquid propellant in the vicinity of the splash plate. A test with a gooseneck probe wherein the probe nozzle was pointed toward the injector face showed somewhat different mixture ratio and temperature distribution from those obtained for a standard probe with the nozzle pointed perpendicular to the motor axis. Wide scatter in data precludes the drawing of firm conclusions relative to the size, kind, and/or amount of liquid drops which may exist in the vicinity of the splash plate and the effect of these drops on temperature measurement.

Fig. 4 shows plots of theoretical and experimental values of chamber temperature and gas composition as a function of local mixture ratio for the Enzian-type injector for pad position 3. Points are identified by test and bottle number as well as by the symbols shown at the top of the figure. Reasonable correlation is seen to exist between temperature and local mixture ratios, the best correlation occurring in regions near the nozzle where the combustion might be expected to be more nearly complete. Appreciable quantities of both free oxidizer and fuel were found only in the center of the motor near the injector (pad position 0) where incomplete combustion might be expected. The measured temperatures at low mixture ratios are higher than those calculated for chemical equilibrium; thus the higher theoretical values calculated using the assumption based on mixing stoichiometric products

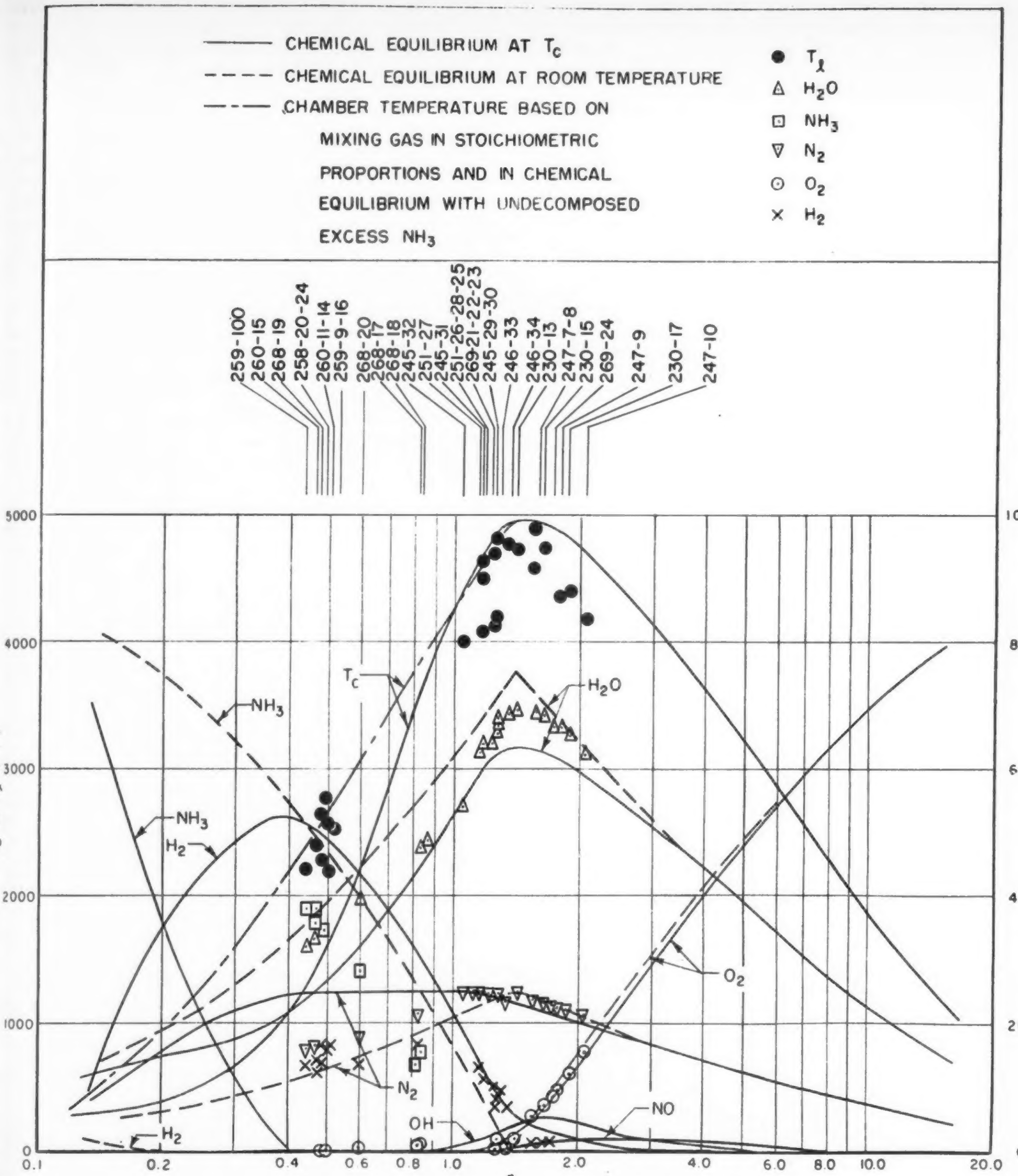

Fig. 4 Experimental values for pad position 3 (Enzian-type injector)

of combustion with undecomposed excess ammonia would seem to be more realistic. The presence of NH_3 in the gas samples in the proportions shown relative to the two theoretical curves of Fig. 4 offers supporting evidence for the validity of this assumption. In addition, consideration of the reaction-kinetic data mentioned would indicate that some such combustion process occurs at low mixture ratios, since calculated time required for homogeneous combustion at low temperatures (corresponding to $r_o \sim 0.5$) would suggest the use of motors of much greater L^* than those found necessary for good performance. Indeed, c^* performance obtained (cf. Fig. 8) shows performance values at $r_o \sim 0.5$ higher than those calculated for chemical-equilibrium conditions. Similar experimental performance results have been obtained, and similar assumptions have been made by other investigators and with other propellant systems. Unpublished data[7] obtained at this Laboratory show performance higher than theoretical based on chemical equilibrium for the ammonia-acid system at low mixture ratios. According to (14), evaluation of hydrazine as a monopropellant depends considerably on the assumptions made for the theoretical calculations. Calculations show large variation in performance as a function of percentage of decomposition of NH_3 (an intermediate in the decomposition of hydrazine). The results of all these investigations are consistent with the assumption and observation that the last step to occur is the endothermic decomposition of ammonia. Because of the absorption of heat in this step,

[7] This experimental work was done by R. B. Canright and Z. A. Typaldos at this Laboratory.

both temperature and c^* may fall to final equilibrium values.

Somewhat similar plots for the like-on-like injector (no. 1) are shown in Figs. 5, 6, and 7. Fig. 5 gives results of tests at 60-deg injector orientation and for pad positions 3, 2, and 1. The 60-deg injector orientation places the probe in line with the radial set of four jets, two oxidizer and two fuel, the other two radial sets each having four jets and spaced at 120-degree increments around the face of the injector. Fig. 6 shows results of tests at pad position 3 for r_o values from fuel-rich to oxidizer-rich and for angular injector orientations of 30 and 0 degrees relative to the probe.

It should be observed by way of comparing the results obtained with both injectors, (*a*) that the variation in r_l for a given r_o with the like-on-like injector is much greater for all pad positions and injector orientations than for the Enzian-type injector (with the exception of results in Fig. 6 at $r_o \sim 0.5$), and (*b*) that measured temperatures less than theoretical are associated with gas samples having appreciable percentages of unreacted propellant. In particular, the values may be compared for both injectors for pad position 3 at mixture ratios near stoichiometric.

Consideration of the relative data for the like-on-like injector at pad positions 3, 2, and 1 at $r_o \sim 1.4$ suggests that a slightly longer motor might permit complete chemical combination of the propellant as distributed, but that a considerable increase in length might be necessary before uniform mixture-ratio distribution could be attained.

The relative performance data for the two injectors shown in Fig. 8 are similar to those reported in (1) and (7) for $r_o \sim 1.4$. The Enzian-type injector gives c^* performance 95 per cent of theoretical based on chemical equilibrium, whereas the like-on-like injector gives performance 81 per cent of theoretical (for the 80-in. L^* motor). The performance for the like-on-like injector is somewhat lower than that reported previously (cf. Ref. 7), and temperature distributions are somewhat different. This variation is attributed to the fact that the injector face had to be replaced before this series of tests because of a burned spot. The burning was probably caused by leakage of oxygen around threads at the base of an orifice insert which became loose during operation. Replacement of the face apparently changed jet alignment. The relative values of performance for the two injectors change considerably at $r_o \sim 0.5$ from their values at $r_o \sim 1.4$. At $r_o \sim 0.5$ the performance for the like-on-like injector is equal to or slightly higher than that for the Enzian-type injector. Performance data for both injectors at $r_o \sim 0.5$ are higher than theoretical based on chemical equilibrium. Performance data for the like-on-like injector are also high at $r_o \sim 4.0$. Better performance, relative to theoretical, at mixture ratios far from (rather than at) stoichiometric seems

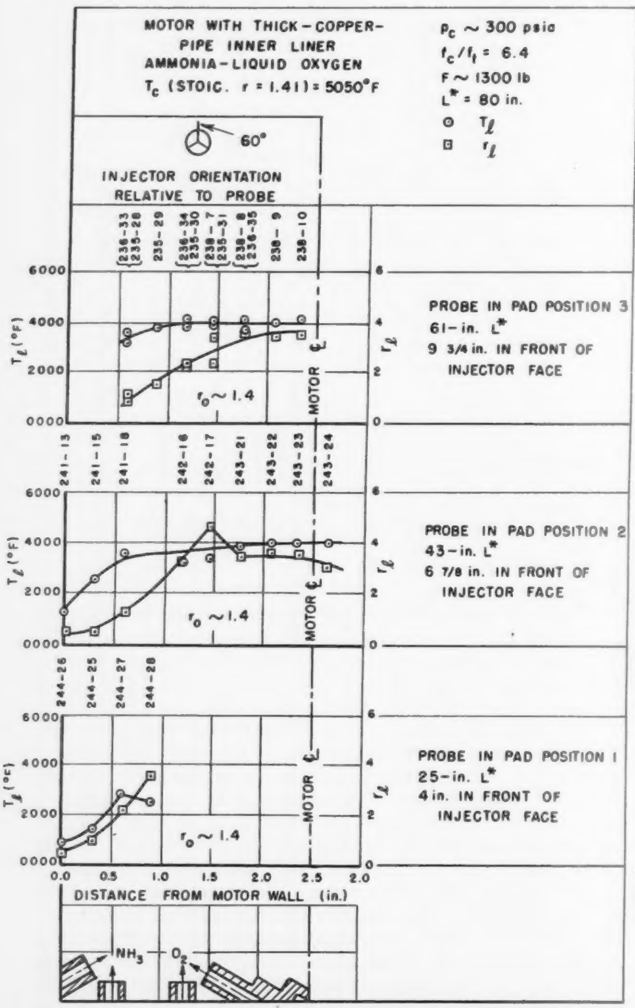

Fig. 5 Temperature and mixture-ratio distributions for like-on-like injector

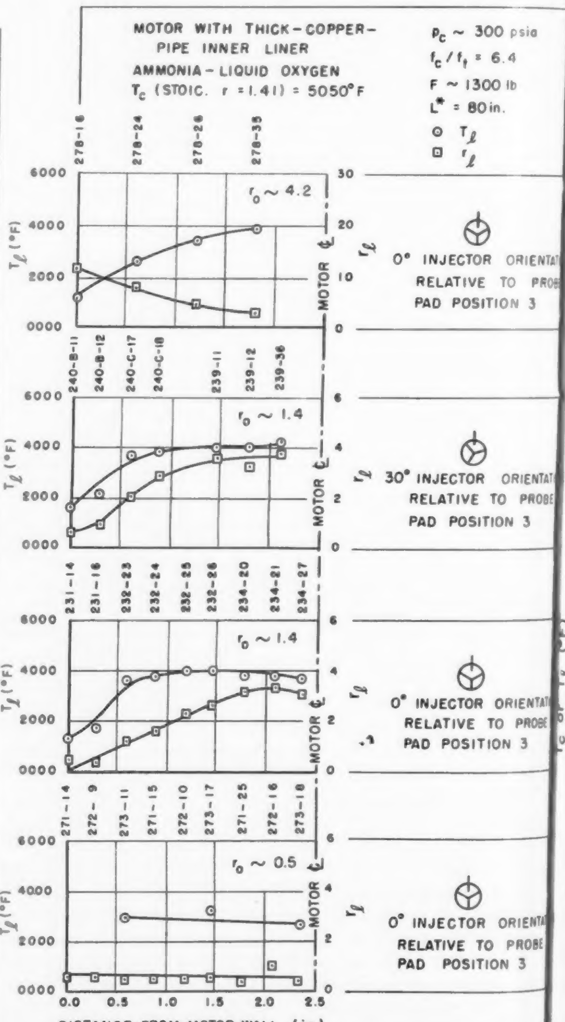

Fig. 6 Temperature and mixture-ratio distributions for various orientations of like-on-like injector

reasonable since more stringent mixing would be required at stoichiometric r for complete reaction. This variation in performance, together with apparent absence of combustion instability for all tests with the like-on-like injector, indicates that one criterion for injector design followed in (1)—i.e., good initial mixing of propellants—might well be modified for r_o values far from stoichiometric. Poor initial mixing may also be desired at times for propellant combinations and mixture ratios where the reaction kinetics are such that diffusion-type combustion is more rapid than homogeneous-type combustion.

4 Conclusions

The use of a pneumatic probe has been found to be of great value for the study of combustion in rocket motors. The ability to measure simultaneously the gas temperature and composition has permitted drawing useful conclusions concerning injectors and combustion processes.

A hypothesis, consistent with the data obtained in this program with available kinetic data and with the assumption in a few cases of nonadiabatic regions in the chamber, has been formulated regarding the combustion process in the oxygen-ammonia rocket motor: Fuel and oxidizer react in stoichiometric proportion, the products of reaction mix with the unreacted propellant, and the unreacted propellant may decompose, dependent on conditions. Coexistence of unreacted fuel and oxidizer was associated with low-temperature measurements, and the absence of such coexistence was associated with equilibrium temperatures, the quasi-equilibrium temperatures predicted for the partial completion of ammonia

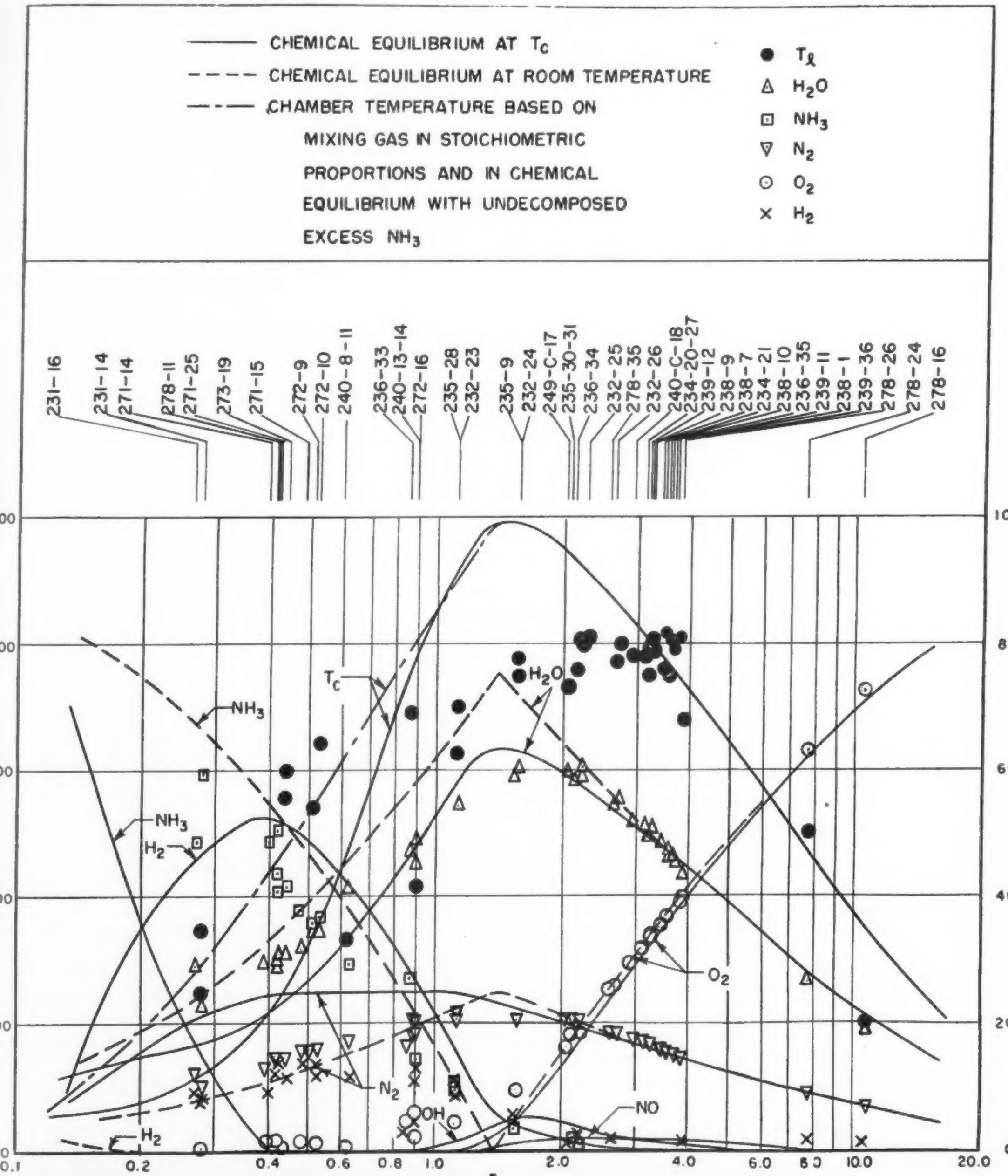

Fig. 7 Experimental values for pad position 3 (like-on-like injector)

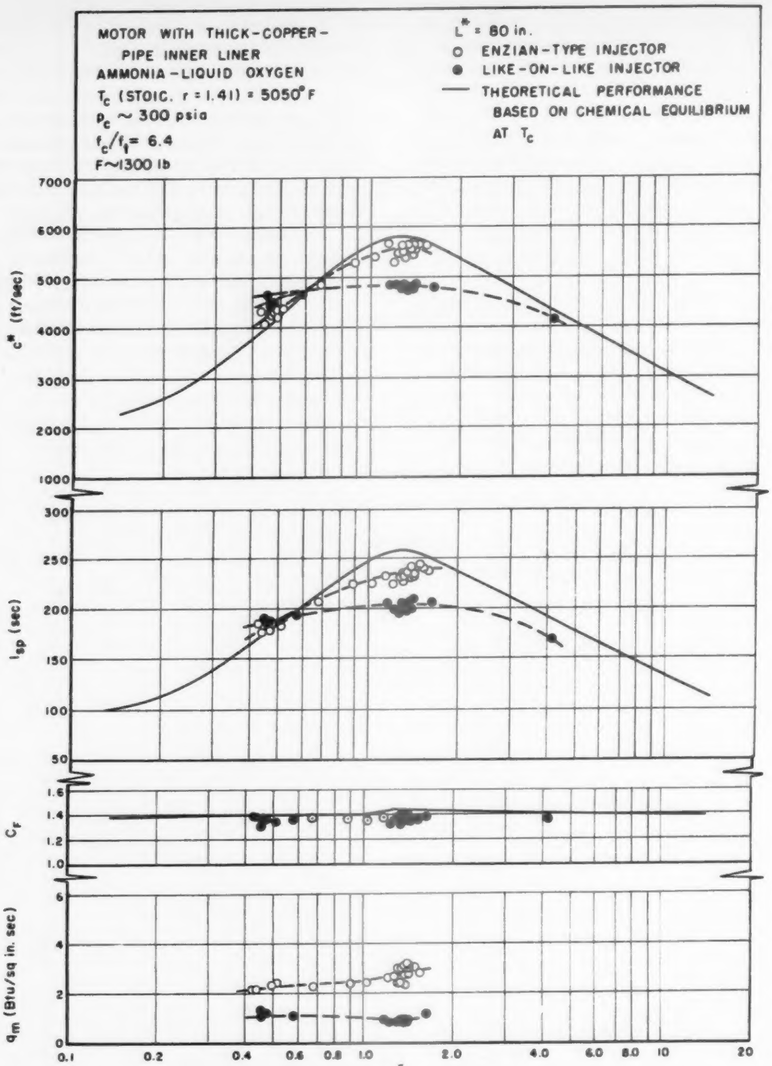

Fig. 8 Performance data for Enzian-type injector and like-on-like injector

decomposition, or nonadiabatic flame temperatures, dependent upon local mixture ratio.

Best rocket motor performance was measured under conditions of over-all mixture ratio near stoichiometric when there was small (if any) variation in local mixture ratio and when the reaction locally had gone to completion before the gases entered the exhaust nozzle. Low performance of the like-on-like injector at mixture ratios near stoichiometric is considered to be caused primarily by wide variation in local mixture ratio and secondarily by locally incomplete reaction.

APPENDIX

Construction and Use of the Pneumatic Thermometer and Gas-Sampling Probe

Construction

THE physical dimensions of a probe which was developed to measure temperature in a rocket motor combustion chamber and which was found to be satisfactory for use with the ammonia-oxygen system are given in Fig. 9. A schematic diagram of the heated line which was used to convey the sampled gases from the probe in the rocket motor to the manifold for the gas-sampling bottles in the control room is also shown. Alternate construction of the probe exit assembly, an alternate construction of the probe tip, and probe details are shown in Fig. 10.

The steps required for assembling the probe are as follows:

1 Helically wrap tubes A and B of Fig. 9 with 0.020-in.-diam copper spacing wire; silver-solder. (Use Handy and Harmon Easy-Flow silver solder.)

2 Silver-solder copper nozzle (N_1) having 0.041-in.-diam throat to tube A.

3 Heliarc tube D to tube B, drill tube B through tube D, and deburr inside of tube B after drilling (this hole is for coolant water).

4 Follow a step similar to step 3 for placing tube E on tube C.

5 Solder tube A to tube B, checking 0.050-in. end clearance between N_1 and the end of tube B. (Use single loops of 0.060-in.-diam wire as filler block between tubes.)

6 Solder tube C to N_1 and tube C to tube B. (Use minimum amount of solder to prevent plugging of coolant passages.)

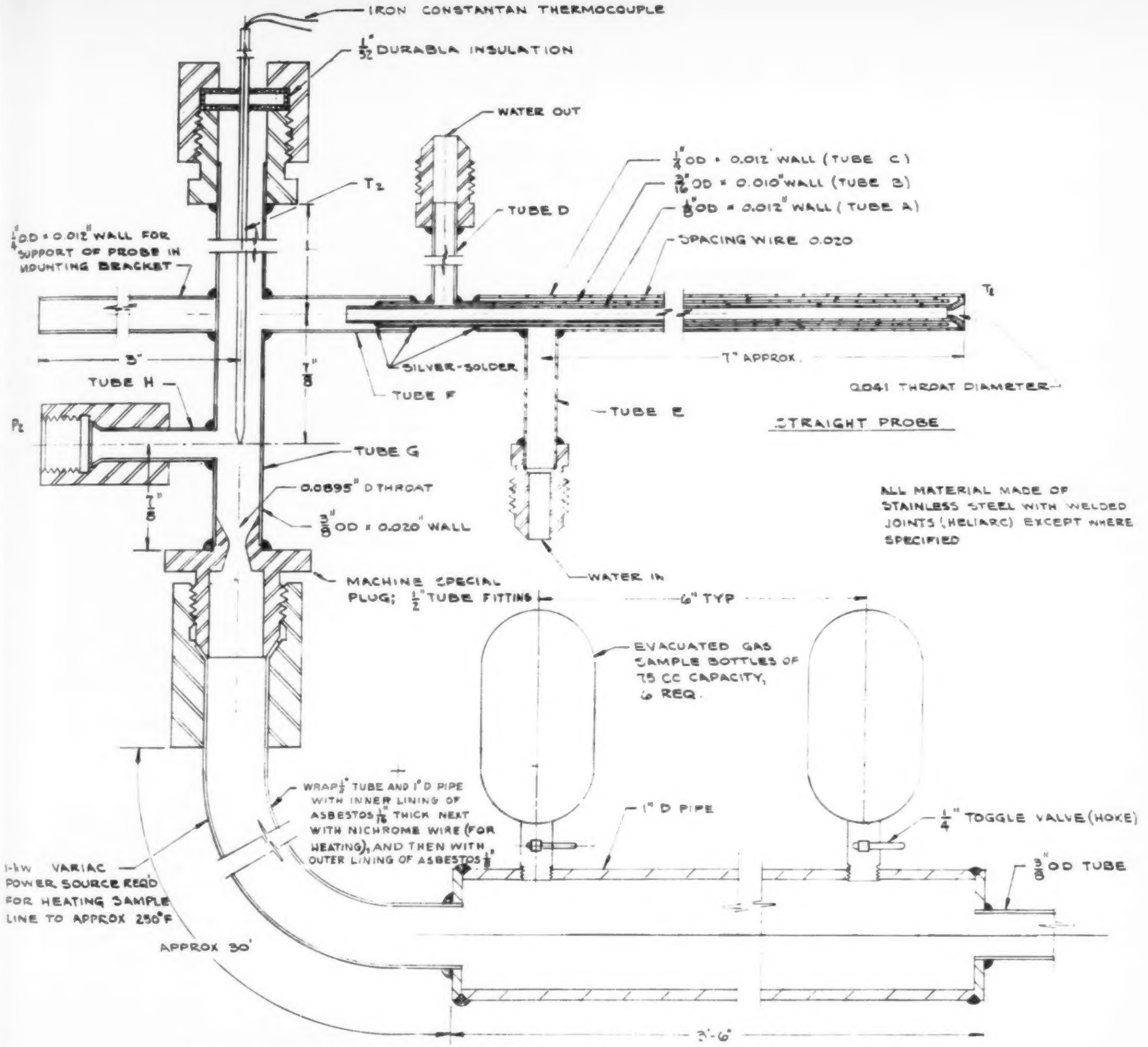

Fig. 9 Schematic diagram of standard double-sonic-nozzle probe and gas-sampling system

7 Leak-test by placing probe assembly under water. (Use 250-psi air pressure.)

8 Check water flow rate through probe with pressure drop of approximately 125 psi. (Flow rate should be between 0.10 and 0.13 lb/sec if coolant-water passages are unobstructed.)

9 Heliarc all joints connecting parts to tube G (cf. Fig. 10 for alternate construction of exit assembly).

10 Silver-solder tube F to tube B in a region which will be cooled by the cooling water.

11 Make bend in the alternate curved probe (cf. Fig. 10) as follows: Fill the coolant passageways and tube A with water, which is then frozen by submerging the probe in liquid nitrogen. The frozen water serves to hold the tubes in alignment while the bend is being made with a standard tube bender.

Use

It is difficult to formulate a general set of rules or limitations for the use of a probe in a rocket motor. Each installation should be evaluated by itself. The probe shown in Fig. 9 has been used successfully in a motor (contraction ratio of 6.4) with ammonia and liquid oxygen. Probes having other physical dimensions were also used successfully in the NH_3-liquid oxygen system. It should be emphasized that, in the use of the probe for rocket-motor development, relative values of temperature from point to point in the combustion chamber are of greater importance than are absolute values. The following precautions, information, and/or rules may be used as a guide either when changing the dimensions of the probe from those given in Figs. 9 and 10 or when applying the probe to another propellant combination:

1 Critical pressure must be maintained at the throat of both nozzles. Small dimensions of the probe, together with heat-transfer requirements at the high and variable temperatures involved, complicate the design of the probe for the criterion of critical pressure drop across each nozzle. Measurement of pressure downstream from the N_1 nozzle is difficult during tests of short duration and makes construction of the probe more complicated (cf. Ref. 1 for details). Theoretical analysis of pressure drop in the tube downstream from the N_1 nozzle is dependent on unknown properties of gases at high temperature and unknown pressure-recovery factors of the sonic jet issuing from N_1 nozzle. Static-pressure measurements for several tests show that pressure drop from a region immediately downstream from N_1 nozzle to a region upstream

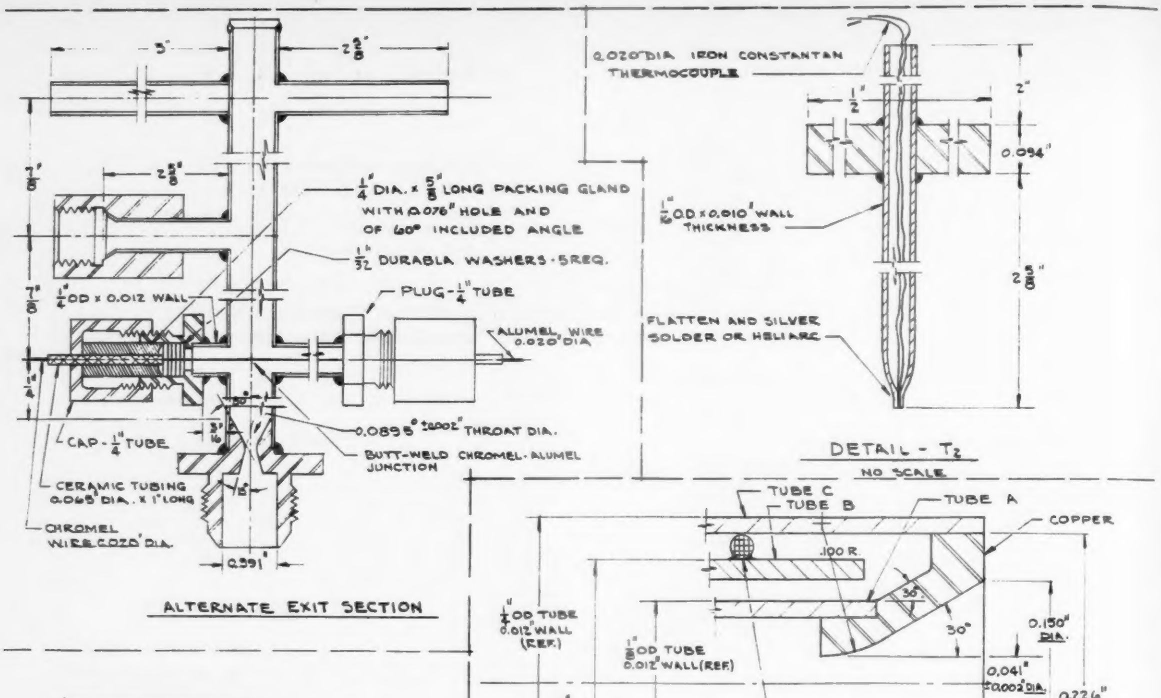

Fig. 10 Alternate designs and details of probe

from N_2 nozzle is less for high-temperature gas flow through the probe than for room-temperature nitrogen gas flow through the probe. [Using a probe having N_1 nozzle throat diam of 0.041 in. and N_2 nozzle throat diam of 0.0895 in. during calibration tests with room-temperature nitrogen at p_c = 300 psia, the pressure drop was approximately 3 psi, whereas for N_1 = 0.051 in., the pressure drop was approximately 13 psi. This result suggests the general criterion that critical flow will be obtained through each nozzle for probes designed such that the calibration constant with nitrogen gas $(p_2/p_c)^2$ is equal to $(CA_1/CA_2)^2$.]

2 T_2 temperature must be high enough to prevent condensation of any component. On the other hand, it must not exceed temperature limitations of the T_2 thermocouple or of the probe construction materials employed. It was found that for tests with gasoline-liquid oxygen the N_1 nozzle throat diam had to be reduced to 0.031 in. in order to reduce T_2 temperatures to less than 1000 F. The high T_2 temperatures during initial tests of gasoline-liquid oxygen with standard probe (N_1 throat diam = 0.041 in.) was attributed to a deposit of carbon on the cold walls of the probe, which caused a reduction in heat transfer from gas to cooling water.

3 A change in dimensions of the nozzle during test or during calibration caused by erosion or by deposits may be encountered under certain circumstances. A small change in diameter can cause a large error in measured temperature since T is a function of diameter to the fourth power. After a successful test with a probe having a 0.051-in. N_1 nozzle throat diameter in an ammonia-nitric acid (7% NO_2) motor, it was found that a deposit of ammonium nitrate had completely plugged the N_1 nozzle. Similar plugging of the N_1 nozzle after a test, and perhaps to a certain extent during a test, was found in tests of gasoline-liquid oxygen with the probe in a fuel-rich region.

4 For any given application, practical changes in the probe characteristics may be effected, p_2 being controlled by varying N_2 and T_2 by varying either N_1 throat diam or the length of the cooled portion of the probe. Great care should be exercised when considering the use of N_1 throat diam much greater than 0.051 in.

References

1 "Combustion Studies of Ammonia-Oxygen Rocket Motors Using a Temperature-Measuring Probe," by Dwight I. Baker, Progress Rep. no. 24-1, JPL, California Institute of Technology, Pasadena, October 21, 1952.

2 "Radio-Frequency Mass Spectrometer for Use in Analysis of Gas Mixtures," by Bertram Keilin, Progress Rep. no. 24-3, JPL, California Institute of Technology, Pasadena, March 4, 1952.

3 "An Improved Radio-Frequency Mass Spectrometer and a New Method for Interpreting Data," by Bertram Keilin, Progress Rep. no. 24-4, JPL, California Institute of Technology, Pasadena, November 25, 1952.

4 P. L. Blackshear, Jr., NACA TN no. 2167, September 1950.

(*Continued on page 234*)

A Combustor Analysis Method Evolved from Basic Flame Stability and Fuel Distribution Research

JOHN W. BJERKLIE[1]

Marquardt Aircraft Company, Van Nuys, Calif.

A method has been devised for aiding the development of ramjet and afterburner combustors which utilize a gutter-type flame holder and a fuel injection system located upstream of the flame holder. The fuel-air ratio range over which a flame holder will stably hold flame is determined from results of applied research into the field of flame holding on bluff bodies in moving air streams. The fuel-air ratio supplied to a flame holder is determined from results of applied research into the field of fuel injection and diffusion in a moving air stream. The relation between the local fuel-air ratio on the flame holder and flame limits of the flame holder is discussed. Methods of adapting the research results to nonideal systems are presented. The analysis is applied to combustion instability, lean and rich engine blowout, and combustion efficiency. This leads to a system for initial design of a burner and for analysis and improvement of an existing burner.

Nomenclature

A = flame holder area
A = duct across section open area
A = area through which fuel is diffusing
D = diffusion coefficient
D_e = equivalent flame holder diameter
e = base of natural logarithm
f/a = fuel-air ratio
h = width of gutter-type flame holder
P = wetted perimeter
P = air static pressure
r = radial distance
R = radial distance from injection point streamline
t = time
T = air static temperature
u = air velocity
w = mass
W_a' = rate of air flow per unit area at the station of interest, lb/sec/ft²
W_f = rate of fuel flow from a nozzle, lb/sec
X = axial distance between injection point and point of interest
μ = air viscosity

Introduction

UNTIL recently most development groups for high heat release burner systems have based a good share of their work on cut-and-try methods. The results have been encouraging enough to start a rapidly growing industry in turbojets, afterburners, rockets, and ramjets, but all the problems have not been solved nor even foreseen or evaluated. However, the results of basic research, initiated upon the advent of these burner systems, are beginning to supersede the cut-and-try methods of development.

The research results are being incorporated into development procedures in some fields of combustion as rapidly as possible. Even in these fields cut-and-try methods have not been eliminated, but development time has been significantly shortened.

Work in the field of flame holding has been done by DeZubay (1),[2] Longwell, et al. (2), Scurlock (3), and others. Flame holders in the shape of cylindrical rods, disks, and bodies of revolution have all been tested.

Most of the applicable work in fuel distribution has been done by Longwell, et al. (4). However, some theoretical work using principles of turbulent diffusion has been done by Beeton (5).

Of the various investigations mentioned, those by E. A. DeZubay and J. P. Longwell showed the most promise for being applied to ramjet and afterburner combustors. DeZubay's work was concerned with the stability limits of a disk type of flame holder immersed in a flowing stream of a prepared fuel-air mixture (1). Longwell's related work was concerned with preparation of the combustible mixture (4).

The typical burner system for the analysis method about to be described is illustrated in Fig. 1. Fundamentally the

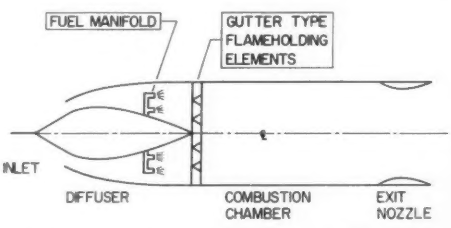

Fig. 1 Typical burner considered in this paper

burner consists of an approach duct, a fuel injection manifold, a gutter-type flame holder, and a combustion chamber. The fuel is injected, mixed with air, and fed to the flame holder. The flame holders then supply the flame source for the combustion that takes place aft of the flame holder in the combustion chamber. The primary concern of this paper is with the region from the fuel manifold to just past the flame holders.

Actual burner systems seldom have uniform velocity distribution across the duct, or straight-walled ducts, etc., as were used in testing for flame holding limits and fuel diffusion. Hence adaptations of both research results were necessary. The full-scale geometry might include changing-area ducts, turning ducts, changing-shape ducts, unsymmetrical ducts, and unsymmetrical and noncoplanar flame holders and fuel manifolds. Actual flow conditions may include pressures and temperatures not in the tested range, and nonuniform profiles for velocity, temperature, and pressure. Emphasis will be laid upon these adaptations in this paper.

Stability Considerations

Reference 1 reports the results of DeZubay's flame holder stability studies. His method of attack was twofold, being theoretical as well as experimental. The theoretical approach

Received August 10, 1954.
[1] Engineer, Thermodynamics Section.
[2] Numbers in parentheses indicate References at end of paper.

tells essentially the type of relation to be expected for the limits of stable flame holding of a bluff body. The model for analysis is pictured in Fig. 2. The experimental approach

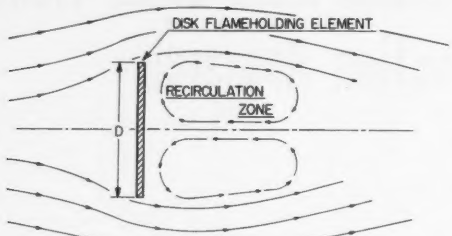

Fig. 2 DeZubay's flame holder model showing air flow

then determined the empirical relation of the type expected. The range of variables tested was quite large. Velocity varied from 40 to 550 fps. The pressure at the flame holder edge varied from 3 to 15 psia. The disk sizes used were 0.25, 0.50, and 1.00 in. in diam. Fuel-air ratio for the premixed gases was varied from lean blowout to rich blowout of the disk-type flame holder. The final relation between blowout fuel-air ratio and the other variables is the curve shown in Fig. 3.

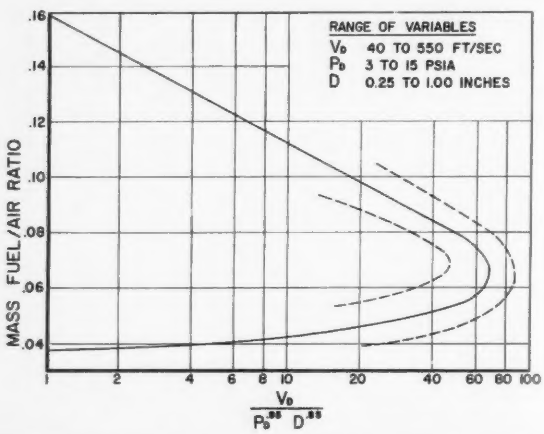

Fig. 3 Correlation of blowout limits for flame holder of Fig. 2. Uniform vapor phase propane-air mixture, velocity from 40 to 550 fps, disk size from 0.25 to 1.00 in., pressure from 3 to 15 psia

DeZubay's curve shows over what range of uniform propane-air mixture ratio flame can be stabilized on the flame holder for any value of the stability parameter $(u/P^{\cdot 95}D_e^{\cdot 85})$. This can be represented by the relation

$$(f/a)_{\text{blowout}} = f\left(\frac{u}{P_D^{0\cdot 95}D_e^{0\cdot 85}}\right) \qquad [1]$$

It should be noted that all testing was done with gaseous propane-air mixtures at a temperature of 550 R.

To apply this stability parameter to development work, it had to be adjusted for other fuels and flame holder shapes besides those tested. The stability curve as found for propane was assumed to hold for all other hydrocarbon fuels in normal use. Full-scale testing showed that this assumption was valid.

The disk diameter term was replaced by another term which would introduce a flame holder shape effect. This term was the hydraulic diameter

$$D_e = \frac{4A}{P} \qquad [2]$$

where

A = area of the flame holder
P = wetted perimeter of the flame holder

Thus, for a gutter-type flame holder

$$D_e = 2h \qquad [3]$$

and for a gutter having a long extension on one side parallel to the flow, $D_e = 4h$, where h is the width across the gutter. Experience has shown that on a gross basis the hydraulic diameter is applicable. The actual cases encountered in practice so far would not allow absolute confirmation of the correctness of the term. Since DeZubay did all his testing at 550 R, a temperature correction term for other temperatures had to be established. DeZubay showed that the limits should depend upon $(T\mu)$ as well as the other variables u, P, D. $(T\mu)$ can be considered to vary as $T^{1.76}$ for temperatures up to 1000 R. Thus, the temperature correction hypothesized is $(550/T)^{1.76}$. Available engine blowout data indicate the correction to be $(550/T)^{1.5}$. The latter term checks the original theory to some extent and is more conservative and so is generally used. The parameter accepted then is $\dfrac{u}{P_D^{0\cdot 95}D_e^{0\cdot 85}}(550/T)^{1.5}$.

The application of the stability work to nonuniform flow conditions consists of finding the local stability parameter and fuel-air ratio for all parts of the flame holder. The velocity profile at the flame holder can be determined from total pressure, static pressure, and static temperature measurements. The static pressure and temperature are usually assumed to be constant across the flow field, thus simplifying the instrumentation required. This is enough information to determine the local stability parameter for all parts of the flame holder. The local fuel-air ratio limits along the flame holder elements can then be read from DeZubay's curve.

Whether or not any portion of the flame holder is holding flame is then determined by comparing the actual local fuel-air ratio with the local fuel-air ratio limits. Here it is considered that the portion of the stream affecting the flame holder is that which extends $^1/_4$ in. laterally outward into the stream from the flame holder lip. The effect of droplets and droplet collection on the flame holder will not be considered here.

Fuel Distribution Considerations

a Basic Point Source Equation

Reference 4 reports the work done by Longwell, et al., in theoretical and experimental determination of the fuel distribution from various nozzles injecting fuel into various air streams. Their determinations show that the basic differential equations hypothesized for fuel spreading holds substantially well if the fuel spreading constant (diffusion coefficient) is properly determined. Experimental work of considerable extent has been undertaken to determine the diffusion coefficient for various conditions.

The basic differential equation is from (4)

$$\frac{\partial w}{\partial t} = -DA\frac{\partial f/a}{\partial r} \qquad [4]$$

This states that the rate of mass transport is proportional to the fuel concentration gradient and the area for diffusion.

The differential equation was solved as shown in (4). If all the fuel issues from a point with no initial velocity, the point source equation applies:

$$f/a = \frac{W_f}{\pi W_a'}\frac{u}{4DX}e^{-(u/4DX)R^2} \qquad [5]$$

This means that the fuel-air ratio at any point is the peak fuel-air ratio reduced by a factor depending upon distance from the peak and upon a fuel spreading term. Fig. 4 shows a

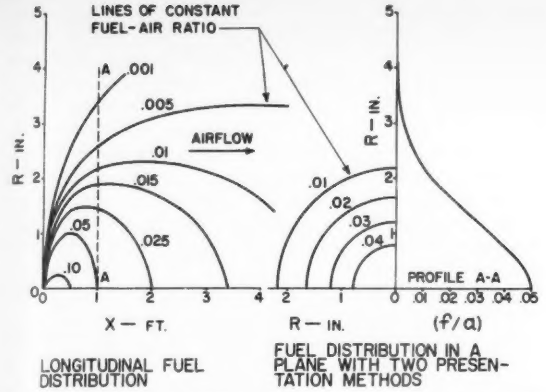

Fig. 4 Calculated fuel distribution from a point source showing lines of equal fuel-air ratio and a profile

$u/D = 200$. R, X, and f/a are the same as in the point source equation.

schematic of a point scource with its accompanying fuel distribution. Fig. 5 depicts the coordinate system and relation between flame holder and injection point.

The point source equation can be integrated over any desired source shape to get the fuel distribution equation for that source shape. The integration for two source shapes other than the point source is presented in (4). The point source equation will be used throughout this paper since it shows the basic relations desired and it is easy to use.

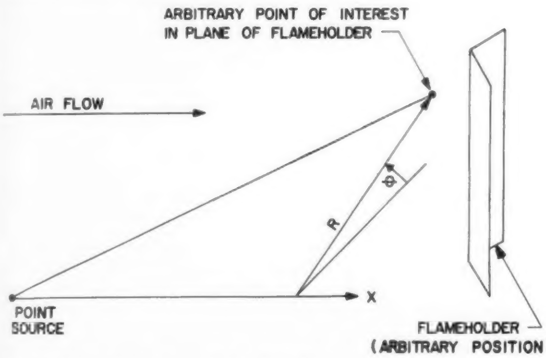

Fig. 5 Coordinate system for fuel diffusing from a point source showing relation between flame holder and injection point

Actually, in application, D becomes a catch-all for many factors, such as the initial longitudinal velocity of the fuel, the state of fuel, induced turbulence due to duct wall and fuel manifold, turbulence due to combustion, etc. Longwell, et al., made quite a complete study of the variation of D with several factors. It was found that u/D remained substantially constant for completely vaporized fuel, while D remained constant for completely liquid fuel. Duct size and gas pressure had little effect on D.

b Use of the Point Source Equation

To apply the methods of fuel distribution to practical systems, it was necessary to find a quick method of plotting and to establish usable diffusion coefficients. Also, initial spreading had to be considered.

The first approximation made is that, for most problems encountered, the point source equation applies. This allows reduction of fuel distribution calculation to graphical or slide-rule techniques.

The fuel distribution calculations can be presented in many ways, but the profile method is one of the most useful. Here, the fuel distribution is calculated along a suitable number of straight lines in the cross-sectional plane of interest.

The fuel-air ratio contribution of one nozzle to any point in the plane of interest can be calculated directly from the point source equation [5].

If $\ln(f/a)$ is plotted vs. R^2, the result is a straight line. From Equation [5] for $R = 0$, the peak value is

$$(f/a)_{\text{peak}} = \frac{W_f}{\pi W_a'} \frac{u}{4DX} \qquad [6]$$

and the slope is

$$\frac{\partial \ln(f/a)}{\partial R^2} = -\frac{u}{4DX} \qquad [6a]$$

The fuel-air ratio for any R, measured from the source streamline, can then be read directly. This plot is shown in Fig. 6.

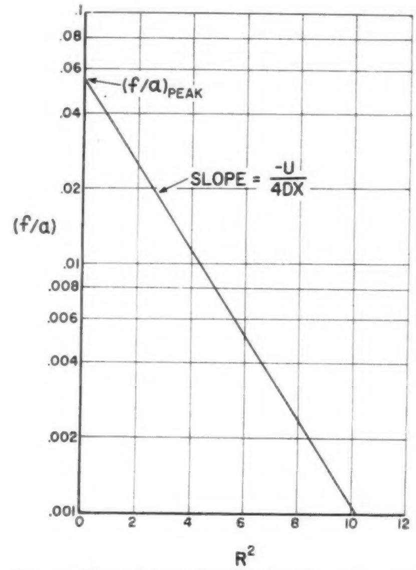

Fig. 6 Plot of fuel distribution from a point source represented on a semilogarithmic plot

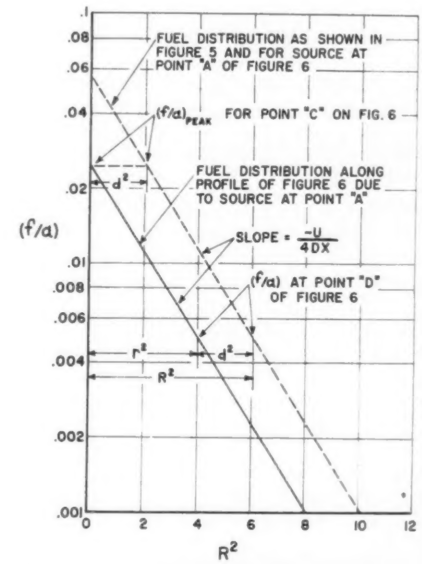

Fig. 6a Plot of fuel distribution from a point source along a line displaced from the source streamline by the perpendicular distance, d

NOTE: "Figure 5" and "Figure 6" indicated on chart should read Figure 6 and Figure 7, respectively.

c Fuel Distribution Profile Calculation

For a uniform velocity distribution, a simple procedure can be used to find the fuel distribution contribution along any profile in a plane perpendicular to the flow, whether or not the nozzle streamline intersects the profile. The radius term in the equation can be divided into two parts: the perpendicular length (d), from the axis of the point source to the profile line, and the distance (r), from this point on the profile to any other point on the profile, Fig. 7. In this figure the profile is being

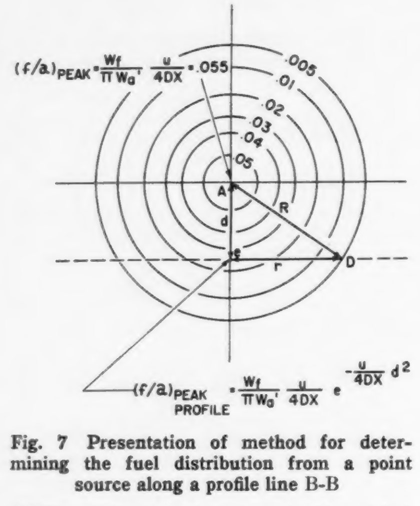

Fig. 7 Presentation of method for determining the fuel distribution from a point source along a profile line B-B

NOTE: "e" indicated on chart should read "c"

found along the line B-B due to the source at A. The point source equation becomes

$$f/a = \frac{W_f}{\pi W_a'} \frac{u}{4DX} e^{-(u/4DX)(d^2 + r^2)} \quad \text{[7]}$$

where

$$R^2 = d^2 + r^2 \quad \text{[8]}$$

from the Pythagorean theorem.

This means that the peak fuel-air ratio at A is reduced to a value at point C by the factor $e^{-(u/4DX)d^2}$ and the fuel-air ratio at C is reduced along the profile by the factor $e^{-(u/4DX)r^2}$. Equation [7] can be written as

$$f/a = \frac{W_f}{\pi W_a'} \frac{u}{4DX} e^{-(u/4DX)d^2} e^{-(u/4DX)r^2} \quad \text{[9]}$$

For the peak fuel-air ratio contribution from the nozzle at A to the profile at point C, where $r = 0$, is

$$(f/a)_{\substack{\text{peak}\\ \text{profile}}} = \frac{W_f}{\pi W_a'} \frac{u}{4DX} e^{-(u/4DX)d^2} \quad \text{[10]}$$

This can be read directly from the original point source graph for $R^2 = d^2$ as shown in Fig. 6. The profile contribution as shown in Fig. 6a will be a straight line parallel to the original line with a peak as indicated above. The fuel-air ratio at point D on Fig. 7 is indicated in Figs. 6 and 6a. To employ Fig. 6a for the fuel contribution of the nozzle at A to the profile, the abscissa is now read as r^2. The contributions of any number of nozzles to the one profile can be found and then added up to give the final profile.

d Adaptation to Velocity Profile

The effect of a velocity profile upon fuel distribution can be of great importance, so Longwell's equations were adapted accordingly. A velocity profile determines the effective position of a source in the plane of interest and the amount of spreading allowed up to the plane of interest. The effective positions of the sources can be estimated by knowing at least two mass flow profiles in the vicinity of the fuel mixing region. The "effective streamline" of the nozzle is assumed to be a longitudinal line on a surface, which includes the nozzle and is concentric with the flow axis that separates the mass flow in the same proportion at all axial positions as it does at the nozzle station. If only two profiles are known, the velocity is assumed to vary linearly from one axial position to the next. If more velocity profiles are known, more accurate estimations of effective streamline positions can be made. Such a procedure also allows determination of value of u to be used in the equation.

The effect of a velocity profile upon spreading is readily calculated if u and D are known, since the basic partial differential equation still holds. If the existing velocity profile is considered to be approximated by any arbitrary number of uniform velocity parts, as in Fig. 8, where only a two-part approximation is shown, at any boundary between parts the fuel-air ratio must be single-valued and the rate of mass spreading must be single-valued. The flow properties are averaged out in each division. Each increment of velocity profile is then considered to have its own fuel-spreading rate.

The easiest way to consider this problem is to think of each part of the air flow being supplied by a fictitious source that can be related ultimately to the real source. One real source and one fictitious source are shown in Fig. 8. The relation

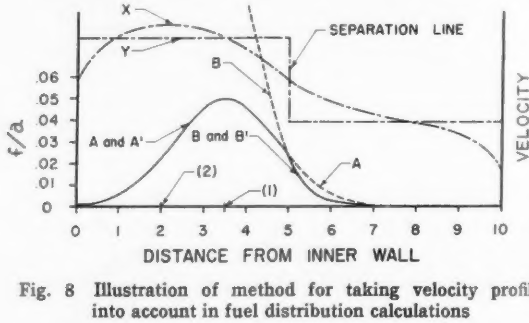

Fig. 8 Illustration of method for taking velocity profile into account in fuel distribution calculations

u/D = 200; A = f/a profile due to nozzle (1), real source, no velocity correction; B = profile due to fictitious nozzle, no velocity correction; A′ = portion of profile A in adjusted f/a distribution; B′ = portion of profile B in adjusted f/a distribution; (1) = nozzle (1), real source, streamline position; (2) = nozzle (2), fictitious source, streamline position; X = actual velocity profile; Y = approximated velocity profile for fuel distribution calculations.

can as easily be carried from one part to the other by relating fictitious nozzle to fictitious nozzle. Writing the fundamental equation for parts 1 and 2 of the velocity profile in Fig. 8, we have

$$\left(\frac{\partial w}{\partial t}\right)_1 = -D_1A_1\left(\frac{\partial f/a}{\partial R}\right)_1 \qquad \text{for part 1} \quad \text{[4a]}$$

and

$$\left(\frac{\partial w}{\partial t}\right)_2 = -D_2A_2\left(\frac{\partial f/a}{\partial R}\right)_2 \qquad \text{for part 2} \quad \text{[4b]}$$

Then the relation

$$D_1\left(\frac{\partial f/a}{\partial R}\right)_1 = D_2\left(\frac{\partial f/a}{\partial R}\right)_2 \quad \text{[11]}$$

must hold since

$$\left(\frac{\partial w}{\partial t}\right)_1 \equiv \left(\frac{\partial w}{\partial t}\right)_2 \quad \text{[12]}$$

at the boundary between parts 1 and 2.

Differentiation of the point source equation, Equation [5] and substitution into Equation [11] leads to the relation

$$D_1 \left(\frac{f}{a}\right)_1 \left(-2R_1' \frac{u_1}{4DX}\right) = D_2 \left(\frac{f}{a}\right)_2 \left(-2R_2' \frac{u_2}{4D_2X}\right) \quad \text{[13]}$$

Then at the boundary between parts 1 and 2

$$D_1R_1' \frac{u_1}{4D_1X} = D_2R_2' \frac{u_2}{4D_2X} \quad \text{[14]}$$

where the primed R's denote radial distances from the boundary to the sources. Fig. 8 shows the real source and the fictitious source for part 2 along with the associated source position and peak values. The profile for the real source, (A) of Fig. 8, is to be used only up to the boundary line of its particular segment 1 of the velocity profile. The profile for the fictitious source (B) is likewise to be used in its particular part of the profile 2 only. The parts to be used in Fig. 8 are shown as solid lines, A′ and B′. Equation [14] and Equation [11] can be used to relate fuel-air ratio gradients at the boundary being considered. The peak values and rates of spreading of the two nozzles can also be related by substituting back into the point source equation the $u/4DX$ and R relations determined above. The fictitious source position (R_2') can be found from Equation [14]. Now the peak f/a for the fictitious source for part 2 can be determined, since at the boundary

$$(f/a)_{\text{boundary}} = (f/a)_{\text{peak}_1}\, e^{-(u_1/4D_1X)R_1'^2} = (f/a)_{\text{peak}_2}\, e^{-(u_2/4D_2X)R_2'^2} \quad \text{[15]}$$

Thus, substituting for R_2'

$$(f/a)_{\text{peak}_2} = (f/a)_{\text{peak}_1}\, e^{-\left[1 - \left(\frac{D_1}{D_2}\right)^2 \frac{(u_1/4D_1X)}{(u_2/4D_2X)}\right] \frac{u_1}{4D_1X} R_1'^2} \quad \text{[16]}$$

The fuel-air ratio gradients in the two parts can therefore be determined if D_1 and D_2 are known. D_1 and D_2 are known if the variation of D with u is known and if u is known. The fuel-air ratio at the boundary depends upon the rate of spreading from the nozzle and can be calculated from the fuel distribution equations of part 1. The fuel distribution in part 2 can then be found with the fictitious source related to the source of part 1 by the above equations. The $u/4DX$ of the second source corresponds to the relation of u to D which is being used. The fuel distribution of Fig. 8 was calculated for constant u/D. The real source and the first fictitious source positions and fuel distribution profiles are given on the figure. If the velocity profile is divided into a large number of parts, the solution can be very accurate. A comparatively small number of parts usually gives results with good engineering accuracy.

A short-cut method may be used with reasonable accuracy. Here the profile is divided into as many parts as there are radial positions of sources, the divisions being made linearly half-way between the source streamline. A sketch of the procedure is shown in Fig. 9. The fuel distribution from one source, for instance, source 1 of Fig. 9, is then calculated as if the whole field were the same as that of the part in which the source is located, as per profile A on Fig. 9. This introduces an error whenever the fuel from a nozzle extends significantly into an adjacent part of the flow field. The contributions are then added directly. There tends to be compensation all along the profile for the error cited so that reasonable accuracy can be achieved for any but the most nonuniform velocity profiles.

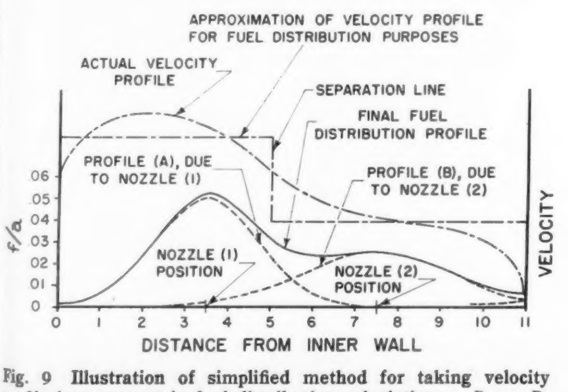

Fig. 9 Illustration of simplified method for taking velocity profile into account in fuel distribution calculations. $D_1 = D_2$

e Experimental Diffusion Coefficient Determination

In the course of analyzing full-scale engine data, a method for the experimental determination of D was developed, making use of measured velocity and fuel-air ratio profiles.

The process of finding diffusion coefficients is simple in concept but tedious in practice. One of the ways to approach the problem is to assume that the point source equation applies to the measured fuel distribution resulting from injection of fuel from an array of nozzles.

If several simultaneous fuel-air ratio values in the duct are known accurately, and if the flow conditions are known reasonably well, the diffusion coefficients can be found. The solution is based on the assumption that a given nozzle has only one basic diffusion coefficient over the whole plane being considered. The problems are considerably reduced in practical applications because usually the significant contributing sources to a point of known fuel-air ratio are few in number. Furthermore, several contributing nozzles may normally be expected to have the same diffusion coefficient. If one combination of diffusion coefficients can be found that allows simultaneous calculation of all the known fuel-air ratio values, the problem is solved, for the solution will be unique. The combination of D's can be found either graphically or analytically, but graphical solutions have proved to be most expedient. The crux of the problem for graphical solution is to hold the D's constant for all nozzles except one, and plot a curve of contributions at the points of known f/a as a function of D from the one nozzle. Then allow the D's of the other nozzles to vary and draw similar curves of contribution vs. D. Study of these curves should then reveal which set of diffusion coefficients will most closely allow all points of known f/a to be matched.

The D's found this way have the initial spreading pattern effect included in them. This fact disallows use of the same D's at any value of X significantly different from the one for which the D's were found. Also, air flow and fuel flow variations for a situation requiring use of the D's must, strictly speaking, be in the same range for which the D's were found.

A more nearly exact analysis would be one in which effective source sizes for such shapes as ring sources or disk sources were found in addition to the diffusion coefficient. It is beyond the scope of this paper to consider such effects in detail, however. Suffice it to say that the measured velocity and fuel-air ratio profiles enable the calculation of diffusion coefficients, the accuracy and usefulness of which depend upon the assumptions made.

Summary

Burner development requires that several characteristics be determined for all operating conditions. Among these are burner fuel-air ratio operating limits at various air flow conditions, combustion stability, and combustion efficiency. These characteristics can be studied closely if the flame holder stability and fuel distribution at all of the burner operating conditions are known.

The fuel distribution techniques which have been described

(Continued on page 234)

Proposed Geodetic Triangulation From an Unmanned Orbital Vehicle by Means of Satellite Search Technique

CLYDE W. TOMBAUGH[1]

Flight Determination Laboratory, White Sands Proving Ground, Las Cruces, N. Mex.

The origin and basis for the search for small natural satellites of the Earth are presented briefly. Next, the fundamental principles and general strategy of the satellite search is described. The three most important features are: (1) An equatorially mounted Schmidt or other fast camera of wide field is driven at a rate to conform with the apparent angular speed of an object across the sky for a given distance. (2) A great many concentric zones are required to avoid excessive magnitude losses from differential drift rates. (3) A small offset in declination is performed near midexposure to create a confirmatory image. With some modification in the declination offset technique, and precisely triggered by radio, it is seen how the satellite search technique could be used for very accurate geodetic triangulation.

IN 1943, a colleague, Mr. Henry Giclas, and I at the Lowell Observatory in Flagstaff, Ariz., attempted to recover the lost asteroid, Adonis. It is one of a dozen discovered whose orbits cross the Earth's orbit. It was expected to be very faint, and its probable position was so poorly known that a fairly large section of the sky had to be explored. At the time, its expected motion thru the starfield was considered fairly rapid (but slow compared to driving rates used in the satellite search today). This was accomplished by frequent resetting of the guiding micrometer thread on a field star in the guide telescope at a rate to conform with the expected apparent motion of the asteroid. The lost asteroid was not found, but it turned my thoughts to the problem of tracking hypothetical bodies at much greater angular speeds.

By 1952, the concept had crystallized into a plan for searching out small satellites of the Earth, if any existed. Under special circumstances, there was the possibility that the Earth with the mechanical aid of the Moon could have captured a few tiny asteroids which cross the Earth-Moon orbit, like Adonis does. Or, there may yet exist some unswept debris from the birth-of-the-Moon process. Because of the rapid angular rates such possible bodies must have in revolving around the Earth, their trails would be too diluted to cross the threshold sensitivity of astronomical plates taken in the usual manner.

Paradoxically, the regions nearest the Earth were virgin fields for exploration. Accordingly, I prepared a 25-page project proposal on how such a search could be conducted, and submitted it to the Office of Ordnance Research, U. S. Army, for their consideration. It was reviewed and approved by OOR. The project was actually started in December 1953, using some of the facilities of the Lowell Observatory at Flagstaff, Ariz.

The basic principle of the Satellite Search is to drive an equatorially mounted Schmidt or other fast camera of wide field at a rate to conform with the apparent angular speed across the sky. The image of any such hypothetical body would be concentrated to a point image or a very short trail. The images of stars would be drawn out into long trails and so diluted that only the brighter ones would record on the film. Fortunately, this removes a very great amount of stellar background junk, and greatly facilitates examination of the films.

Another very important principle employed is what is called the "declination offset." The exposure is broken into two sets of images by giving a quick, small offset in declination near midexposure. This gives a confirmatory image to check spurious images, and eliminates about 98 per cent of the possible satellite suspects. By breaking the exposure into two unequal parts, not only do we have a means of confirmation, but also one of immediately determining its distance. With the F 1.6 Schmidt that is used, one cannot give more than 5 minutes exposure per film frame because of the buildup of sky background density, even on moonless nights. After 3 minutes run on a frame, the declination offset is quickly made without closing the shutter and the exposure continued for two more minutes. The shutter is opened and closed to the split second. The result is that there are two sets of star trails of unequal length. If there should be a satellite body moving exactly the speed of the drive, there will be two dot images exactly in a north-south direction, but of unequal brightness. The brighter one will correspond to the 3-minute exposure, the fainter one to the 2-minute exposure. It is much more likely that the driving rate will not correspond perfectly. If an object is beyond the exact drive-rate distance, it will exhibit two short trails of

A contact print of a typical Satellite Search Project film, taken with an F 1.6 Schmidt camera at Flagstaff, Ariz., in 1954

Note the long star trails (the result of high driving rate), and "declination offsets" to create dual images. A small satellite would show as two dots, one above the other and separated by the same amount as the offset in the star trails, if the driving rate of the camera coincided perfectly with the apparent motion of the satellite. If the driving rate was not quite matched, the satellite images would appear as a pair of short trails.

Presented at the Ninth ARS Annual Convention, New York, N. Y., December 2, 1954.

[1] Chief, Research Evaluation. Mem. ARS.

unequal length, the longer component being in the same direction as the longer star trail. If an object is inside the drive-rate distance, it will be outrunning the Schmidt, and the long and short segments will be reversed in order. By adding or subtracting the object's short trail to or from the long star trail, and allowing for the Earth's rotation and parallax, and applying Kepler's law, one knows the period and when and where to shoot for it again on the basis of approximate parallax and a circular orbit. The amount of departure on an expected return will yield data on the eccentricity of the orbit, etc. The askewness of the short trail with the star trails would yield information on the inclination of the object's orbit.

If an object trailed a little, there would be some loss in magnitude. Thus, the exploration zones in depth have to be spaced according to how much loss of magnitude one is willing to tolerate for possible objects midway between zones.

As the search work progressed, many interesting aspects of geometry and observational procedure unfolded. The problem of arranging the photographic observations to get all the sectors of an orbital zone through an accessible observing arc resulted in the establishment of several types of procedure. The most suitable type of observing procedure is selected for a given zone. In a few types, all of the photographic exposures are centered on the observer's meridian, in which case there are two observing periods during the night. One observing arc lies between the limits of evening twilight and the intersection of the satellite orbit with the Earth's shadow. The other arc lies between the east edge of the Earth's shadow and morning twilight. The further out a zone lies, the wider are its observable arcs. Other types of procedures involve progressive settings in hour angle so as to just miss the Earth's shadow, and photographs may be taken continuously throughout the entire night. Some of the latter types involve progressive variations in drive rate and pointing of the optical axis in hour angle and declination. Each of these quantities have to be calculated for each successive photograph. The whole night's run is carefully planned beforehand with every minute of time of the run assigned on a prepared observation sheet. For many zones which require several nights for coverage of all the longitudinal sectors, a timetable graph is kept so that a sector lost by a cloudy night can be recovered later when it should traverse the observing arc. The great range in periods of revolution makes this chore a rather intricate one. Some zones are very difficult because of peculiar astronomical circumstances, and several hours of deliberation are required to plan an effective exploration of one zone.

The reach of this method and modest equipment is almost fantastic. It records dot images of stars to the 15th magnitude in two minutes of exposure on fast film. A V-2 rocket seen broadside and in nearly "full phase" would show as a 15th magnitude star at the distance of the moon by merely reflecting the sunlight from a flat-white painted surface. Or, that of a clean white tennis ball only half illuminated to the observer at 1000 miles up! It would also be capable of recording as a dot image a dark meteorite about one foot in diameter at a height of 1000 miles. But the range in apparent angular speeds over a relatively small span of distance is so great that hundreds of different drive rates must be employed. This requires an enormous amount of work.

So much for the methods and techniques of the Satellite Search. With small modifications, and firing times after sunset, this kind of optical instrumentation would be particularly effective and accurate for gathering ballistic data on extremely high-altitude multistage rockets.

Suppose that an artificial satellite is sent up to revolve around the Earth at the classical height of 1075 miles. If its orbit were circular, its period would be exactly two hours. After a few months' observation, its orbit would be known with great accuracy. Then by using Satellite Search technique from two or more camera stations separated from each other by hundreds of miles, with solenoids electronically controlled and triggered by radio to give two or more star trail offsets, very accurate distances and azimuth angles could be obtained for geodetic triangulation. By establishing a complex triangulation net, positions of stations probably could be gotten to within an accuracy of a few feet on the Earth with respect to points thousands of miles apart.

Although the parallax would not be as sensitive, a simpler method would be to erect an artificial satellite at 26,180 miles from the Earth's center. It would then remain stationary in the observer's sky. But even so, the parallax is ten times more sensitive than observing occultations of stars by the moon. The accuracy would probably be much better than tenfold because there would not be the problem of the profile of the moon's mountains.

Certainly the benefit to geodetic triangulation would justify the erection of a small unmanned artificial satellite.

References

1 "On the Utility of an Artificial Unmanned Earth Satellite," Appendix E, "The Geodetic Significance of an Artificial Satellite" by John O'Keefe, Army Map Service, JET PROPULSION, vol. 25, February 1955, pp. 75–76.

2 "Practical Plan for a Space Satellite," *Life*, Jan. 24, 1955, p. 30.

3 "Man Will Conquer Space Soon," *Colliers*, March 22, 1952, "Crossing the Last Frontier," by Wernher von Braun.

4 "Across the Space Frontier," edited by Cornelius Ryan, Viking Press, 1952, "Prelude to Space Travel," by Wernher von Braun, pp. 12–70.

A Combustor Analysis Method

(*Continued from page 231*)

are used to determine the fuel distribution in a burner for an existing fuel manifold.

The flame holding study methods are used in conjunction with the fuel distribution studies. Together, these determine the over-all fuel-air ratio limits which correspond to the local limits at any given point on the flame holder. These values over the whole flame holder can then be used together with observed test results to study the over-all operation of the burner.

The calculation techniques presented have been put to use to analyze the performance of full-scale ramjet engines and afterburners. The local flame holding limits and local fuel-air ratios over the whole flame holder were calculated from the known velocity profile for a number of over-all fuel-air ratios. Correlation of these data with test observations were used to study the following: 1 Combustion instability; 2 lean and rich engine blow-out; 3 combustion efficiency of a burner system.

Development time of a particular burner item can be cut considerably if tests are coordinated with on-the-spot fuel distribution and flame holder stability analyses by using the results of the afore-mentioned studies. The analyses should reveal the desired direction of fuel manifold or flame holder change to give improved performance. Such a procedure need not even require that accurate quantitative values of stability and local fuel-air ratio be established. For most manifold types relative values are entirely satisfactory for this type of analysis.

The accuracy of the calculations and calculation methods improves with accumulation of information. For instance, as data for a particular engine are accumulated, diffusion coefficient estimation, etc., improves. The accumulation of enough data should eventually allow correlation of various factors between burners and allow accurate prediction of diffusion coefficient, effective streamline position, etc., for new burners.

The procedures described herein have been used in afterburner and ramjet development work. Significant improvement in performance and reduction of development time have been realized. The classified nature of such work, however, precludes detailed discussion. Suffice it to say that the practical application of two applied research programs has been very fruitfully employed in several full-scale burner development programs.

Acknowledgment

The author wishes to acknowledge the contributions of many members of the Marquardt Aircraft Co. Engineering staff. In particular, invaluable assistance was extended by G. W. Koffer, G. S. Bahn, C. H. Builder, and W. J. Bennet.

References

1 "Characteristics of Disk-Controlled Flame," by E. A. DeZubay, *Aero Digest*, vol., 61, July 1950, pp. 54–56, 102–104.

2 "Flame Stabilization by Baffles in a High Velocity Gas Stream," by J. P. Longwell, J. E. Chenevey, W. W. Clark, and E. E. Frost, Third Symposium on Combustion, Flame and Explosion Phenomena, p. 40. Williams and Wilkins, Baltimore, 1949.

3 "Flame Stabilization and Propagation in High-Velocity Gas Streams," by A. C. Scurlock, Meteor Report no. 19, Fuels Research Laboratory, M.I.T., July 1948.

4 "Mixing and Distribution of Liquids in High-Velocity Air Streams," by J. P. Longwell and M. A. Weiss, *Industrial and Engineering Chemistry*, vol. 45, March 1953, pp. 667–676.

5 "A Theoretical Expression for Point-Source Diffusion in Turbulent Flow," by A. B. P. Beeton, *NGTE Rep.* R.152, March 1954.

Fabrication of Titanium Components

(*Continued from page 216*)

filler wire addition; the internal fillet was cast against the copper backup blocks. Following this, the leading edge of the strut was through-welded in a similar manner. The fixture was removed from the chamber, disassembled, and the trailing-edges resistance seam welded. Fig. 17 shows the struts prior to and following welding.

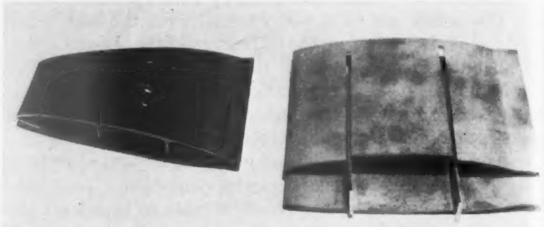

Fig. 17 Titanium airfoil strut. Left: welded and trimmed strut. Right: parts prior to welding

Conclusion

A review has been herewith presented of some of the commonly applied fabricating techniques for the making and assembly of titanium components. It will be noted that no attempt has been made to discuss various machining operations such as milling, drilling, tapping, grinding, etc. The data on these methods have been made available and are so complex as to be well beyond the scope of this report. It will be sufficient to say that on the grade of titanium discussed herein, no radical departure from stainless steel machining practices has been required.

The hot-forming and spinning methods developed, as well as the helium-filled welding chamber, are relative innovations which are particularly useful for pilot production. Modification and simplification of the principles involved will most certainly be forthcoming when titanium fabrications enter the field of large-scale production.

Mixture Ratio Surveys of Rocket Motor Combustion Chambers

(*Continued from page 226*)

5 P. W. Moore, Jr., *Aeronautical Engineering Review*, vol. 7, no. 5, 1948, pp. 30–34.

6 W. A. Wildhack, *Review of Scientific Instruments*, vol. 21, no. 1, 1950.

7 "Temperature Surveys of Rocket-Motor Combustion Chambers," by Dwight I. Baker, Progress Rep. no. 24–5, JPL, California Institute of Technology, Pasadena, November 28, 1952.

8 "Development and Appraisal of a Photographic Technique for Rocket-Motor Combustion Study," by G. A. Agoston, Rep. no. 25-1, JPL, California Institute of Technology, Pasadena, January 29, 1954.

9 T. B. Enzer, Rep. no. 578, Aerojet-General Corporation, Azusa, Calif., July 8, 1952.

10 "Operational Characteristics of a Radio-Frequency Mass Spectrometer," by Ralph Bowersox, Rep. no. 25-3, JPL, California Institute of Technology, Pasadena, January 29, 1954.

11 David Altman and Henry Wise, Publication no. 19, JPL, California Institute of Technology, Pasadena, May 27, 1953.

12 "The Thermal Decomposition of Ammonia upon Various Surfaces," by C. N. Hinchelwood and R. E. Burk, *Journal of the Chemical Society*, vol. 127, 1925, pp. 1105–1117.

13 "On the Burning of Single Drops of Fuel in an Oxidizing Atmosphere," by M. Goldsmith and S. S. Penner, Guggenheim Jet Propulsion Center, California Institute of Technology, Pasadena, November 1953.

14 "Evaluation of Hydrazine as a Monopropellant and a Gas Generant," by David Altman and Delbert D. Thomas, Progress Rep. no. 9-36, JPL, California Institute of Technology, Pasadena, April 17, 1949.

Technical Notes

Automatic Safety Devices for Rocket-Propelled Aircraft

FERNAND FLORIO[1]

Société d'Etude de la Propulsion par Réaction, Villejuif (Seine), Paris, France

Introduction

THE "Société d'Étude de la Propulsion par Réaction (SEPR) was founded in 1944 and has since designed and developed a certain number of solid- and liquid-propellant rocket units, for aircraft and missile propulsion

In the aircraft rocket-unit field, the best known developments are the SEPR 25, SEPR 251, and SEPR 481 which are respectively fitted on the SNCASO 6025, SNCASO 6026, and SNCASO 9000 aircraft. All these various rocket units use nitric acid as oxidizer.

They all have the characteristic of being fully automatic. The pilot has only one starting control and, for certain units, a control insuring thrust variation. Furthermore, any failure or malfunction immediately causes the switching-off of the unit and it is then impossible to switch it on again.

The subject of this paper is to deal with the development of some indispensable safety devices for operation on a manned aircraft. Some of them are intended for protection of the aircraft in case of light liquid leaks, others are for abnormal increase in temperature of turbine feed gases (in case of a self-contained turbopump unit) and can be integrated in the general automatic safety system.

Liquid Leak-Detecting Devices

The starting circuit will permit the opening of the various distribution units only if the propellant pressures have reached suitable values. Conversely, in case of leaks causing a drop in those pressures, the rocket unit will stop burning.

These pressure-detecting units, however, will not react for light leaks which might, though, deteriorate electric circuits, the aircraft structure, or even cause a fire if it is a fuel leak.

A leak-detecting device therefore had to be developed.

Such a device should meet the following requirements

(a) It should detect the liquid in less than one second; (b) it should not be sensitive to these liquid vapors, nor to water or air humidity; (c) it should control enough energy from the aircraft battery to light up a warning light or to operate a relay; (d) it should be of reduced dimensions in order to permit housing in small nooks where liquids can be stored; (e) it should be easily handled and quickly connected and fastened.

Principle and operation diagram

The principle consists in obtaining an electrolyte by action of the liquids on a chemical compound set between two electrodes (Fig. 1).

Development of an acid detecting unit. Performances

The reactive is caustic soda, wrapped in a gum-based coating. This soda-proof coating is, on the reverse, instantaneously destroyed by liquid nitric acid, though it resists nitric vapors. It is furthermore waterproof.

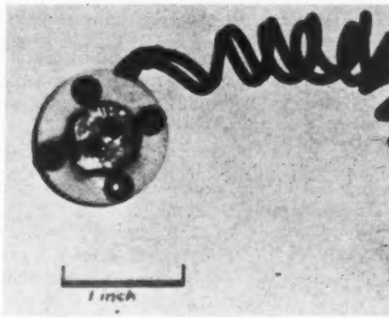

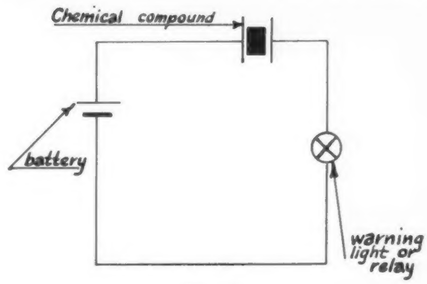

Fig. 1

The small bag containing this chemical compound is located between two silver-sheet electrodes, the whole being maintained fastened by two perforated teflon supports. Assembling is carried out by riveting. A wire connects one electrode to the positive pole of the battery; the other one is grounded to the aircraft structure.

Insulation of these detecting units ranges about 10 MΩ. Effect of water or nitric acid vapors, even after lengthy periods (15 days), on this small bag does not carry the insulation value below 1 MΩ. One single drop of nitric acid is sufficient to establish in $^2/_{10}$ of a second an electric current higher than 150 milliampere.

Similar developments enable the detecting of the presence of liquid fuels.

These detecting units, of a simple construction, are very strongly built and vibration-proof. Their small dimensions permit the housing of several units in various locations in the aircraft. Parallel-mounted, they operate either a warning light provided in the cockpit, or a relay if this detecting unit is to be integrated in the automatic safety system of the power plant.

Thermal Shutting-Off Unit

Temperature of the gas-generator exhaust can abnormally increase in case of failure of the cooling system, and result in melting the turbine inlet manifold. Evolution of the temperature is then very fast, and a conventional regulator has a time delay much too high to be usable in this case. A special device was therefore designed and developed.

Operating conditions

A record of gas temperatures at turbine inlet shows a rate of increase of about 400 F per $^1/_{10}$ of a second in case of cooling-

Presented before Cleveland-Akron, N. E. New York, and Alabama Sections of ARS in September 1954.

[1] Chief Engineer, SEPR.

EDITOR'S NOTE: This section of JET PROPULSION is open to short manuscripts describing new developments or offering comments on papers previously published. Such manuscripts are published without editorial review, usually within two months of the date of receipt. Requirements as to style are the same as for regular contributions (see first page of this issue.)

liquid injection failure. Destruction of the turbine inlet manifold then occurs about 1 second later.

The detecting device and the system which will cause the gas-generator to stop should therefore react in a total time of about $^{5}/_{10}$ of a second.

Description of tested devices

Vapor pressure switch. Among the various usable liquids, mercury can be chosen because its pressure-vs.-temperature curve gives a good sensitiveness at point of adaptation.

The mercury tank, of 0.03-cu in. capacity, is set in the gases circuit (Fig. 2). When the device was tested, a 1-sec time delay was found and judged incompatible with the specific problem.

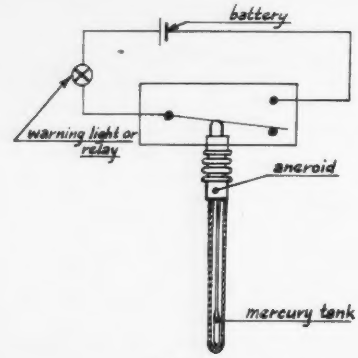

Fig. 2

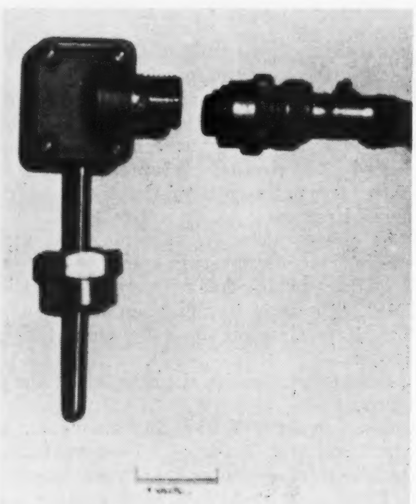

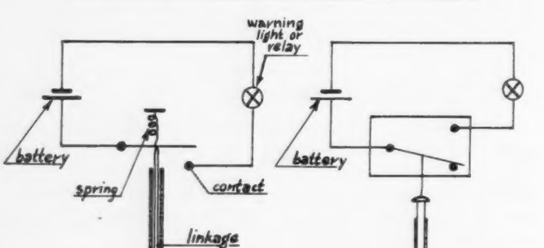

(a) (b)

Fig. 3

Units using fusible alloys. Usual alloys have melting-points ranging from 400 F to 1850 F and cover the turbopump units operating temperatures. With some of these alloys, two types of detecting-units have been developed.

In the type shown in Fig. 3a, the fusion of a rod housed in a tube causes a spring-loaded contact to close.

In the type shown in Fig. 3b, fusion of the tip made of a metallic alloy, melting at a well-defined temperature, gives the gases passage to a piston which, when moving upward, switches on an electric circuit.

It should of course be acid-tight and acid-proof.

Performances

A record shows the operation of the thermal shutting-off unit and points out the time delays of the various elements in the gas-generator system until it comes to a stop.

A temperature increase has been purposely caused by a sudden stop in cooling-liquid circulation. The thermal shutting-off unit was set at 1100 F.

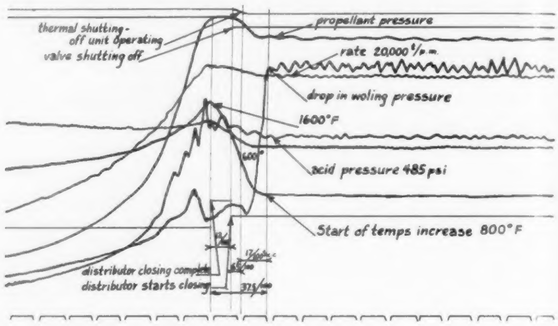

Fig. 4

Time 0 sec.: stop in cooling system.

at 17/100^{s}: temperature t = 1100 F, operating temperature of the thermal shutting-off unit.
at 23/100^{s}: the control shutting-off liquids inlet is operating.
at 37/100^{s}: closing is complete.
at 39/100^{s}: temperature reaches a maximum and then decreases. Maximum value attained is 1600 F.

The temperature of the turbine inlet manifold has reached a maximum at 1300 F.

Systematic tests have shown that there is a ± 50 F clearance on operating temperature of control shutting-off liquids inlet (Fig. 4).

This second type has been thoroughly and successfully tested and finally accepted.

Conclusion

The leak-detecting device and the thermal shutting-off units integrated in the general automatic safety system of the rocket unit protect the aircraft against leaks and overheating. They do not require any special attention from the pilot.

These devices have permitted all SEPR rocket units to be operated successfully on test stands as well as on aircraft without any incident occurring.

ERRATA

In Jet Propulsion for February 1955, the following revisions should be made in the paper, "One-Dimensional, Steady Flow With Mass Addition and the Effect of Combustion Chamber Flow on Rocket Thrust" by E. W. Price.

(*Continued on next page*)

Discussion of "The Mechanics of Film Cooling"

ARTHUR B. GREENBERG[1]

Purdue University, West Lafayette, Ind.

IN a recent paper (1)[2] Knuth presented an interesting treatment of the phenomena of film attachment and film stability as related to film cooling. The latter work closely parallels a research program which has been in progress at the Purdue University Rocket Laboratory since 1948, under the auspices of Project SQUID (2, 3, 4). Consequently, some interesting comparisons of results can now be made.

In his investigations of film attachment and film stability Knuth employed an injector comprising a series of holes arranged circumferentially in a tube wall through which a turbulent gas stream flowed. Corresponding experiments at Purdue University have utilized an injector consisting of a continuous circumferential slot in the duct wall formed by two spaced, parallel, washer-shaped disks. These two types of liquid injectors have distinct mechanical and flow characteristics which suggest applications wherein each type is preferable. Such characteristics are indicated below.

1. *Multiple-Hole Injectors:* (a) are easily fabricated; (b) are not susceptible to thermal distortion; and (c) may be designed to provide sufficient pressure drop at low liquid flow rates to insure good liquid flow control; but (d) have a fixed liquid flow area; (e) provide no liquid film on the duct wall in the vicinity of a clogged hole and incomplete, relatively thin film coverage of the duct wall for some distance downstream of the point at which the liquid films spreading from adjacent injector holes join; and (f) do not provide a flow field which is amenable to analysis.

(Obviously, the deleterious effects of a clogged hole suggested in (e) can be minimized in a specific application by a proper selection of the size and spacing of the injector holes according to data relating the spreading characteristics of liquid films to the liquid and gas flow conditions. However, such data have not been published.)

2. *Continuous-Slot Injectors:* (a) are easily fabricated (although somewhat greater precision is required than for multiple-hole injectors); (b) may be designed to have adjustable liquid flow area; (c) may be designed to provide either low or high pressure drop at high liquid flow rates; (d) provide uniform liquid films on the duct wall even under moderate clogging conditions, when such clogging is caused by foreign particles in the liquid; and (e) provide a flow field which is amenable to analysis; but (f) require careful initial adjustment to provide a uniform liquid flow passage; and (g) are adversely affected by thermal distortion when the axis of the liquid slot forms an acute angle with the duct wall.

In view of the differing characteristics of the two types of liquid injectors, it cannot be generally stated (and it has not been so claimed in the references cited by Knuth) that either type of injector is superior to the other. Indeed, a combination of the two types (for example, circumferential holes feeding a shallow circumferential slot) would provide some of the best characteristics of both types of liquid injectors. However, continued studies of both types of injectors are warranted in order to provide the data by which the injectors may be successfully applied.

Knuth correlated the data for film attachment that he obtained with multiple-hole injectors by plotting the momentum ratio of the gas and liquid streams versus a function of the gas stream Reynolds number, the liquid stream Reynolds number, and a modified cavitation parameter. The correlation represents his data reasonably well. However, when the same parameters are used for correlating the Purdue data for film attachment obtained with continuous-slot injectors over substantially the same range of variables, the result is a field of data points. Inasmuch as the attachment phenomena for both types of injectors are basically the same, a single correlation effective for either attachment mechanism should be attainable.

The Purdue data for film attachment with continuous-slot injectors, obtained by four different investigators (including Knuth), have been correlated by a single curve by using as dimensionless parameters the momentum ratio of the liquid and gas streams, the ratio of the characteristic dimensions of the flow passages for the liquid and gas streams, and the gas stream Reynolds number. It was observed that when the gas stream bulk velocity is small (for example, 40 fps) the film attachment phenomenon occurs with very low liquid injection velocities (approximately 4 fps). Under such conditions of flow of a viscous liquid there could be no point in the liquid flow field where the velocity is sufficiently high to cause cavitation effects. Consequently, cavitation was not deemed pertinent to the correlation of the film attachment phenomenon. Furthermore, although the velocity distribution of the liquid in the injector passages may influence the attachment phenomenon, the Reynolds number of the liquid would have little effect in the correlation because the liquid flows encountered in the experiments were in the laminar regime.

At this time the data for film attachment obtained at Purdue do not include a significant variation in the gas stream density and gas stream viscosity. The effects of the latter parameters are currently being investigated. After the above studies are completed the results of the entire investigation will be reported.

The foregoing comparisons of the results reported by Knuth, and some of the unreported studies conducted at the Purdue University Rocket Laboratory, indicate that more research is required to establish the details of the mechanisms of film attachment.

Received March 30, 1955.

[1] Research Assistant, School of Mechanical Engineering.

[2] Numbers in parentheses indicate References at the end of discussion.

References

1 "The Mechanics of Film Cooling—Part 1," by Eldon L. Knuth, JET PROPULSION, vol. 24, November–December 1954, pp. 359–365.

2 "Progress Report on the Stability of Liquid Films for Cooling Rocket Motors," Technical Report no. 23, by M. J. Zucrow, C. M. Beighley, and E. L. Knuth, Purdue University, Lafayette, Ind., November 1950.

3 "The Stability and Flow of Liquid Films Injected into an Air Duct Through Spaced Parallel Disks in the Two- and Three-Dimensional Cases" (MS Thesis in Aeronautical Engineering), by Arthur B. Greenberg, Purdue University, Lafayette, Ind., August 1952.

4 "The Effect of Air Duct Diameter Upon the Stability of Liquid Films Injected Radially into an Air Duct Through Spaced Parallel Disks" (MS Thesis in Mechanical Engineering), by Robert K. Louden, Purdue University, Lafayette, Ind., January 1954.

(Errata continued)

Page 62, left column. Line 15 from bottom should read: "(which is the Mach number squared and multiplied by the ratio . . .)"

Page 64, Equation [21]. The first factor in the numerator should be

$$[\gamma\delta_i^2 - (1 - [1 - \delta^2]^{1/2})]^{(\gamma/\gamma-1)}$$

Page 66, Equation [1]. The equation should be

$$r = Cp^n(1 + ku)$$

(This is also called for in the expression in the Summary, page 78.)

Jet Propulsion News

Alfred J. Zaehringer, American Rocket Company, *Associate Editor*

Rockets, Guided Missiles

DOUGLAS Aircraft is establishing a Charlotte (N. C.) Division for expanded production of Nike missiles. Production is expected at the new site early in 1956. Nike is currently being produced at the Santa Monica (Calif.) Division of Douglas. Nike has successfully completed cold-weather testing—at minus 35 F—in joint Canadian-U. S. tests near Fort Churchill, Canada.

● Indicative of the operational status of other new missiles, the Air Force has revised its missile designation into tactical, strategic, and air defense groups. For example, the Matador is a tactical missile and is called the TM-61. Snark, a strategic missile, now is the SM-62. The guided aircraft missile, Rascal, is designated as the GAM-63, while the guided aircraft rocket, Falcon, is the GAR-98. Bomarc, an interceptor missile, will be known as IM-99. Pilotless aircraft designation will no longer be used.

● The Northrop Snark, currently being tested at Cocoa, Fla., is turbojet powered and has a range capability hinted at 4–5 thousand miles. Thrust is provided by a P&W J57 turbojet while additional take-off power comes from solid propellant booster rockets. Snark cruises at near sonic speed and is said to be guided by a star-tracking inertial system. Rascal, by Bell, is launched in the vicinity of a target by its mother plane in a manner similar to the start of the X-1 rocket plane. Propulsion for Rascal comes from a triple bank of rocket engines and the speed is reported to be near 1000 mph. Guidance comes from the mother plane which is expected to be the B-36 or B-47. Wraps have been taken off the Hughes Falcon rocket which is now in production and is to be used to arm the Northrop F-89H Scorpion and the delta wing Convair F-102. Falcon, automatically guided to its target, weighs somewhat over 100 lb, is 6 ft long, and has a diameter of 6 in. Propulsion is from a high thrust solid propellant rocket motor giving it supersonic speed and a range of several miles. Bomarc, now in the development stage, is a ground-to-air missile which has a range of up to 250 miles. Launching is by means of a rocket motor while two ramjet engines provide sustaining thrust for cruise.

● In the long-range class, two other missiles, the North American surface-to-surface SM-64 Navaho, and the Convair intercontinental ballistic missile, Atlas, are in the news. Navaho, with ranges hinted at up to 5000 miles, is launched by high thrust rocket engines and receives sustaining thrust from ramjets. The missile is reported to be capable of cruising at 75–90 thousand ft and at a speed of Mach 2.5–3. Guidance is probably a celestial system. The Atlas, on the other hand, is powered completely by high thrust rocket engines. With range capabilities of about 5000 miles, Atlas may have a burning time of 12 min, a Brennschluss velocity of 22,000 fps, and have a peak trajectory altitude of about 800 miles. Atlas may be equipped with a hydrogen bomb warhead and be able to reach its target in about 30 min.

● Official disclosure has been made of an entire series of jet propelled pilotless aircraft (photo). Built by Radioplane Company of Van Nuys, Calif., are the YQ-1B turbojet; its prececessor, the XQ-1A turbojet; the XQ-1 (modified) pulsejet; and the XQ-1 pulsejet. The drones are recoverable and are used for targets. Some of the drones have been in operation since 1950 at Holloman AFB.

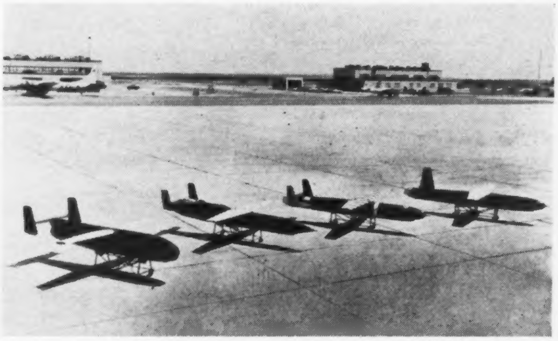

Northrop Aircraft

Radioplane Company target drones. Left to right: YQ-1B, XQ-1A, XQ-1 (modified), and the XQ-1

● The Viking high-altitude research rocket may soon be fired from the *USS Norton Sound* near Norway to obtain data about the upper atmosphere in northern climes.

● New tests are expected at the Woomera rocket range on new British rocket-propelled pilotless bombers. Ranges of about 500 miles have been mentioned.

● The de Havilland Super Sprite is the first British rocket engine to be certified for service use. Hydrogen peroxide is employed as the oxidant; a solid metal catalyst is used to decompose the peroxide; kerosene or gasoline is used as a fuel. Total impulse is 120,000 lb sec. Maximum thrust is 4200 lb; operating time is 40 sec; dry weight is 620 lb. Super Sprite is used as an ATO unit for jet bombers and can be employed as an integral mount or jettisonable installation.

● The Air Force is predicting that military aircraft of 10 to 20 years hence will fly at an altitude of 100,000 ft and at speeds of Mach 5.

● Quantity production of the Snecma Vulcain turbojet engine developing over 13,000-lb thrust is scheduled this year.

Combustion Courses Offered

The College of Engineering of the University of Michigan is offering in June two intensive courses in the jet propulsion field: *Combustion,* covering the latest developments such as gas kinetics, basic chemical kinetics, gas dynamics, deflagrations, and detonations; *Gas Turbines and Free Piston Engines,* dealing with centrifugal and axial compressors, turbine performance, axial turbines, high temp materials, fuels, etc. Date: June 13–17; Location: Ann Arbor, Mich.

EDITOR'S NOTE: The information reported in this Section has been selected from approved news releases originating with the Department of Defense, private manufacturers, universities, etc., and from published news accounts in journals and newspapers. The reports are considered generally reliable, although no attempt has been made to verify them in detail.

LRWE

The town of Woomera

Typical Woomera house

Air freighter delivers equipment and personnel

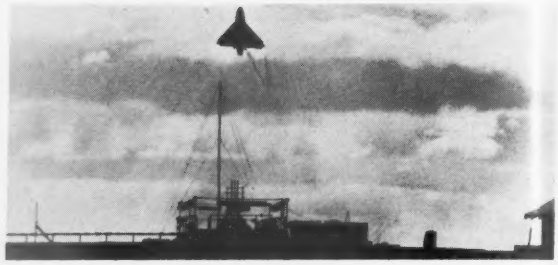

Launching of Fairey VTO research model

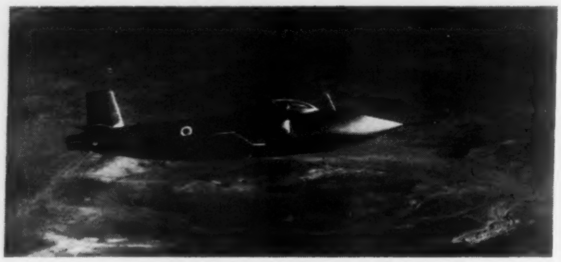

Pika, piloted version of Jindivik

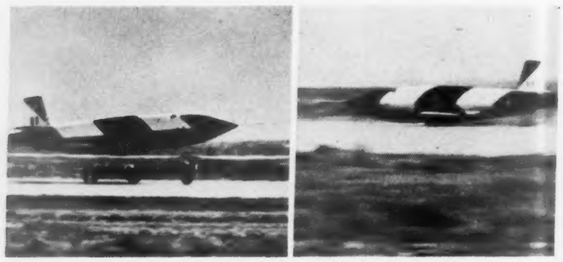

Jindivik target takes off and lands

Down Under at Woomera

SHORTLY after World War II, a joint British-Australian rocket range, known as the Long Range Weapons Establishment (LRWE), was established at Woomera (aboriginal word for spear launcher) in the "gibber" desert country of Australia. Woomera is located some 270 miles NNW of Adelaide in a vast desert resembling our southwest. The average annual rainfall is about 6 inches and only bluebrush and saltbrush flourish on the desert floor which is littered with black and red stones known as gibber to the aborigines. The rocket range covers about 1 million square miles and extends 1200 miles northwest to the Indian Ocean; ultimate extension of the range to Christmas Island, 2700 miles away, is possible.

Over 1200 personnel were used in the construction of the vast installation. Railroads, highways, airfields, utility lines, shops, laboratories, and homes were among the items which took shape during the past few years. A permanent fabrication facility and a control and launching site were recently placed into operation.

Since establishment in 1946, over 1500 missiles have been tested at LRWE. Early work was with pilotless drones for use as target aircraft in testing new missiles under development in Britain. Typical of these was the Jindivik jet propelled drone which was first a piloted model. Later unmanned models, able to take off and land without auxiliary power, were checked out. Many aerodynamic models later evolved into operational craft. An example is the Fairey Aviation VTO which is powered by two Beta rocket motors of 900 lb thrust each. Two solid propellant booster rockets, developing 600 lb thrust each, are also used at launch. In Ministry of Supply tests, the Fairey models are used to study launching of aircraft under low accelerations from restricted area take-off sites.

Many of Britain's more than 100 aircraft and missile firms have personnel based at LRWE. Two British missiles are completing testing at Woomera and are nearing operational status. One is the English Electric two-stage AA guided missile, resembling our Nike, but which can reach speeds of Mach 2 and altitudes of over 50,000 ft. The other is the Armstrong Whitworth-Sperry Gyroscope naval AA guided rocket. The latter rocket, to be used on special fleet guided missile ships, has a range of about 20 miles, and is launched by means of multiple booster rockets; the missile contains its own homing device.

Australian missiles are also currently undergoing development at LRWE, and Canada may also soon be doing testing here. Because of tremendous area of the Woomera facility, LRWE may be expected to play an increasingly prominent role in rocket development.

ARS SECTION PRESIDENTS

Alabama: Joseph Wiggins, *Thiokol Chem. Corp.;* **Arizona:** R. H. Hansen, *Hughes Aircraft Co.;* **Central Texas:** B. S. Adelman, *Phillips Petroleum Co.;* **Chicago:** V. J. Cushing, *Armour Research Foundation;* **Cleveland-Akron:** John Sloop, *NACA;* **Detroit:** Laurence M. Ball, *Chrysler Corp.;* **Florida:** R. S. Mitchell, *Pan American World Airways;* **Indiana:** A. R. Graham, *Purdue Univ.;* **Maryland:** W. G. Purdy, *Glenn L. Martin Co.;* **National Capital:** E. C. Page, *Page Communications, Inc.;* **New Mexico-West Texas:** R. C. Sherburne, *New Mexico A & M;* **New York:** C. W. Chillson, *Curtiss-Wright Corp.;* **Niagara Frontier:** T. Zannes, *Bell Aircraft Corp.;* **Northeastern New York:** Kurt Berman, *General Electric Co.;* **Northern California:** M. A. Pino, *California Research Corp.;* **Pacific Northwest:** R. M. Bridgforth, *Boeing Airplane Co.;* **Princeton Group:** Irvin Glassman, *Princeton Univ.;* **St. Louis:** Norton B. Moore, *McDonnell Aircraft Corp.;* **Southern California:** C. M. McCloskey, *ONR;* **Southern Ohio:** W. J. Mizen, *Bendix Aviation Corp.;* **Twin Cities:** J. J. Schons, *Univ. of Minnesota.*

ARS to Meet in Boston; Four Sessions Scheduled June 22–23

First meeting of the Society ever to be held in Boston will take place during the ASME-ARS Semi-Annual Meeting, June 19–23.

Sessions sponsored or co-sponsored by ARS will be held on Wednesday afternoon, June 22, and on Thursday, June 23, during the morning, afternoon, and evening.

An ARS banquet will feature the meeting, to be staged at the Hotel Statler. The banquet will be on Wednesday evening, June 22. Toastmaster will be past-president Frederick C. Durant III, of Arthur D. Little, Inc.

Two of the sessions—organized by ARS alone—will feature combustion in bipropellant rockets, rocket instrumentation, vibration analysis of turbine blades, a system for handling and storing low boiling propellants, stabilization of oscillation in liquid rockets, and flame stability as topics. Two sessions to be co-sponsored with the ASME Aviation Division will consist of papers on stall flutter, aerodynamics, fluid flow, and Mach number determination.

The complete program will be published in the June issue of Jet Propulsion.

Nike Tactical Plan Revealed to New York Section

A group of Civil Defense directors attended the March 18 meeting of the New York Section in order to hear a Nike expert give details on how the weapon is to be used in protecting the New York metropolitan area from attack.

The Civil Defense leaders, invited by Section president C. W. Chillson as a public service, represented communities in which Nike installations are slated to be built. Co-operating with the Section in releasing the list of 24 such communities was Major General N. A. Burnell II, Commanding General, 1st Antiaircraft Regional Command, Fort Totten, N. Y.

The speaker, Lt. Col. Glenn Crane, resident ordnance officer at Bell Telephone Laboratories, prime systems contractor for Nike, detailed the Nike's tactical strategy and pointed out the space and manpower requirements for each installation. About 100 officers and men will be required to man an installation, one third of whom require extensive field training. Officers are all college graduates with engineering or science degrees.

Karsch on the V-2

President R. K. Sherburne of **New Mexico-West Texas** reports on a March 31 meeting at La Posta restaurant in Old Mesilla, N. Mex.: "About 70 members and their wives enjoyed program chairman Lou Stecher's French 75's and the New Mexican menu at La Posta. After the dinner Herb Karsch gave a short talk on his experiences in collecting V-2's in Germany and showed a color film of early V-2 activities."

National Capital Meets with AHS on Rocket-Powered Helicopters

A joint meeting of the **National Capital** Section with the Washington Section of the American Helicopter Society drew an audience of 150 in March.

Following a steak dinner, the following experts held forth on the application of rockets to helicopters: L. Goland, Princeton University; N. Stefano, American Helicopter Div., Fairchild Engine & Airplane Corp.; W. R. Brown, Reaction Motors, Inc.; and J. B. Nichols of Hiller Helicopters. Joint chairmen of the meeting were Peter Torrey, vice-president of AHS, and Robert C. Truax, vice-president of the ARS **National Capital** Section and national director.

Sikorsky Aircraft, *Aero Digest* magazine,

First European Corporate Member is SNCASO

France's Société Nationale de Constructions Aéronautiques du Sud-Ouest of Paris is the first European organization to become a Corporate Member of ARS. Shown above in front of the company's SO-9000 Trident, a rocket-powered interceptor, are the five SNCASO engineers who become ARS members: (Left to right), Jean Girard, chief engineer in charge of flight test; Lucien Servanty, chief engineer and designer of the SO-9000; Fernand Vinsonneau, technical director; Jacques Cornillon, U. S. technical representative; Georges Delval, attaché to the technical board.

ARS Meetings Calendar

		Theme
June 22–23	ARS Summer Meeting, Boston	see above
Aug. 1–6	Sixth IAF Congress, Copenhagen	
Aug. 22–24	ARS-Northwestern University Gas Dynamics Symposium, Evanston, Ill.	Combustion
Sept. 19–21	ARS Fall Meeting, Los Angeles	General
Nov. 13–18	ARS-ASME Annual Convention, Chicago	General

Abstracts or manuscripts for all meetings are invited. They should be submitted to the Program Chairman, American Rocket Society, 500 Fifth Ave., New York 36, N. Y., 120 days prior to the meeting date.

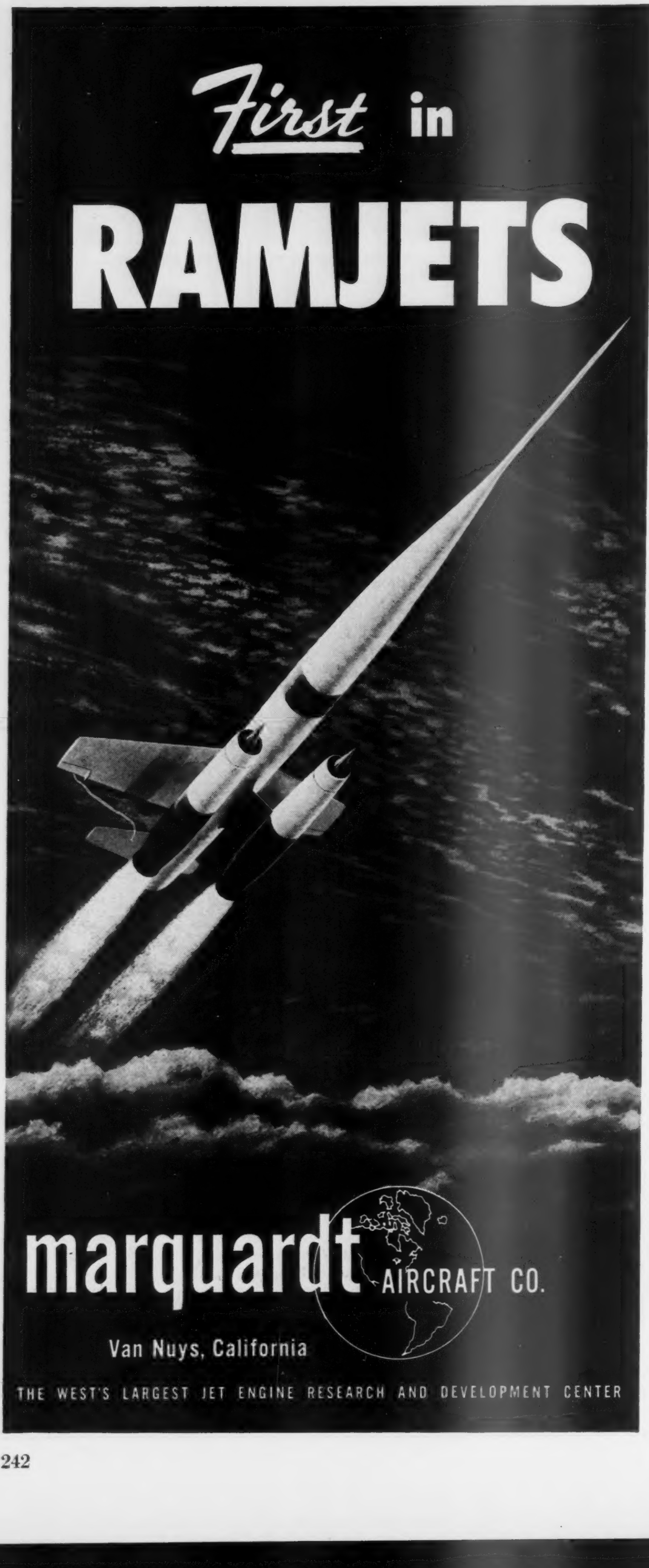

and Glenn L. Martin Co. supplied door prizes for the meeting, which was preceded by a steak dinner.

More Hear Dornberger

A TURNOUT of 250 heard Walter R. Dornberger speak on his "Rocket-Powered Commercial Airliner" at a March 3 meeting of the **Pacific Northwest** Section at the University of Washington, Seattle.

Dornberger was introduced by Lysle A. Wood, director of pilotless aircraft at Boeing.

A questionnaire on preferences for future programs was distributed to the audience, with "space flight" nosing out a host of more specific categories as the subject of greatest interest.

Mitchell New Florida President

RICHARD S. Mitchell, division manager, Guided Missiles Range Division, Pan American World Airways, Patrick AFB, is the new president of the **Florida** Section, succeeding Keith K. McDaniel of Boeing Airplane Company, who continues as a director.

Elected vice-president at a March 23 meeting of the Section was Verl O. Smith, Chief, Missile Test Facility, Northrop Aircraft. Paul B. Campbell and William Risley, both of Boeing, were made secretary and treasurer, respectively.

The other new directors are: George C. Gentry, Patrick AFB; G. L. Lakey and G. L. Rhodes of Boeing; R. L. Lewis and E. H. Munsey of Northrop; and Maj. Gen. D. N. Yates, Commander, AFMTC.

High-Speed Turbojets

OWEN Welles of Pratt & Whitney Aircraft spoke to a March 8 meeting of the **Indiana** Section at Purdue University on "Developing Turbojet Engines for High Speed Flight."

Two Southern Ohio Meetings

DARRELL Romick of Goodyear Aircraft spoke on "The Dawn of the Age of Space Flight," and Walter Kleczek of General Electric's Guided Missiles Division on "Developments in Rocketry in the Last Ten Years" at recent meetings of the **Southern Ohio** Section.

Section Guide "in the Works"

A HORDE of facts, some excellent suggestions, and a few lusty "gripes" on how or how not to run a Section, were included in the questionnaires recently filled out by officers, directors, and committeemen of the various Sections, at the request of the national office.

Returns from all but six of the Sections are in. As soon as these are heard from, a compilation will be made and a "Section Guide," designed to assist Sections in planning and programming their activities,

taking care of their finances, etc., will be printed and distributed.

Blarney in Ohio

"MY, how the blarney flew as they reported on the year's activities," says the **Cleveland-Akron** newsletter of a St. Patrick's Day meeting of the Section's officers and committee chairmen.

No blarney, however, was the disclosure that the Section's membership had increased from 80 to 102 over the previous twelve months.

Cleveland-Akron has sent questionnaires to all members asking for ideas for future programs.

Solid Rockets in the USAF

TRISTAN J. Keating, chief of the nonrotating engine branch at Wright Air Development Center's Power Plant Laboratory, spoke to the **Chicago** Section on the application of solid propellant rockets in the Air Force at a March 23 meeting.

The discussion, held at the Technology Center, dealt with the difference between the needs of the Air Force and the other services.

Rocket and Guided Missile Museum

ARS has been requested to publish the following notice:

"The Department of the Army has approved Research Project Ord 139, Compilation, Assemblage and Preservation of Historical Materiel Pertaining to the Development of Rockets and Guided Missiles and assigned it to the 3353rd Research and Development Unit (U. S. Army Reserve), Huntsville, Ala. The Commanding General of Redstone Arsenal is co-operating in the project by giving logistic support, making equipment which has fulfilled its original purpose available, and designating a building at the arsenal for housing the Museum.

"Part of the display will cover the historical development from the Chinese firesticks to more recent developments. Co-operation of individual members of the American Rocket Society in this portion of the presentation especially will be appreciated. In addition, information on recent or current developments of individuals, foreign sources and other services is desired."

"Correspondence on this subject should be directed to the Unit Project Officer, Lt. Col. R. Preston Watts, 1305 Matthews St., Huntsville, Ala."

ARS is informed further that the museum will have both classified and unclassified sections. Credit will be given any donor of materiel, models, photos, manuscripts, drawings, or other material, and donors should include biographical data with their contributions.

Book Reviews

C. F. Warner, Purdue University, Associate Editor

Rare Metals Handbook, edited by C. A. Hampel, Reinhold Publishing Co., New York, 1954, 657 pp. $12.

Reviewed by T. J. Hughel
Purdue University

This book is a useful compilation of reference data on over thirty metallic elements which have not in the past been commonly used engineering materials. Actually the number of elements covered is considerably greater than thirty if one counts those elements which are grouped together; e.g., the rare earths and the platinum metals. The term "rare" as used in the title of this book does not refer to the rarity of the element in nature, but rather to the rarity of its application in traditional engineering practice. In fact, some of the metals included, such as titanium and molybdenum, are not only fairly common in the earth's crust but are well on their way toward becoming well-established engineering materials.

Each element or group of elements is the subject of a chapter written by an author or authors expert in the metallurgy of the particular element. In general the chapters consist of an introduction and sections on occurrence, production statistics, recovery and purification processes, physical properties, chemical properties, toxicity, alloys, fabrication techniques, and present applications. Where elements have additional important properties, such as biological effects or radioactivity, these are discussed. Mechanical properties and corrosion data are also given for those metals for which such data are available. The final chapter of the book is a compilation of data on the properties of all metals, rare or otherwise. These data are presented in tabular form, which is most convenient for comparing the properties of all the metals. One interesting table in this section lists the metals on the basis of current price per lb and per cubic inch.

This book will prove to be a most valuable reference work for those metallurgists and engineers who are striving to develop materials having properties superior to those of conventional engineering metals. The book itself may serve to make several of the metals it discusses less rare in their application.

Control-System Dynamics, by Walter R. Evans, McGraw-Hill Book Co., Inc., New York, 1954, 277 pp. $7.

Reviewed by E. M. Sabbagh
Purdue University

The design of control systems requires the selection of components to meet specified values relating to load, speed of response, settling time, overshoots, transient oscillations, steady-state errors, etc. From the analysis of an already designed system, the response can be found from the solution of the differential equations relating the output to input. The solution, though obtained by operational calculus, is long and time-consuming. After the answer is obtained, if the results show that the specifications have not been met, the designer has to depend upon his experience to alter some parameters, hoping that the change will cause the specifications to be met. With the change he proceeds to analyze his system again.

In order to avoid such groping in the dark, the frequency transfer function method of analysis and synthesis was adapted, and correlation between the frequency response and dynamic quantities were developed. In 1948, W. R. Evans introduced his root-locus method of analysis and synthesis, with which the transient solution can be easily obtained. Furthermore, it is well adapted to design. The effect of a change of a parameter on the response is easily seen and evaluated. In the later chapters of this book the root-locus method is explained and well illustrated. The frequency response is also obtained by this method.

The first five chapters of the book explain the problems met in control design, the translation of the physics of the components into mathematical equations, the Nyquist diagrams, and the Bode plots.

In chapter 6 the transient response is obtained from the frequency response. From chapter 7 to chapter 12, the author explains the root-locus method and applies it to the analysis and synthesis of control systems, to the solution of high-order differential equations, and to setting up block diagrams of circuits. He also devotes some space to the signal flow diagram. Chapter 12 deals with the phase plane of nonlinear circuits and their describing functions.

This book will be of great value to anyone working with control systems.

Book Notices

Fluid Dynamics and Heat Transfer, by J. G. Knudsen and D. L. Katz, University of Michigan Press, 1954, 243 pp. $3.50.

Knudsen and Katz present a review of modern fluid mechanics in the first 172 pages of this University of Michigan Bulletin, and discuss the general concepts of convective heat transfer in the remainder of the book. A short presentation of liquid metal heat transfer is included.

Jet, by Sir F. Whittle, Philosophical Library, New York, 1954, 320 pp. $6.

An interesting biographical story of the development of the English turbojet engine by its inventor. The major portion of the book deals with the three-way battle fought by the British Air Ministry, Power Jets, and various private contractors for the development of the turbojet engine. A true companion volume to "V-2" since, together, they present the development story of today's two most important types of jet power plants.

Please Note: In the Book Reviews Section for March 1955, Mr. John L. Barnes, Ramo-Wooldridge Corp., should have been listed as the reviewer for "The New Warfare," page 136.

Technical Literature Digest

M. H. Smith, Associate Editor **and M. H. Fisher,** Contributor
The James Forrestal Research Center, Princeton University

Jet Propulsion Engines

Methods for Rapid Graphical Evaluation of Cooled or Uncooled Turbojet and Turboprop Engine or Component Performance (Effects of Variable Specific Heat Included), by Jack B. Esgar and Robert R. Ziemer, *NACA TN* 3335, Jan. 1955, 45 pp.

Fuel Requirements of Pre-Vaporizing Type Gas Turbine Combustors, by W. W. Horsman and J. L. Jackson, *Woods River Research Lab., Shell Oil Co., 8th and 9th Quart. Prog. Rep.,* March and June 1954.

Thermodynamics of Supersonic Straight Thrust Diffusers (in German), by E. Sänger, *Ing.-Archiv.,* vol. 22, 1954, pp. 368–377.

A Novel Cooling Method for Gas Turbines, by Edward Burke and G. A. Kemeny, *Trans. ASME,* vol. 77, Feb. 1955, pp. 187–195.

Some Applications of Gas Turbine to Helicopter Propulsion, by John Brown, *J. Helicopter Assoc. Gt. Brit.,* vol. 8, Jan. 1955, pp. 87–111.

Jet Lift (Rolls-Royce Flying Bedstead), *Flight,* vol. 67, Feb. 1955, pp. 134–135.

Tests to Determine the Effect of the Exhaust Cone Support Strut Fairings on the Performance of a Turbojet Engine, by W. Deacon, *Gt. Brit. Natl. Gas Turbine Estab. NGTE.* M222, July 1954, 8 pp.

The Bristol Olympus Type-Tested at 10,000 lb., *Aeroplane,* vol. 88, Feb. 1955, pp. 135–136.

What Comes After the Turbojet?, by Robert W. Bonner, *Aero Digest,* vol. 70, Jan. 1955, pp. 65–68.

An Analysis of Thrust Estimation, by W. R. Cushing, *Aircr. Engng.,* vol. 27, Jan. 1955, pp. 9–13.

An Investigation of the Flutter Characteristics of Compressor and Turbine Blade Systems, by Chi-Teh Wang, Frank Lane, and Robert J. Vaccaro, *IAS Preprint,* Jan. 24–27. 1955, 20 pp.

The Influence of Turbojet Engine Design Parameters on Noise Output, by D. M. A. Mercer and Ira Dyer, *IAS Preprint,* Jan. 24–27, 1955, 16 pp.

Recent NACA Investigations of Noise Reduction Devices for Full-Scale Engines, by Edmund E. Callaghan, Newell D. Sanders, and Warren J. North, *IAS Preprint,* Jan. 24–27, 1955, 8 pp.

The Control of Turbojet Engines, by Donald F. Winters, *IAS Preprint,* Jan. 24–27, 1955, 11 pp.

Power Plants for Rotary Wing Aircraft, by A. Graham Forsyth, *Fourth Aeronaut. Confer.,* London, Sept. 15–17, 1953, pp. 325–356.

Dart Development (Rolls-Royce, Ltd.), *Flight,* vol. 67, Jan. 1955, pp. 45–48.

Vibration Testing, *Flight,* vol. 67, Jan. 1955, pp. 62–63.

A Study of Surge in Compressors and Jet Engines, by Carl E. Pearson, *J. Aero. Sci.,* vol. 22, Jan. 1955, pp. 10–16.

A Standardized Range of Small Gas Turbines (Blackburn-Turbomeca), by G. Waller, *Oil Engine and Gas Turbine,* vol. 22, Oct. 1954, pp. 238–240.

U. S. Gas Turbine Coach and High-power Car (General Motors Corp.), *Oil Engine and Gas Turbine,* vol. 22, Nov. 1954, pp. 277–281.

Annular Combustion for Turbine Engines, by M. A. Stokes, *Aeroplane,* vol. 88, Jan. 1955, pp. 48–52.

Miniature Power Pack has Gas Turbine Driven Generator, *Design News,* vol. 10, Jan. 1955, pp. 26–27.

Effect of Fuel Type on the Performance of Aero Gas Turbine Combustion Chambers, and the Influence of Design Features, by J. G. Sharp, *J. Roy. Aeron. Soc.,* vol. 58, Dec. 1954, pp. 813–825.

Calibration and Description of the Exhauster Section of the High Altitude Test Plant, by E. Simpson and F. S. Margrie, *Gt. Brit. Royal Aircr. Estab.* Aero 2303, May 1954, 24 pp.

Booster Ramjets for Helicopters, by P. R. Payne, *Flight,* vol. 66, Dec., 1954, pp. 939–941.

Rocket Propulsion Engines

Thermodynamic and Propulsive Aspects of Rocket Motors (in Italian), by E. Macioce, *Aerotecnica,* vol. 34, Aug. 1954, pp. 196–203.

Thrust and Drag in Rocket Propulsion (in Italian), by E. Mattioli, *Aerotecnica,* vol. 34, Aug. 1954, p. 204–206.

Notes on Development of JATO, by H. D. Greenburg, *Picatinny Arsenal. Ordnance Res. Dev. Div. P.A. Notes* no. 62, June 1953, 16 pp.

Heat Transfer and Fluid Flow

Prandtl Number Determination by Means of Recovery Factor Measurements, by R. A. Seban, S. Scesa, and A. Levy, *Proj. Squid, TR* UCB-1-R, Sept. 1954, 26 pp. (published only on microcard).

Dynamic Response of Turbine-Blade Temperature to Exhaust Gas Temperature for Gas Turbine Engines, by Richard Hood and William E. Phillips, Jr., *NACA RM* E52A14, Feb. 20, 1952, 41 pp. (Declassified from Confidential 10/29/54.)

Some Aerodynamic Problems of Compressors and Turbines, by William R. Sears, *Maryland Univ. Inst. for Fluid Dynamics Appl. Math. Lecture Ser.* no. 30, Nov. 1953, 24 pp.

Prediction of Losses Induced by Angles of Attack in Cascades of Sharp-Nosed Blades for Incompressible and Subsonic Compressible Flow, by James J. Kramer and John D. Stanitz, *NACA TN* 3149, Jan. 1955, 45 pp.

On the Significance of Non-dimensional Coefficients in Heat Transfer, by A. F. Fritzsche, *Cornell Aero. Lab.* (translated from *Schweiz. Bauzeitung,* vol. 70, no. 40, 1952, pp. 580–582).

Shock-tube Measurements of Vibrational Relaxation, by Edward Stanley and Ernst H. Winkler, *J. Chem. Phys.,* vol. 22, Dec. 1954, pp. 2018–2022.

A Study of Surge in Compressors and Jet Engines, by Carl E. Pearson, *J. Aero. Sci.,* vol. 22, Jan. 1955, pp. 10–16.

The Early Development of Spherical Blast from a Particular Charge, by F. J. Berry, D. S. Butler and M. Holt, *Proc. Roy. Soc.,* vol. A227, no. 1169, Jan. 1955, pp. 258–270.

Secondary Flows and Boundary-Layer Accumulations in Turbine Nozzles, by E. Rohlik, Milton G. Kofskey, and Hubert Allen, *NACA Rept.* 1168, 1954, 32 pp. (Formerly *NACA TN* 2871, 2909, 2898.)

The Structure of Turbulence, by Theodore Theodorsen, *Maryland Univ. Inst. Fluid Dynam. Appl. Math. TN* BN-31, May 1954, 17 pp.

Free Jet and Ejector Studies, by Richard V. DeLeo and R. Hermann, *Rosemount Aero. Lab. Univ. Minnesota, Rep. of Progress,* June-Aug. 1954, 30 pp.

Compressible Two-Dimensional Jet Mixing at Constant Pressure, by H. H. Korst, R. H. Page, and M. E. Childs, *Illinois Univ. Engng. Exper. Sta. ME TN* 392-1; *OSR TN* 54-82, April 1954, 22 pp.

Analysis of Viscous Laminar Compressible Flow Through Axial Flow Turbomachines with Finite Blade Spacing, by P. W. Born, F. C. Hall, and others, *Illinois Univ. Engng. Exper. Sta. TR* no. C-TR-2, March 1953, 38 pp.

Nozzle Thrust and Momentum Data for Supersonic Flow, by C. M. King, *Frankfort Arsenal Pitman-Dunn Labs. Dept. Memo. Rep.* no. MR-590, Aug. 1954, 9 pp.

Ingestion of Foreign Objects into Turbine Engines by Vortices, by Lewis A. Rodert and Floyd B. Garrett, *NACA TN* **3330,** Feb. 1955, 23 pp.

Experiments on Turbulent Flow Through Channels having Porous Rough Surfaces with or without Air Injection, by E. R. G. Eckert, Anthony J. Diaguila, and Patrick L. Donoughe, *NACA TN* 3339, Feb. 1955, 45 pp.

Kinetic Theory of Evaporation Rates of Liquids, by E. F. Lype, *Trans. ASME,* vol. 77, Feb. 1955, pp. 211–223.

Pulsating-Flow Measurement—a Literature Survey, by A. K. Oppenheim and E. G. Chilton, *Trans. ASME,* vol. 77, Feb. 1955, pp. 231–248.

A Theoretical and Experimental Study of Shock-tube Flows, by I. I. Glass and G. N. Patterson, *J. Aero. Sci.,* vol. 22, Feb. 1955, pp. 73–100.

Thermodynamic Properties of Air and Combustion Products of Hydrocarbon Fuels. Part 3. The Flow of Gases of Varying Specific Heat, by D. Fielding, J. E. C. Topps, and W. R. Thomson, *Gt. Brit. Natl. Gas Turbine Estab. NGTE* no. R.160, June 1954, 24 pp.

Heat Transfer to Boiling Water Forced

Editor's Note: This collection of references is not intended to be comprehensive, but is rather a selection of the most significant and stimulating papers which have come to the attention of the contributors. The readers will understand that a considerable body of literature is unavailable because of security restrictions. We invite contributions to this department of references which have not come to our attention, as well as comment on how the department may better serve its function of providing leads to the jet propulsion applications of many diverse fields of knowledge.

Through a Uniformly Heated Tube, by J. F. Mumm, *Argonne National Lab., ANL* 5276, Nov. 1954, 57 pp.

Combustion

Burning Velocities in Deuterium-Bromine and Hydrogen-bromine Mixtures, by Stone D. Cooley and Robbin C. Anderson, *J. Amer. Chem. Soc.*, vol. 77, Jan. 1955, pp. 235–237.

Calculations of Burning Velocities for Hydrogen-bromine and Hydrogen-Chlorine Flames, by Katherine Hellwig and Robbin C. Anderson, *J. Amer. Chem. Soc.*, vol. 77, Jan. 1955, pp. 232–234.

Activation Energies of Reactions of Methyl Radicals with Organic Molecules, by Francis Owen Rice and Robert E. Varnerin, *J. Amer. Chem. Soc.*, vol. 77, Jan. 1955, p. 221–224.

Flame Propagation. V. Structural Influences on Burning Velocity. Comparison of Measured and Calculated Burning Velocity, by Paul Wagner and Gordon L. Dugger *J. Amer. Chem. Soc.*, vol. 77, Jan. 1955, pp. 227–231.

Carbon Formation in Pre-mixed Flames, by J. C. Street and A. Thomas, *Fuel*, vol. 34, Jan. 1955, pp. 4–36.

Decomposition Flame of Gaseous Ethyl Nitrate. I., by W. G. Wolfhard, *Fuel*, vol. 34, Jan. 1955, pp. 60–67.

Flame Stability of Preheated Propane-air Mixtures, by Gordon L. Dugger, *Indust. Engng. Chem.*, vol. 47, Jan. 1955, pp. 109–114.

Flame Velocity and Preflame Reaction in Heated Propane-Air Mixture, by Gordon L. Dugger, Robert C. Weast, and Sheldon Heimel, *Indust. Engng. Chem.*, vol. 47, Jan. 1955, pp. 114–116.

The Thermal Decomposition of Ammonium Perchlorate. II. The Kinetics of Decomposition, the Effect of Particle Size, and Discussion of Results, by L. L. Bircumshaw and B. H. Newman, *Proc. Roy. Soc.*, vol. A227, no. 1169, Jan. 1955, pp. 241–251.

Fuels, Propellants and Materials

The Synthesis of Resin Intermediates by Reactions with Ethylene Oxide, by Peter L. Nichols, Jr., John D. Ingham, Walter L. Petty, and Alan B. Magnusson, *Calif. Inst. Tech. Jet Prop. Lab. Rep.* no. 20–84, Sept. 1954, 44 pp.

Cermets—a New Solution for Thermal Shock, by J. A. Stavrolakis, *Aero Digest*, vol. 70, Jan. 1955, pp. 22–26.

The Direct Synthesis of Boron Hydrides, by A. E. Newkirk and D. T. Hurd. *J. Amer. Chem. Soc.*, vol. 77, Jan., 1955, p. 241.

Suggested Solutions for Liquid Hydrogen Handling Problems, by T. B. Dufur, *J. Space Flight*, vol. 7, Jan. 1955, p. 8.

Titanium Metallurgy. A Bibliography of Unclassified Report Literature, by Hugh Voress, *Atomic Energy Comm.* TID 30–39, April 1953, 57 pp.

Development of a New Gas Turbine Super Alloy, GMR 235, by D. K. Hannick, F. J. Webbere, and A. L. Boegehold, *SAE Preprint* no. 435, Jan. 1955, 22 pp.

Magnetic Susceptibility of Liquid Ozone-Oxygen Mixtures, by Callaway Brown, Charles K. Hersh, and Abraham W. Berger, *J. Chem. Phys.*, vol. 23, Jan. 1955, pp. 103–108.

High Temperature Heat Content and Entropy of Lithium Oxide and Lithium Hydroxide, by C. Howard Shomate and Alvin J. Cohen, *J. Amer. Chem. Soc.*, vol. 77, Jan. 1955, pp. 285–286.

A Turbine-Blade Alloy, Castable and Low in Cobalt and Columbium, by W. Siegfried and F. Eisermann, *Metal Progress*, vol, 67, Jan. 1955, pp. 141–146.

The Manufacture of Blades, Buckets and Vanes for Turbine Engines, by A. T. Colwell, *SAE Preprint*, Jan. 10–14, 1955, 35 pp.

Instrumentation and Experimental Techniques

Optical Considerations and Limitations of the Schlieren Method, by G. S. Speak and D. J. Walters, *Gt. Brit. A.R.C. Rep. Mem.* no. 2859 (formerly *ARC Tech. Rep.* 13066; *Roy. Aircr. Estab. TN* IAP 968), 1954, 25 pp.

Instrumentation for Jet Transports, by Christopher Dykes, *Aero. Engng. Rev.*, vol. 14, Jan. 1955, pp. 24–32.

A Strobe-Control System for Motion Picture Cameras, by Eric Laue, *Calif. Inst. Tech. Jet Prop. Lab. Memor.* no. 20–95, July 1954, 8 pp.

The Accuracy of Radiation Pyrometers. I. (in German), by Joachim Euler, *Arch. für Tech. Messen* no. 227, Dec. 1954, pp. 277–280.

Corrected Photoelements. I., by D. Geist (in German), *Arch für Tech. Messen* no. 227, Dec. 1954, pp. 281–284.

Launching Control for Guided Missiles, *Electronics*, vol. 28, Feb. 1955, pp. 122–127.

The Reduction of Data from the Rocket-Grenade Experiment, by W. G. Stroud, *Fort Monmouth Signal Corps Engng. Labs. Tech. Memo.* no. M-1570, April 1954, 33 pp.

Air-Driven Afterburner Fuel Pump, by M. C. Toth, *Aero Digest*, vol. 70, Feb. 1955, pp. 58–60.

A Panoramic Mass Spectroscope for Kinetic Studies, by Edouard G. Leger, *Canadian J. Phys.*, vol. 33, Feb. 1955, pp. 74–95.

Space Flight, Astrophysics, Aerophysics

RTV-N-12a Viking, *Glenn L. Martin Co. Progress Rep.* no. 36, *Engng. Rep.* no. 6373, Dec. 15, 1953–March 15, 1954, 17 pp.

USAF Aerobee Nos. 38, 39, 40, 41, 42, 43, by Eldon E. Rasmussen, *Holloman Air Force Base, Holloman Air Devel. Center Final Field Test Rep.*, Rep. nos. HADC-TR-54-9, 10, 11, 12, 13, 14, April 1954.

Terrestrial Flight, Vehicle Design

James Clayton Lecture: Guided Missiles, by G. W. H. Gardner, *Chartered Mech. Eng.*, vol. 2, Jan. 1955, pp. 5–22.

Engineers Probe Barriers to IBM Flight, by David A. Anderton, *Aviation Week*, vol. 62, Feb. 28, 1955, pp. 26–32.

Atomic Energy

Nuclear Powered Aircraft, by D. M. Walley, *Res. Rev* . (*Office of Naval Res.*), Jan. 1955, pp. 1–5.

Atomic Energy—the Power of the Future, *Interavia*, vol. 10, 1955, pp. 46–47.

Liquid Metal Cooled Reactors, by C. R. Stahl, *Mech. Engng.*, vol. 76, Dec. 1954, pp. 978–980.

Radiation Rules Out Reactors for Small Planes and Autos, by Kenneth Kasschau, *SAE J.*, vol. 62, Dec. 1954, pp. 17–20.

Index to Advertisers

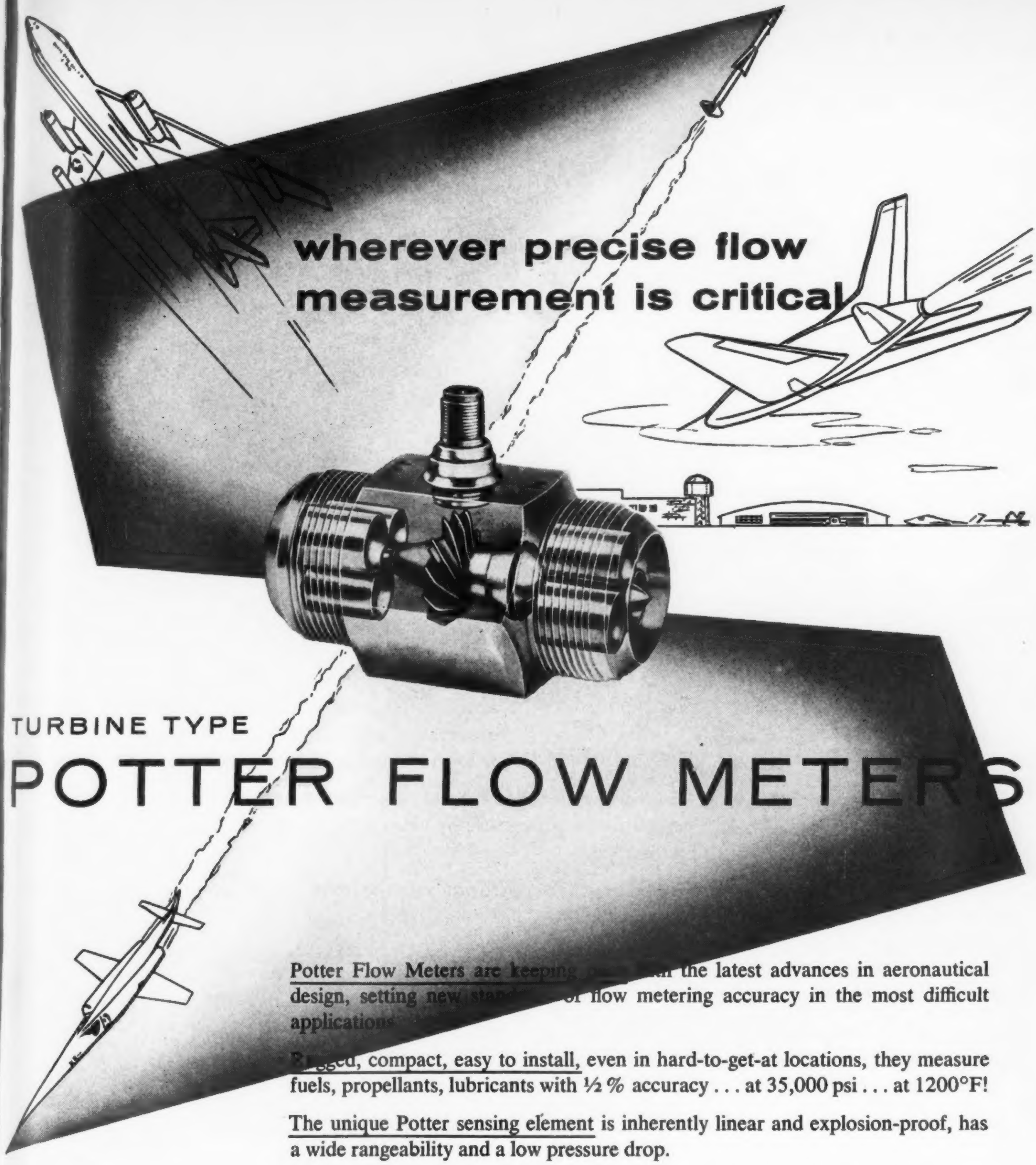

Potter Flow Meters are keeping pace with the latest advances in aeronautical design, setting new standards of flow metering accuracy in the most difficult applications.

Rugged, compact, easy to install, even in hard-to-get-at locations, they measure fuels, propellants, lubricants with ½% accuracy . . . at 35,000 psi . . . at 1200°F!

The unique Potter sensing element is inherently linear and explosion-proof, has a wide rangeability and a low pressure drop.

The Potter meter holds its calibration because it is designed for dependability with no complex linkages and no thrust bearings.

Find out how you can fit this meter into a Telemetering System, A Flow Recorder, or a Fuel Control System to meet your needs.

Write for bulletin AF 1 today.

POTTER AERONAUTICAL COMPANY

Route 22 • Union, New Jersey • Phone MUrdock 6-3010

Makers of "Potter Engineered" products